

**Page Denied**

CONFIDENTIAL

DOCUMENT NO. \_\_\_\_\_  
NO CHANGE IN CLASS.   
 DECLASSIFIED  
CLASS. CHANGED TO: TS <sup>S</sup>  
NEXT REVIEW DATE: 2012<sup>C</sup>  
AUTH: HR 70-2  
DATE: 25/5/82 REVIEWER: 037169

CONFIDENTIAL  
ELFIN III FINAL REPORT

SGG-1C6  
ORD # 673-64

1 August 1963

CONFIDENTIAL

## 1. INTRODUCTION AND SYSTEM CONCEPT

The purpose of the Elfin program is to develop electroplating techniques for the passive integration of microwave field intensities. The word Elfin itself is an acronym derived from electromagnetic-field-integration. Elfin I was a program to investigate the feasibility of developing electroplating cells hereafter called E-Cells, to integrate DC currents at high sensitivity. In particular, a sensitivity was specified such that the E-Cell would reproducibly measure an electric charge with an accuracy of one-tenth microcoulomb. E-Cells were developed under the Elfin I program which have a sensitivity two orders of magnitude greater than the original goal. Currents smaller than a millimicroampere can be integrated with E-Cells to an accuracy of approximately 1 millimicrocoulomb.

The Elfin II was a program to develop an instrument to measure microwave field intensities at hazardous levels. This program, supported by the Navy, developed instruments which would provide a digital readout of the integrated microwave energy over a thirty second time interval. This phase of the program is continuing with instruments currently being tested which provide acoustic warning signals when the integrated power level exceeds certain specified values.

The present report is the Final Report of the Elfin III program which had as its goal the development of small passive integrators to measure very low microwave field intensities. The range of field intensities which are of importance for this program are in the region of one-tenth to one-hundredth of a microwatt per square centimeter. The goal of the Elfin III program was to produce such devices and demonstrate the feasibility by means of field tests. A subsidiary goal was to investigate the feasibility of determining the frequency of the microwave field by noting the relative signal integration using antennas tuned to different wavelengths.

The goals of the Elfin III program have been substantially met, as stated above, with devices having been constructed which will measure microwave field intensities at distances from 1000 to 5000 feet from a radar antenna. Indication has also been obtained that the frequency of the radar can be determined by these techniques to an accuracy of approximately 10-20%. Portable instrumentation to read the accumulated charge in the E-Cells has also been constructed and tested under field conditions.

The Elfin device for measuring low intensity microwave fields consists in its simplest form of an antenna, a diode, a switch and an E-Cell for integrating the current generated by the diode. Some improvement in sensitivity is added if a small capacitor is connected in parallel across the diode when narrow pulses are to be integrated. The feasibility tests of the Elfin devices have been completed and the design sufficiently established that operational equipment can now be constructed to operate with a high degree of reliability.

The remainder of the report is divided into several sections and two Appendices. These sections describe tests performed on diodes and E-Cells of different designs and the selection of components for the final field tested equipment. A description of the field test equipment is provided and instructions for using the various components. The first Appendix contains a very brief summary of the large volume of electrochemical research which went into the development of the latest version of the E-Cell being used in the Elfin devices. The second Appendix is a discussion of the application of E-Cells to timers and is included because of its general qualitative discussion of E-Cell characteristics and circuitry to be used with E-Cells. A reader not familiar with many of the concepts associated with the E-Cells would be advised to read this discussion of cell characteristics in Appendix B before undertaking the remainder of this report.

## 2. DIODE TESTS AND MICROWAVE EQUIPMENT

In addition to the E-Cell the device requires an antenna diode, a capacitor, and a switch. Of these additional components the diode is the most critical. For the sake of simplicity, it was decided to use a microwave video diode which is enclosed in a small glass bead with leads protruding from either end rather than the cartridge type which has to be mounted in a special container coupled to coaxial cable. By using the diode with leads extending from each side it was necessary only to trim the leads to the proper length in order that the diode could serve as a half-wave dipole antenna. Two wires soldered to these leads at right angles serve as the DC path to the E-Cell so that no microwave linkage is needed in the system eliminating coaxial connections and waveguide.

*at what freq?*

Before a diode was chosen for this system, tests were conducted on several potential diodes to find the one most suitable for the application in mind. It had been found in previous work that at very low current levels the E-Cell acts as a relatively large resistance compared to its behavior at higher current levels. Since we would be operating at low field intensities the current generated by the diode would be relatively small and for that reason high sensitivity E-Cells were developed. The increase in resistance of the E-Cell at low current level also occurs for diodes for the same theoretical principle. This can be seen in Figure 2.1 which gives typical values for open circuit voltage and short circuit current of the diode at various power levels. It will be seen that the internal resistance of the diode is approximately 15K at a power level of 1 microwatt whereas it is less than 1K at a milliwatt. Since the high sensitivity cells which were developed under the previous phase of the program had a resistance at very low current levels of 1 megohm the diode resistance becomes relatively unimportant and the current through the E-Cell is determined primarily by the open circuit voltage of the diode. Therefore, this is the factor which is considered in evaluating the

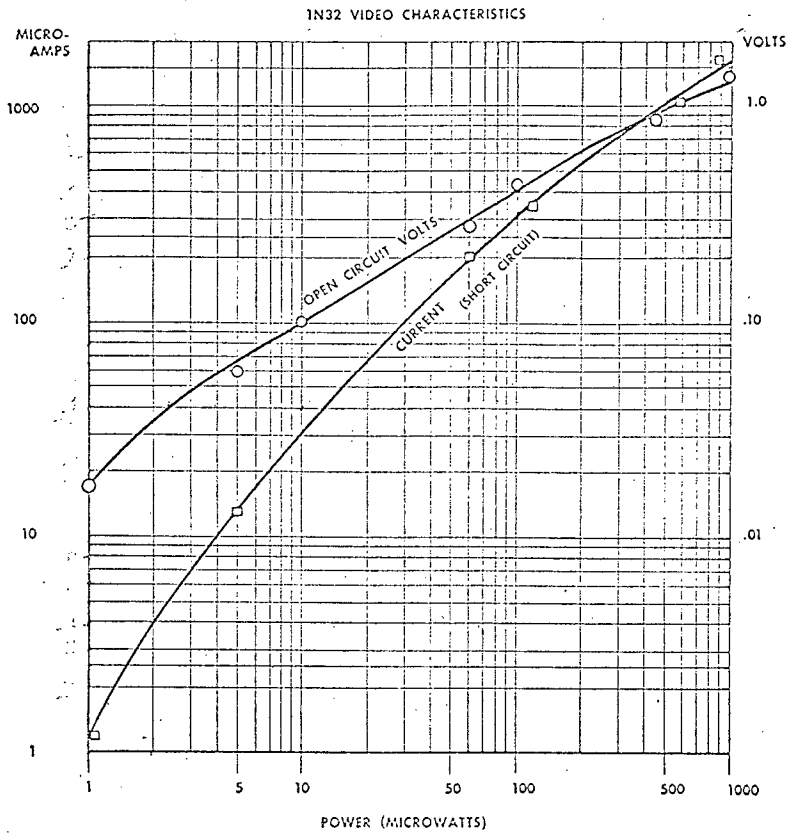
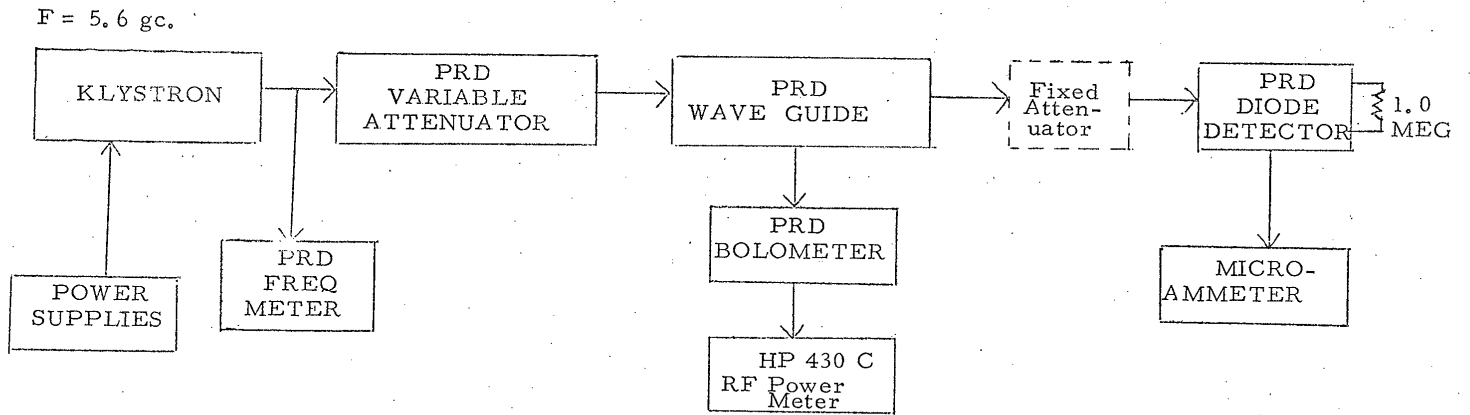


Figure 2.1

relative merits of the diodes.

Before the glass diodes were tested, an experiment was set up to measure the characteristics of a IN23C diode which is a capsule mounted diode unsuitable for our application but useful in some laboratory measurements. Its characteristics were found to be very similar to those shown in Figure 2.1 and will not be repeated here. Figure 2.2 shows the microwave setup used for making these measurements. The agreement with the data in Figure 2.1 provided some confidence that this means for making the open circuit voltage measurements was relatively sound. A 5.6 gigacycle Klystron was coupled by means of waveguide into a PRD variable attenuator with an absorption type frequency meter coupled to the waveguide. Beyond the attenuator was a waveguide section in which one quarter of one percent of the energy in the waveguide was picked off and coupled into a Bolometer to monitor the output power of the Klystron. The main portion of the power passed through a fixed attenuator to reduce the power level sufficient for diode detection. The diode was mounted in a section with a stub tuner which was tuned to provide maximum voltage output from the diode at a fixed power level of the Klystron. The current from the diode passed through a 1 megohm load and a Hewlett-Packard microvolt ammeter.

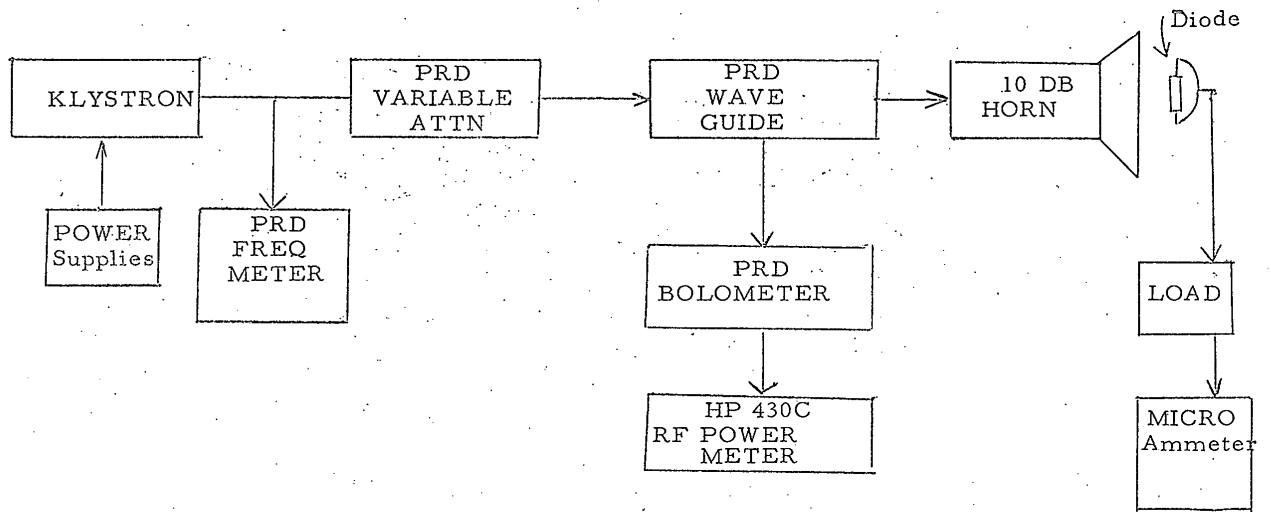
The microwave equipment setup used for making the measurements on the glass diodes was very similar to that shown for the IN23C diode and is illustrated in Figure 2.3. In place of the fixed attenuator and diode mount a 10 DB horn was mounted on the end of the waveguide. The diodes were then tested by cutting their leads so that the length of the diode would be resonant to the Klystron frequency, the length being one-half the radiated wavelength. DC pickoff leads were then soldered to the resonant diode leads in the manner that they would be used in operation. However, rather than passing the current from the diode through an E-Cell, it was passed in series through a 1 megohm load. The voltage across the 1 megohm resistor was monitored by the same microvolt ammeter used before.



IN23C DIODE CURRENT MEASUREMENTS  
TEST SET-UP BLOCK DIAGRAM

Figure 2.2





DIODE CURRENT  
TEST SET-UP

Figure 2.3

Three diodes were chosen from those available in the literature on the basis of their predicted performance for video operation at the microwave frequency and power levels under consideration. The results of these measurements on the MA 4123A, MA 4123, and IN833 diodes are shown in Figure 2.4. The Microwave Associates diode MA 4123A performed about a factor of two better than the other two for all power levels investigated and this is the diode that was chosen for our experimental equipment.

It will be noted from the data that the results for these diodes are about an order of magnitude less than the voltage reported as being typical in Figure 2.1. This is the result, however, of the fact that the RF power given as the independent parameter in Figure 2.4 is actually the total power being radiated from the 10 DB horn and is not the power intercepted by the diode. Although the diode antenna combination was placed very close to the aperture of the horn, the fact that it received only about one-tenth of the radiated power is quite reasonable. Indeed external monitoring of the radiated power with and without the diode in place showed no significant difference.

These voltage measurements were made with the Klystron operating in the CW mode so that they do not reflect the peak voltages which would be obtained for the same average power level if a pulsed source were used. Such peak voltages would not be readily measured at the lower levels with the microvolt ammeter because of its long integrating time constant. It will be noted, however, that the CW voltage generated by the diode at the 20 microwatt CW level is approximately 10 millivolts. An estimate of the spread of the energy out of the 10 DB horn allows one to make an estimate of the power density at the diode. 20 microwatts radiated power over 200 sq. cm. area yields a power density of approximately one-tenth microwatt per square centimeter which is typical of the field intensities which will be found in practice. Therefore, one should expect

KEUFFEL & ESSER CO. MADE IN U.S.A.  
3 X 5 CYCLES

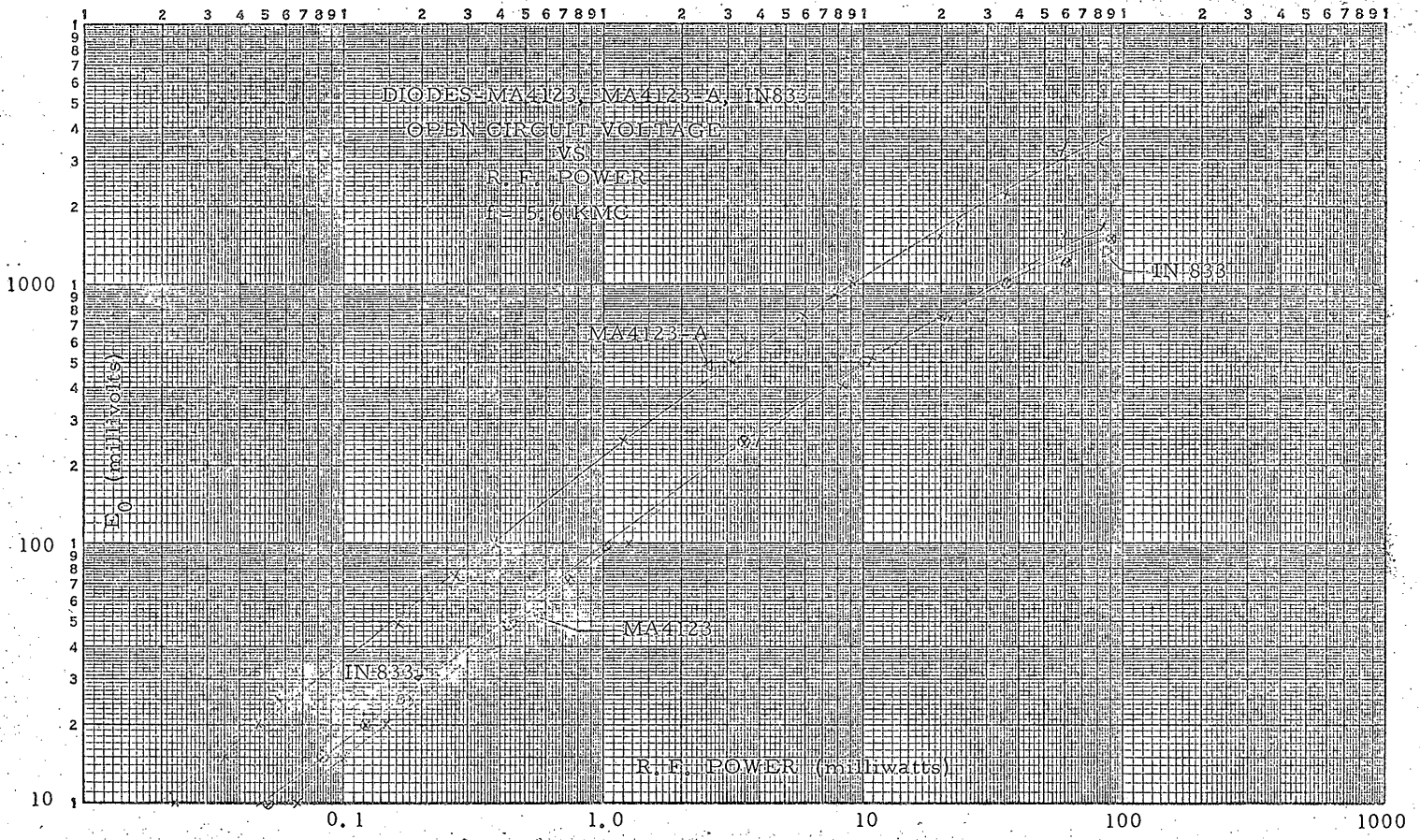


Figure 2.4

peak voltages out of the diode in excess of 10 millivolts. This is important since previous work with the E-Cells indicated that voltages below 10 millivolts are very ineffective for passing currents through the cells. This question will be examined in more detail in a later section.

### 3. TESTS ON B-CELLS

#### 3.1 INTRODUCTION

The first phase of the Elfin program was concerned with the development of an electroplating integrator subsequently called the E-Cell which would integrate currents as small as a tenth micro-ampere and reproducibly measure charge to the order of one-tenth microcoulomb. During the course of that program successive steps were made in improving cell sensitivity so that ultimately currents smaller than one millimicroampere could be integrated with charge sensitivity of the order of one millimicrocoulomb, two orders of magnitude beyond that which was required.

However, the analysis of the application which indicated the one-tenth microcoulomb sensitivity requirement assumed a cell resistance which was somewhat lower than the actual cell resistance encountered. It was also found that the more sensitive cells had higher internal resistances so that their sensitivity was offset by the fact that smaller currents would automatically be passed through them when a constant voltage source was applied. More specifically, cell resistance of 10 K was assumed in the sensitivity analysis and resistances of approximately 1 megohm were obtained in the sensitive B-Cells at one-hundredth microampere current level. Therefore, the increased sensitivity of the cells nearly compensated for the increased sensitivity requirement due to the larger cell resistance. Nevertheless, with this consideration it still appeared practical to meet the operational system requirements of integrating very small microwave field intensities.

In addition to the large resistance problem with the high sensitivity B-Cells, other problems were observed when the cells were used in other than controlled laboratory operation. There were periods in which the cell operation appeared quite erratic and a batch of cells would not yield consistent results among the individual mem-

bers. Furthermore, if silver were deposited on to one of the electrodes and allowed to stand overnight the recovered silver was often not very close in quantity to the original plated charge.

All of these characteristics indicated that much work would need to be done to take the laboratory type cell and convert it into a device which would be reliable under a variety of field operating conditions. Many of the experiments which were done on the high sensitivity B-Cells are summarized in the following sections to illustrate the problems which led to the development of a cell of somewhat less sensitivity but greater reliability and better matching characteristics to the microwave diode. This new cell, the DB-Cell, is described in more detail in Section 4.

### 3.2 SENSITIVITY TESTS OF B-CELLS

Tests were made on B-Cells containing 0.1N Ag NO<sub>3</sub> electrolyte. Several freshly prepared cells were tested for sensitivity to low levels of applied voltage and current, revealing unexpected characteristics. An attempt was made also to test several cells that had been stored for approximately fifty days, but they could not be made operational.

Voltage and current for the cells were supplied by the laboratory cell testing unit. Continuous measurements were made with two Hewlett-Packard Model 425A DC microvolt ammeters, one measuring the current and the other the voltage. The outputs of these meters were used to operate a Sanborn Dual Channel DC amplifier-recorder. This unit provided a continuous plot of the voltage and current versus time.

#### Stored Cells

Measurements were made on five cells which had been stored for a period of approximately fifty days. An open-circuit voltage ( $E_0$ ) of 100 millivolts and a short-circuit current ( $I_s$ ) of 1.0 microamps

were used as the power source. The results for each cell were the same: as the silver deposit was transferred successively from one electrode to the other, the amount transferred consistently diminished with each transfer until finally no measurable current flowed through the cell. The applied voltage was then varied from 10 mv to 500 mv, but no appreciable current could be detected.

#### Cell B-34

This cell was freshly prepared on 29 January, 1963, and tested on 31 January, 1963. The conduction values of current (I) and voltage (E) were obtained from the Sanborn Recorder plots for given values of  $E_0$  and  $I_s$ . \* R is the conduction resistance of the cell calculated from the average values of E and I for each transfer (a transfer is defined as the time interval during which silver is transferred from one electrode to the other). In cases where E and I changed significantly during successive transfers for a given value of  $E_0$ , the maximum and minimum averages were recorded. Figure 3.1 is a plot of conduction resistance versus  $E_0$  using the data obtained.

The various effects resulting from the tests are discussed in the following paragraphs. In all cases, measurements with  $E_0$  less than 100 mv were begun with approximately half the total silver deposit on each electrode.

a. In the first series of runs (a run consists of measurements at a given  $E_0$ ) it was found that when  $E_0$  was reduced from 100 mv to 1 mv and then increased, no measurable results were obtained until  $E_0$  became 30 mv. However, when  $E_0$  was decreased following the 30 mv run, significant measurements were obtained down to 10 mv. At this point the series was concluded.

b. In the second series of runs on this cell readings at  $E_0 = 20$  mv and above were found to be consistent with the first series of data. Below 20 mv, it was found that by preceding each run with a run at 100 mv, significant results were obtained for the smaller

\* Open circuit voltage and short circuit current.

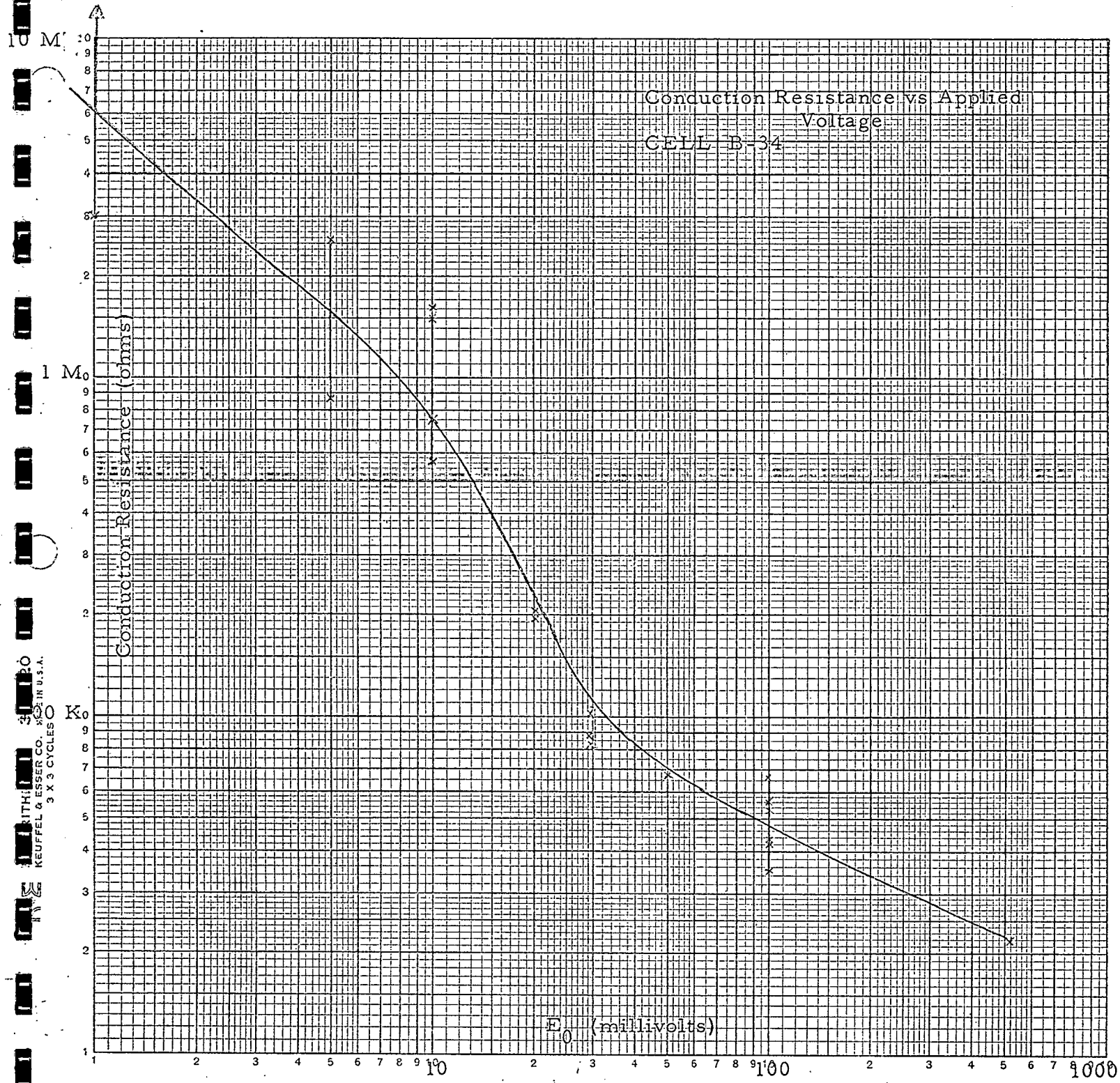


Figure 3.1



values of  $E_0$ . If  $E_0$  was decreased directly to successively smaller values, either no cell current could be measured or it would decrease from a measurable value to insignificance after two or three transfers of a run.

c. Another effect noted was a change in the total charge being transferred with different runs at  $E_0 = 100$  mv. The charge transferred in the initial run of the first series,  $E_0 = 100$  mv, shall be taken as 100% charge transfer for purposes of discussion. Subsequent runs at  $E_0 = 100$  mv (all in the second series) yielded charge transfers of 95%, 78%, 90%, 78%, 79%, and 65%, respectively. Preceding the run yielding 65%, a run was made with  $E_0 = 500$  mv (prior to this run,  $E_0$  was never greater than 100 mv). The 500 mv run gave 82%, 79%, and 75% values in three successive charge transfers. Then  $E_0$  was returned to 100 mv and the last run was made, giving three successive transfer values of 68%, 65%, and 63%; i. e., after 500 mv was applied to the cell, the total charge transfer consistently decreased with subsequent transfers. No data was obtained for total charge transfers with  $E_0$  less than 100 mv. Figure 3.2 compares a transfer of the initial run at 100 mv to the first transfer of the final 100 mv run. \*

d. A study of the Sanborn plots of current versus time revealed that after some of the runs with  $E_0$  other than 100 mv, the initial transfer that occurred when  $E_0$  was again made 100 mv had a "tail"; i. e., towards the end of the transfer the current dropped sharply to about 70-80% of its peak value and continued at this level for a period of time. This effect was most pronounced after the successful 1.0 mv run. In the 100 mv run which followed, the tail appeared in four successive transfers, and in fact, appeared to increase with each transfer. In the third transfer of this run, the tail accounted for about 15% of the total charge. Figures 3.3 and 3.4 illustrate this effect for 100 mv runs which followed runs at 1.0 mv, 10 mv, and

---

\* Current is on the left and voltage on the right. Time runs from bottom to top at one millimeter per second.

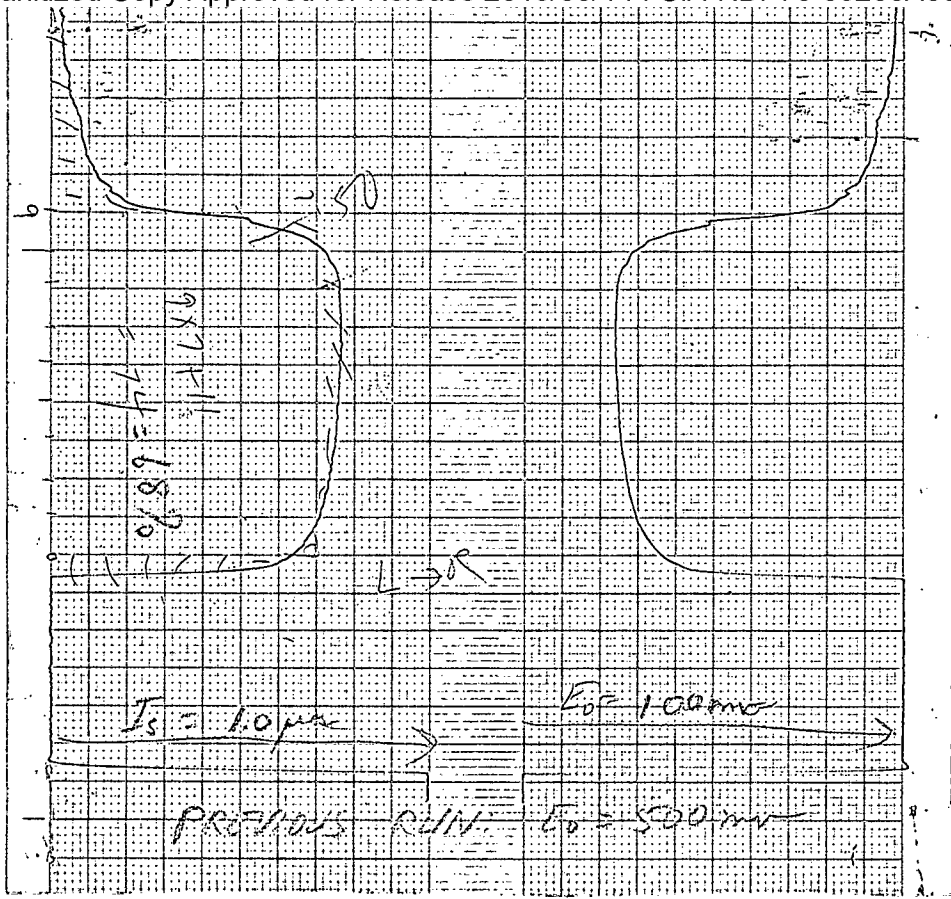


Figure 3.2

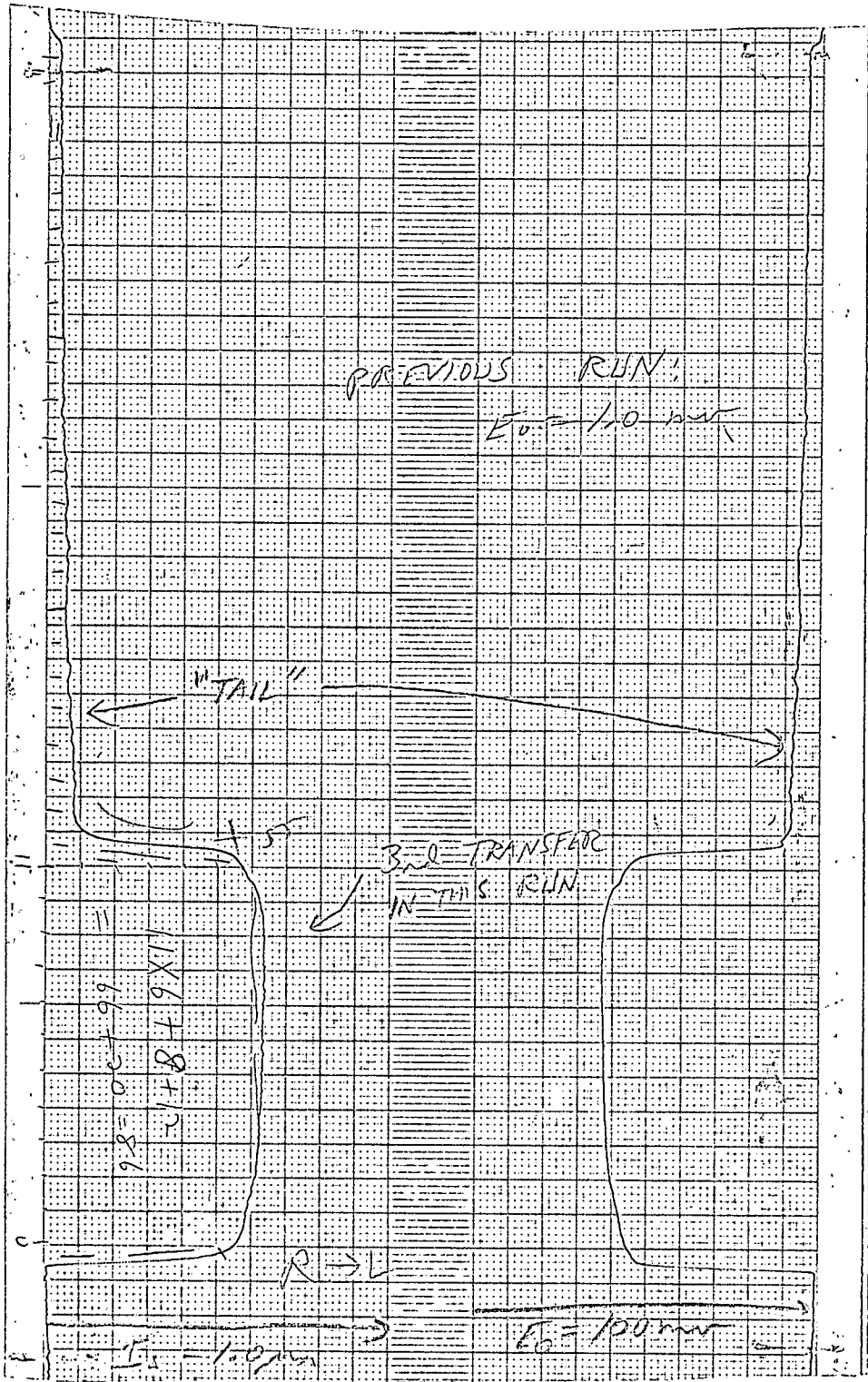


Figure 3.3

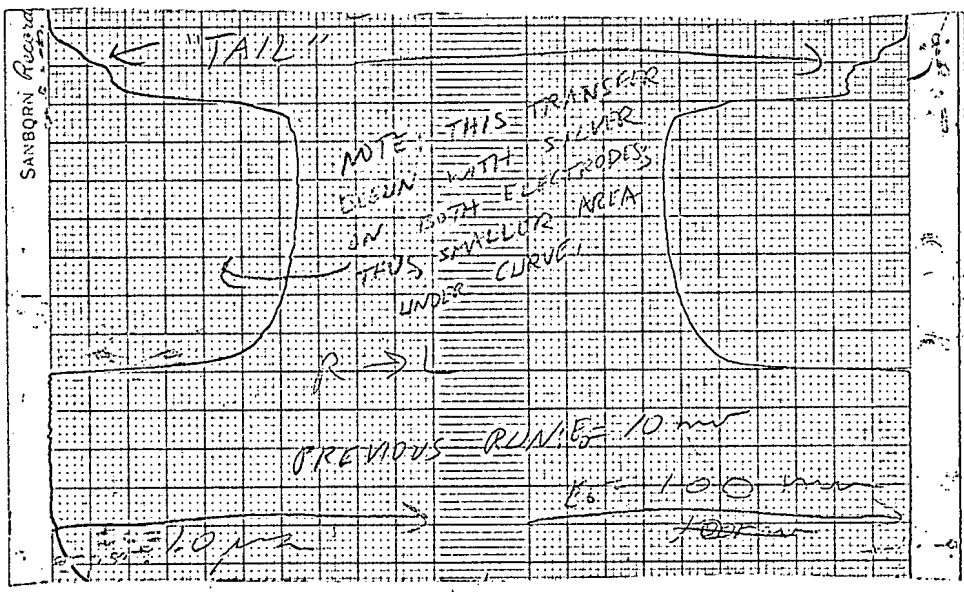
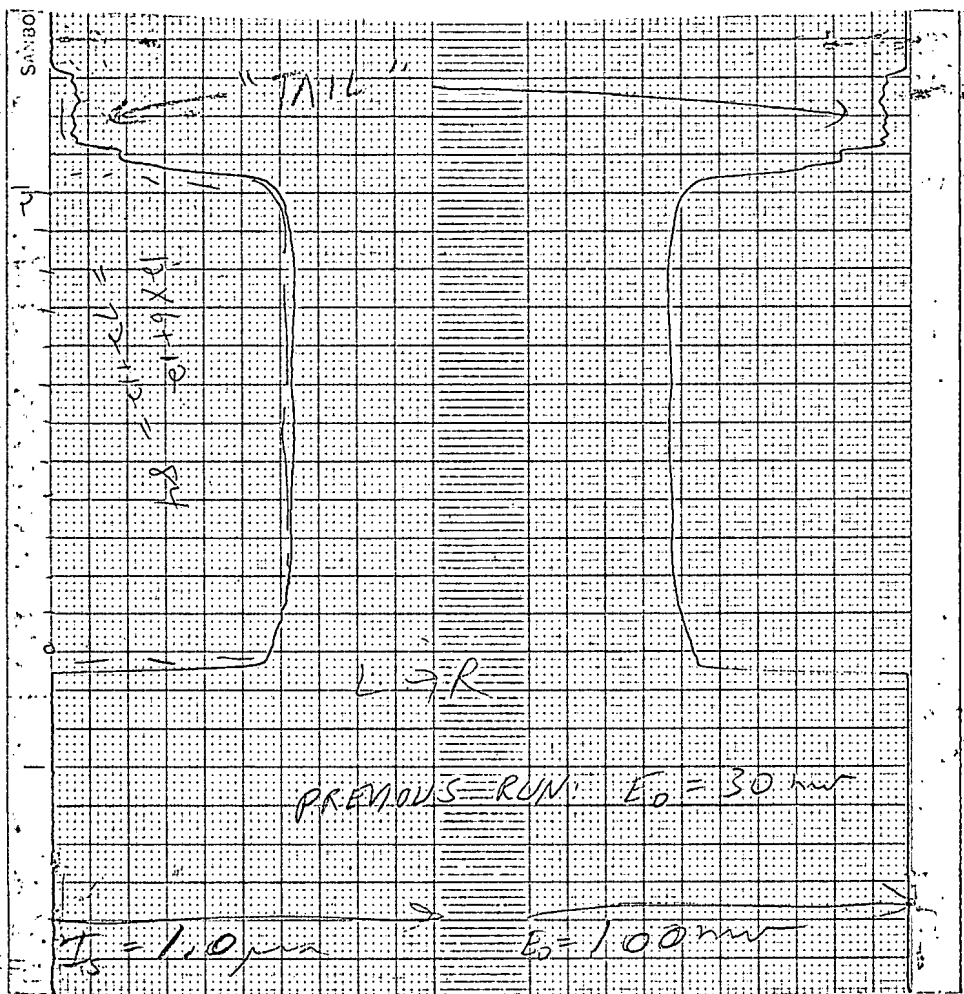


Figure 3.4

30 mv. These should be compared with the initial transfer of Figure 3.2. Note also in Figure 3.2 the tail on the transfer which followed the 500 mv run.

e. At  $E_0 = 10$  mv and less, the conduction resistance of the cell was found to consistently increase within a run. That is, the transfer current decreased and the transfer voltage increased with successive transfers for a given value of  $E_0$ . For values of  $E_0$  between 10 mv and 100 mv, this effect could not be determined due to an insufficient number of transfers per run. At  $E_0 = 100$  mv, the conduction resistance appeared to decrease slightly with successive transfers, but this is believed due to a "dip" effect discussed in the next paragraph. However, the aggregate of runs at  $E_0 = 100$  mv showed a trend of increasing conduction resistance with each run until the 500 mv run was made. In the 100 mv run which followed the latter, the conduction resistance was less than in any of the previous 100 mv runs, while at the same time, it increased slightly with successive transfers. Figures 3.5 and 3.6 show the trend of increasing resistance at  $E_0 = 10$  mv (note: the current scale has been decreased in Figure 3.6).

f. When the initial condition of the cell consisted of part of the silver deposited on each electrode, a "dip" phenomena occurred after the silver was transferred completely to one electrode. To illustrate this effect, assume one-fourth of the silver is on the right electrode and three-fourths on the left electrode. The first transfer, say from right to left, deposits the fourth of silver from the right onto the left electrode. Then a total transfer is made from left to right. As the point at which the original condition existed ( $1/4 R - 3/4 L$ ) is reached during the transfer, the conduction resistance increases approximately 10-20% and then returns to its previous value of the transfer, forming a "dip" in the current and voltage time plots. Subsequent transfers are then normal (no "dip"), with a slightly lower value of conduction resistance. Total transfers were made with the above initial conditions only at 100 mv, and the effect was

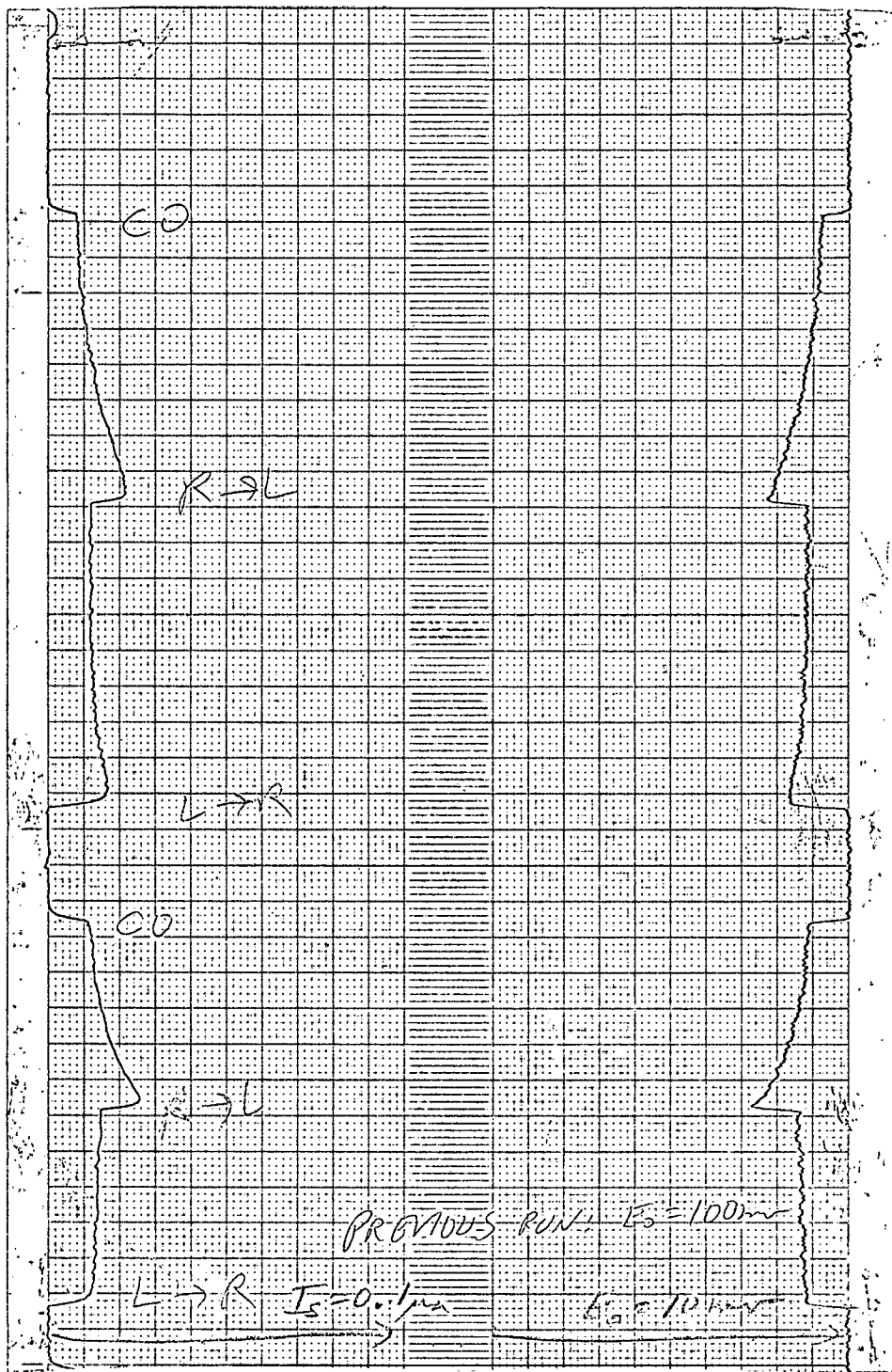


Figure 3.5

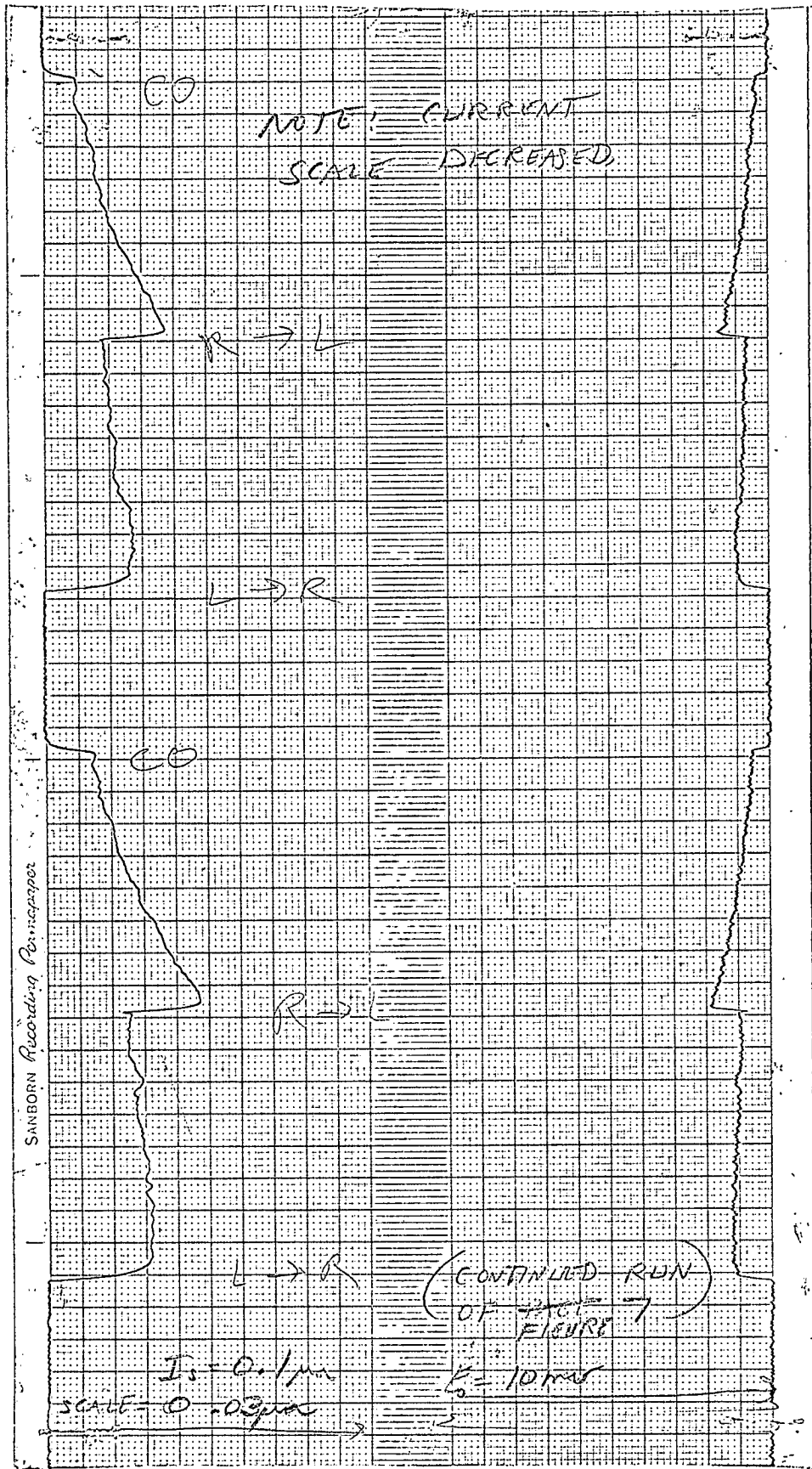


Figure 3.6

observed in every case. It occurred with various initial distributions of silver deposit and appeared independent of whether the first transfer was made right to left or left to right. Figure 3.7 is a plot of the "dip" effect.

#### Cell B-35

This cell was freshly prepared on 29 January, 1963, and used for some preliminary test on 30 January. The measurements of this report were made on 31 January, at which time the cell displayed a pronounced effect of consistently decreasing the total amount of silver transferred, whatever value of  $E_0$  was applied. Taking the initial transfer of the first run at 100 mv as 100%, the last transfer of the fourth run (also at 100 mv) was found to have decreased to 30% of the initial value. Total transfers were not made at values of  $E_0$  less than 100 mv.

Readings were obtained with this cell down to  $E_0 = 10$  mv, where  $E_0$  was decreased directly to this value from 50 mv. The procedure used with cell B-34 of returning to 100 mv before proceeding to small values of  $E_0$  was not used with this cell, and readings were not obtained at 1.0 mv, the next run attempted after 10 mv.

Figure 3.8 is a graph of conduction resistance versus  $E_0$  for the cell, obtained from the data. The single value of R plotted for  $E_0 = 10$  mv is assumed questionable, based on information obtained from cell B-34.

#### Conclusions

To summarize the effects discussed above:

a. When  $E_0$  was initially decreased from 100 mv to 1 mv, and then increased to 5 mv, 10 mv and 20 mv, negligible current flowed at any of the values below 100 mv. At 30 mv satisfactory results were obtained;  $E_0$  was then decreased to 20 mv and 10 mv with positive results.

b. Below 20 mv, when  $E_0$  was returned to 100 mv before



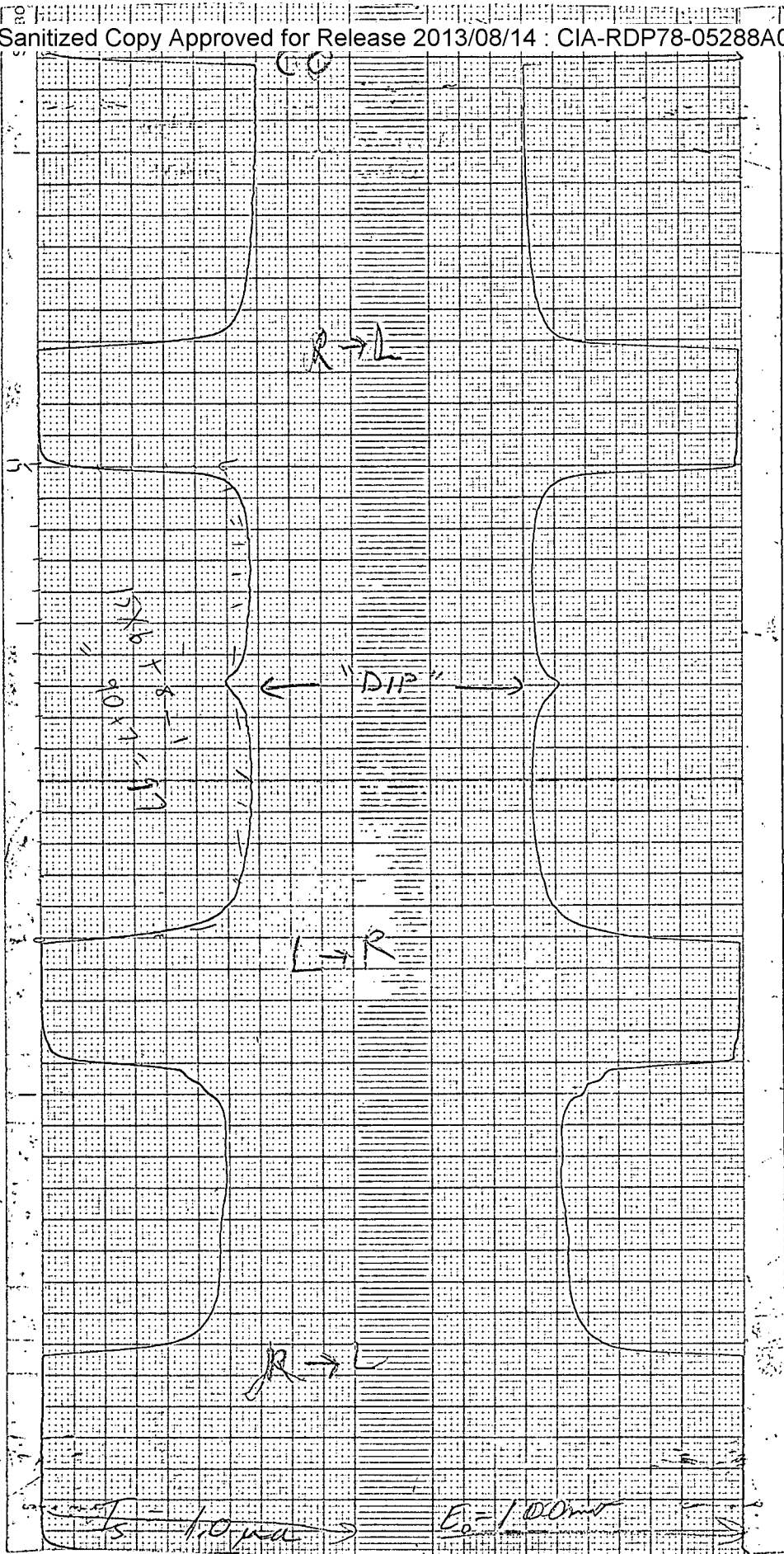


Figure 3.7

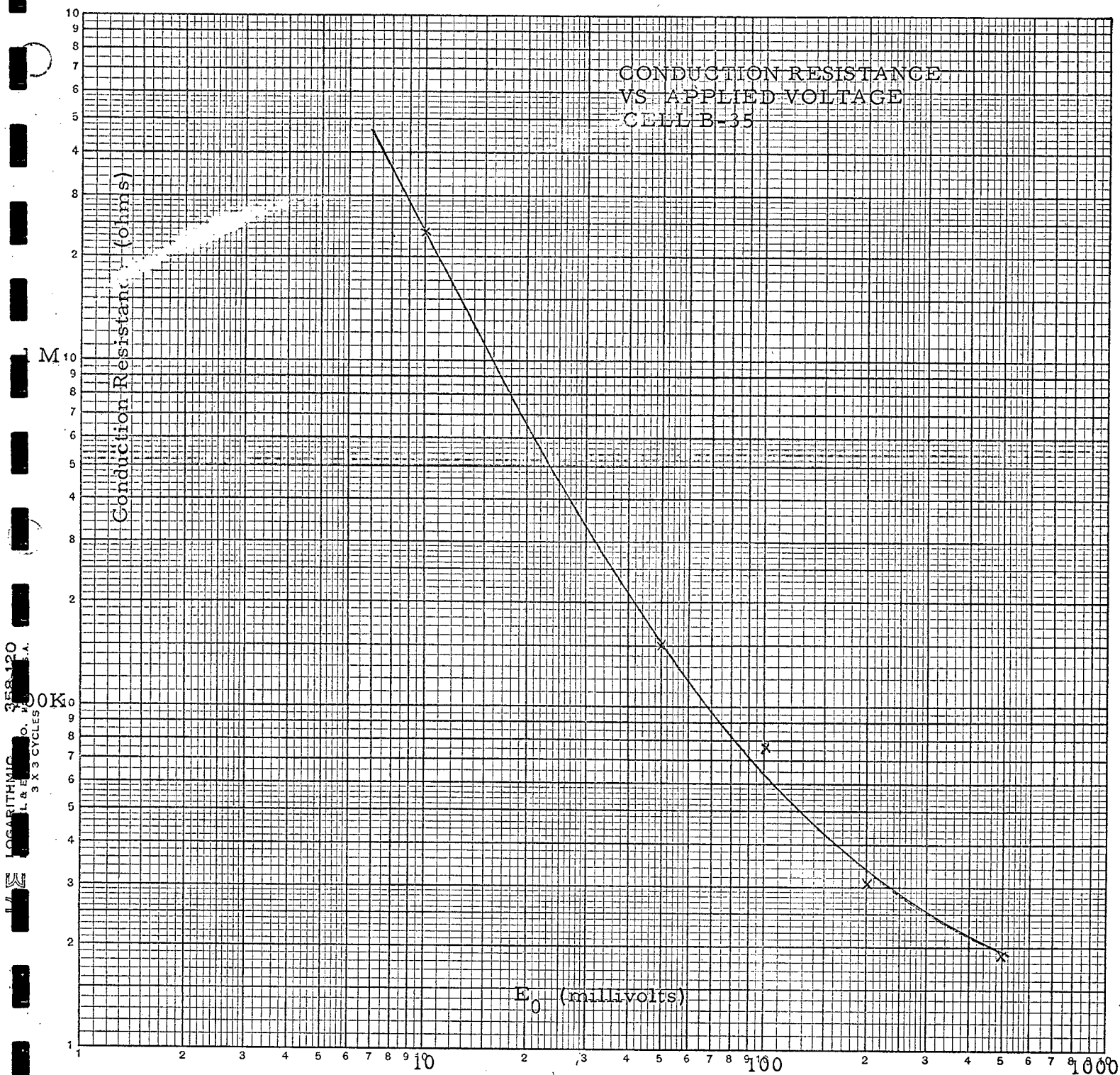


Figure 3.8

going to each of the smaller values, performance was greatly improved over the results obtained when  $E_0$  was decreased directly to the smaller values.

c. Total charge transfer decreased with subsequent runs at 100 mv. After 500 mv was applied, successive transfers consistently decreased in amount of charge.

d. "Tails" occurred on 100 mv total transfers after some runs at other values of  $E_0$ . This was very pronounced after the 1.0 mv run.

e. Below 10 mv, the conduction resistance of successive transfers consistently increased within a run.

f. "Dips" occurred in transfers at 100 mv when the silver deposit was initially on both electrodes.

The results indicate inconsistent operation of the cells may be expected below 30 mv. While some of the difficulties encountered at low voltages might be overcome by operational techniques, the effect of increasing conduction resistance with time would seem a difficult problem to solve in this manner. In addition, no information was obtained concerning the effects of prolonged time intervals between transfers.

### 3.3 B-CELL R. F. POWER MEASUREMENTS

A freshly prepared cell, B-35, was tested for response to a microwave power source. The R. F. power, at a frequency of 5.6 kmc, was detected with a IN23C crystal diode in a PRD microwave detector. Figure 3.9 is a block diagram of the test setup.

The general procedure was to first transfer all the silver of the cell to one electrode, then transfer approximately half back to the other electrode, the exact amount being determined from the Sanborn current time plot. The laboratory test unit was then disconnected and the cell connected to the diode. The R. F. power was then turned to the desired power level (by changing the attenuator

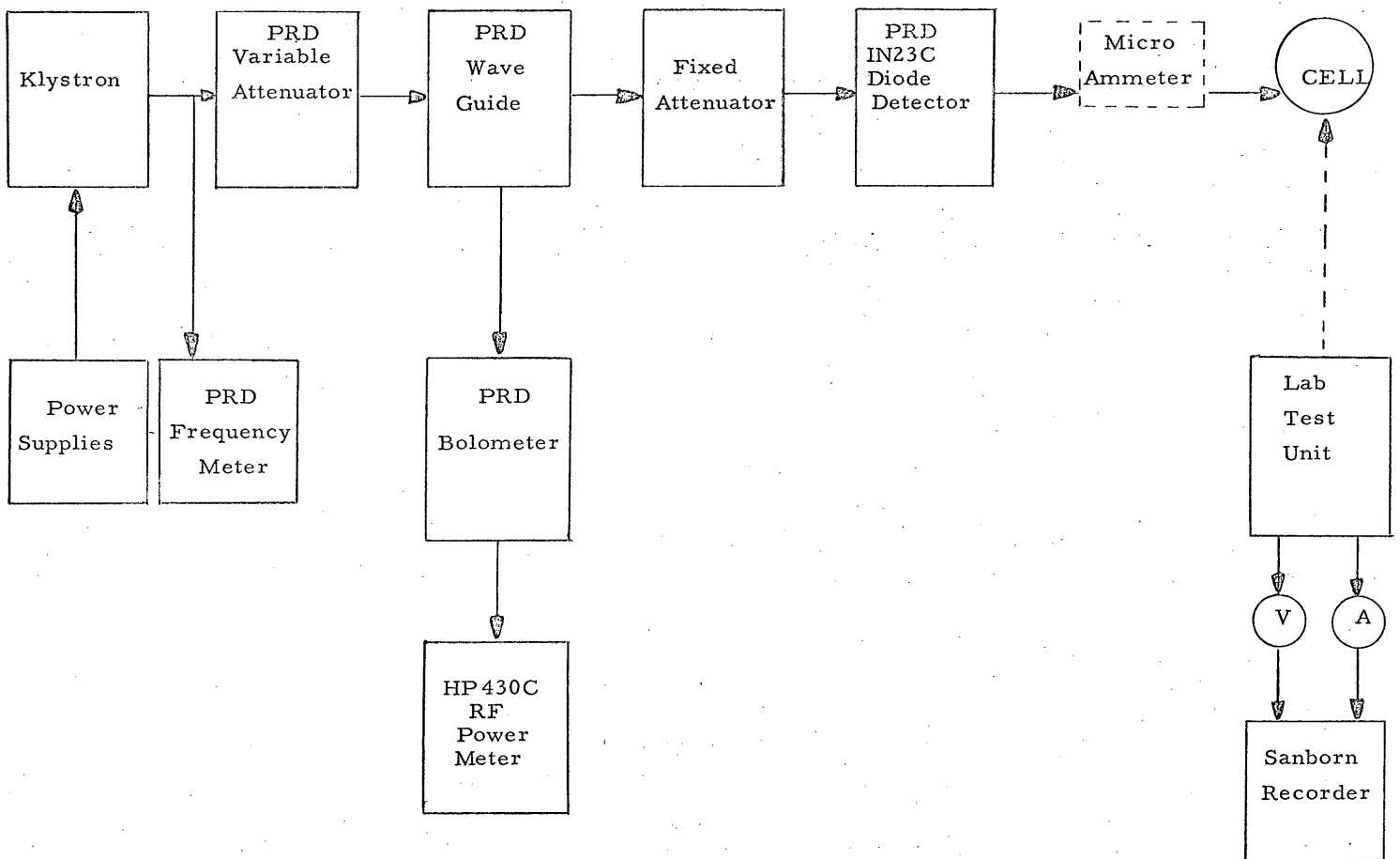


Figure 3.9 RF Power Measurements With B-Cells Test Set-Up.

setting) for the specified exposure time. The last step was to reconnect the lab test unit and transfer the remaining silver back to the original electrode. The amount of this final transfer was determined from the Sanborn current time plot. In all runs with the lab test unit, the open circuit voltage  $E_0$  was 100 mv and the short circuit current  $I_s$  was 1.0 microamps.

The difference between the transfers before and after the R. F. was applied to the cell is the amount of charge deposited by the R. F. diode current. Thus, the diode current may be calculated.

The first set of measurements was obtained using a microammeter with a 10 K $\Omega$  internal resistance in series with the cell and diode. The data is given in Table 3.1. Due to the experimental procedure used, there was a possible error of +20% in the exposure time. Thus, the current calculated from the charge transfer is in agreement with the measured current through the cell. These measurements were made only at the relatively high current levels shown in the table to establish the correct operation of the cell at a level known previously to give good response.

The second set of measurements, Table 3.2 was then made to determine the cell's response to low R. F. power levels. The ammeter was removed from the circuit and the cell connected directly across the diode. The R. F. power input to the diode detector was measured and the cell current calculated from the resulting charge transfer.

Multiple readings were taken at power levels of 16.9 mw, 15.0 mw, and 13.4 mw at various exposure times. It can be seen from the table that consistent results were not obtained in this region. This might be due in part to the procedure used in setting the R. F. power level for each run. The attenuator was varied from maximum attenuation to the desired reading at the beginning of the run and returned to maximum attenuation at the end. This allowed considerable error in the exposure time and the attenuator dial setting. The error in the attenuator setting is estimated at  $\pm$  0.5 db. However, previous

TABLE 3.1

## R. F. MEASUREMENTS -- CELL B-35

<u>Run Number</u>	<u>Measured Diode Current (<math>\mu</math>amps)</u>	<u>Exposure Time (sec) <math>\pm</math> 20%</u>	<u>Calculated Diode Current From Cell (<math>\mu</math>amps)</u>	<u>% Error</u>
1.	1.0 $\mu$ a	15 sec	1.13 $\mu$ a	+13%
2.	1.0 $\mu$ a	15 sec	1.10 $\mu$ a	+10%
3.	1.0 $\mu$ a	15 sec	1.23 $\mu$ a	+23%
4.	1.0 $\mu$ a	15 sec	1.04 $\mu$ a	+ 4%
5.	0.50 $\mu$ a	15 sec	0.51 $\mu$ a	+ 2%

Table 3.2  
 RF Measurements - Cell No. 35  
 (Measured RF Power)

Run No.	RF Power ( $\mu$ watts)	RF Diode $E_o$ (millivolts)	Exposure Time (sec) <u>+3 sec.</u>	RF Diode Current ( $\mu$ amps)	(Calculated from Cell read-out)
1.	134 $\mu$ w	270 mv	15 sec.	1.23 $\mu$ a	
2.	86	200	15	1.0	
3.	53.5	140	15	0.37	
4.	33.6	90	30	0.13	
5.	13.4	42	60	0.050	
6.	13.4	42	120	0.017	
7.	21.2	63	120	0.14	
8.	13.4	42	180	- -	
9.	16.9	50	120	0.16	
10.	16.9	50	60	0.099	
11.	15.0	46	120	0.054	
12.	15.0	46	180	0.038	
13.	13.4	42	300	0.056	
14.	13.4	42	180	0.0067	

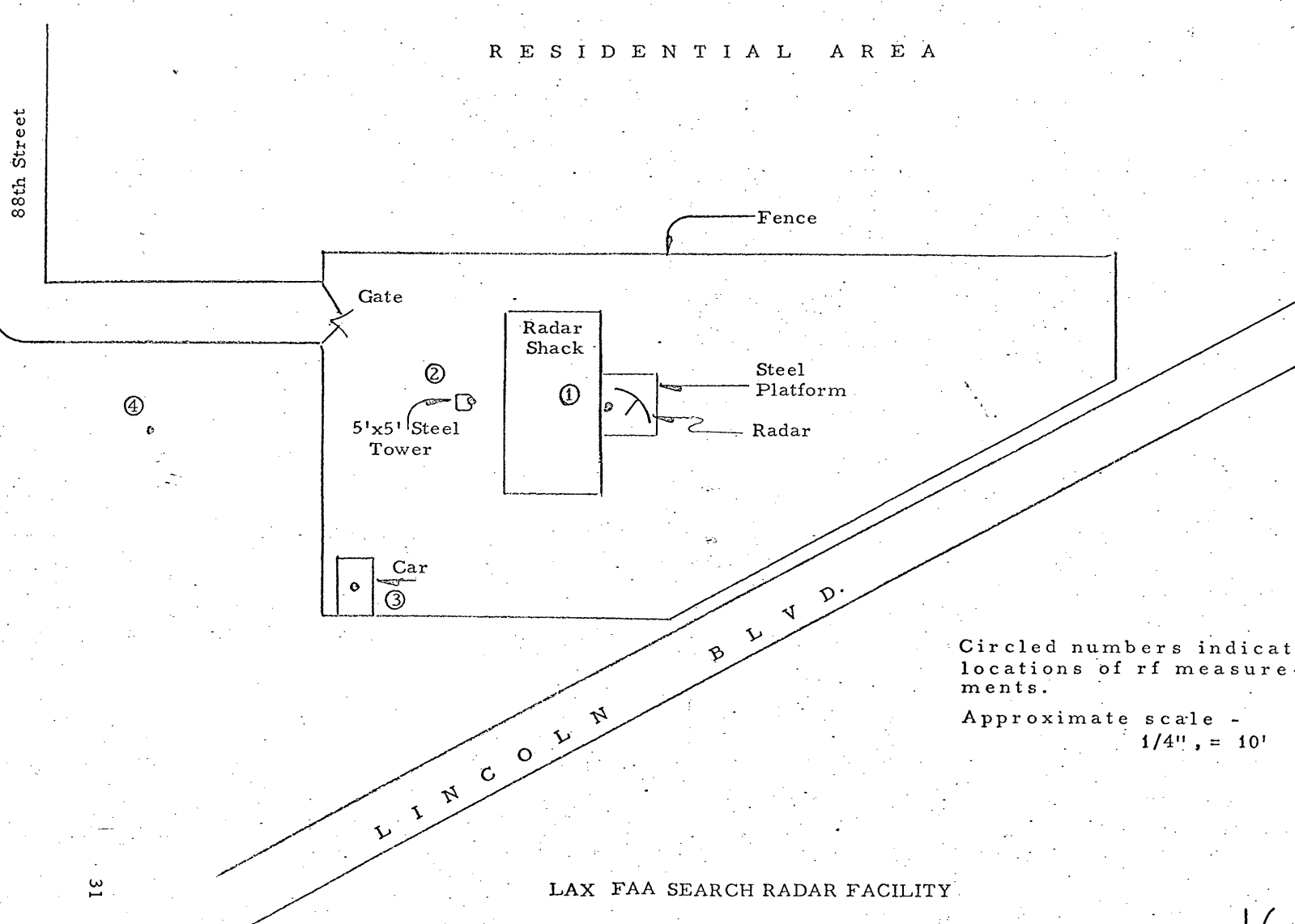
work with these cells has shown them to be inconsistent at applied voltage levels below 50 mv, which corresponds in this case to power levels below 20 microwatts.

#### 3.4 B-CELL FIELD TESTS

Five high sensitivity B-Cells were prepared for field testings. These were cells B-27, B-29, B-32, B-33, and B-34. The cells had been prepared in the manner of previous laboratory experiments and filled with one-tenth normal silver nitrate solution. The cells were each charged with approximately 20 microampere seconds of silver on each electrode. Then the cells were sealed with Teflon tape. The current source in the field was an S-band antenna, a tunable crystal diode mount containing a IN23C diode, and external leads to which the B-Cells were attached. The tests were conducted at the Los Angeles International Airport Radar Facility. A sketch of the facility is shown in Figure 3.10. A low sensitivity microwave radiation monitor using A-Cells rather than the high sensitivity B-Cells, was also taken along on the test. This instrument gave integrated reading at Positions 1 and 2 shown in the figure. No reading was obtained in Position 3. The B-Cells were all exposed one hundred feet from the antenna at Position 4, as shown in the figure. They were exposed for a range of time intervals from a few seconds up to several minutes. Figure 3.11 is a Xerox reproduction of a photograph showing an exposure taking place. The antenna diode and cell combination was hand held for all the exposures.

The airport radar radiates at a frequency approximately 2900 megacycles with pulses 1 microsecond wide and a pulse repetition frequency of approximately 1000 pulses per second. The antenna gain was given to be 34db with a  $1\ 1/2^\circ$  beam width in the azimuth. The maximum of the beam is tilted approximately  $3^\circ$  above the horizontal. The average power of the antenna was given to be approximately 290 watts with a peak power close to .500 kilowatts. The antenna rotates once every twelve seconds.





Circled numbers indicate locations of rf measurements.

Approximate scale -  
1/4" = 10'

LAX FAA SEARCH RADAR FACILITY

Figure 3.10

N

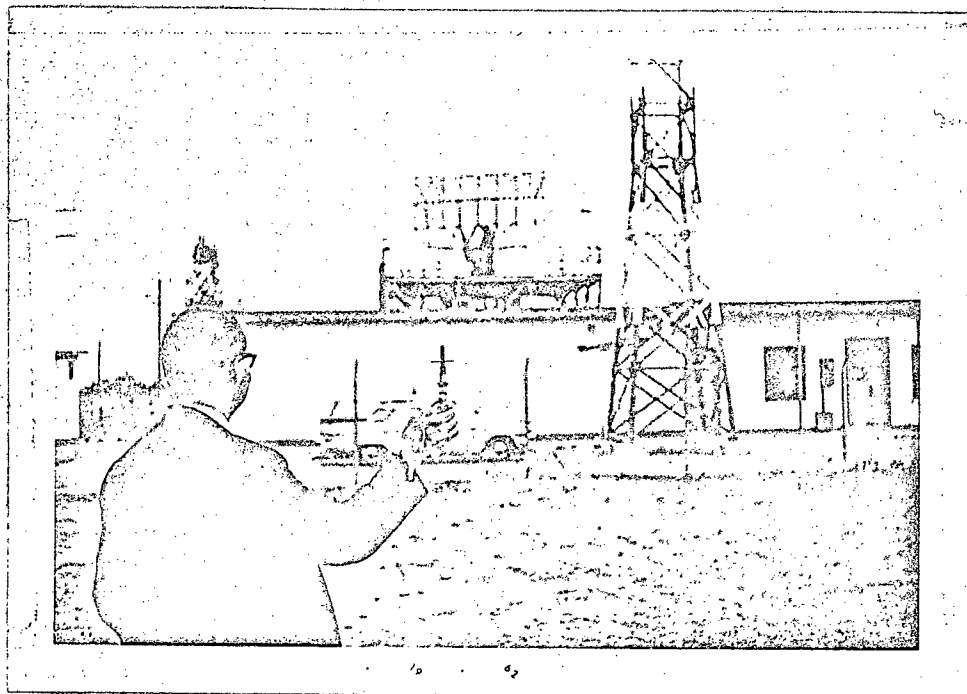


Figure 3.11

The B-Cells were charged with silver in the lab prior to being taken to the radar <sup>site</sup> sight and were brought back to the lab for discharge and determination of the integrated current. Figures 3.12 and 3.13, respectively, show the charge process and the discharge record for cell B-29. These are the current-time and voltage-time plots taken with the Sanborn recorder. In Figure 3.12 it will be noticed that the silver was put upon the right electrode and then integrated from right to left, from left to right again, and then approximately half the silver from right to left. When the cell was brought back to the laboratory, the plating from right to left was continued and then re-cycled from left to right, then right to left.

It will be noticed on this particular cell that the sum of the integrals before and after the radar exposure is very close within the experimental error to the total integral of charge put on the electrode. In other words, no detectable transfer of silver occurred during the exposure at the radar sight. The "dip" effect will be noticed during the plating period shown in the center of Figure 3.13. The result for cell B-29 is typical of the results for all five cells and in no case was a detectable amount of plating measured during this field test.

Previous results and subsequent analysis in the laboratory with the cells using a laboratory source which closely simulated the airport radar revealed that the cell resistance at low power levels was too large and its integration of narrow pulses too poor to have produced measurable results under the operational situation described for the test. The results of this test and other laboratory investigations, some of which are described above, suggested strongly that another cell be built which would have characteristics which better matched the video diodes being used and the field intensities which it would be necessary to measure.

This test also indicated that it would be desirable to have equipment in the field which could provide readout for the cells in order to save considerable amount of time in transportation between the radar sight and the laboratory. Laboratory tests also indicated

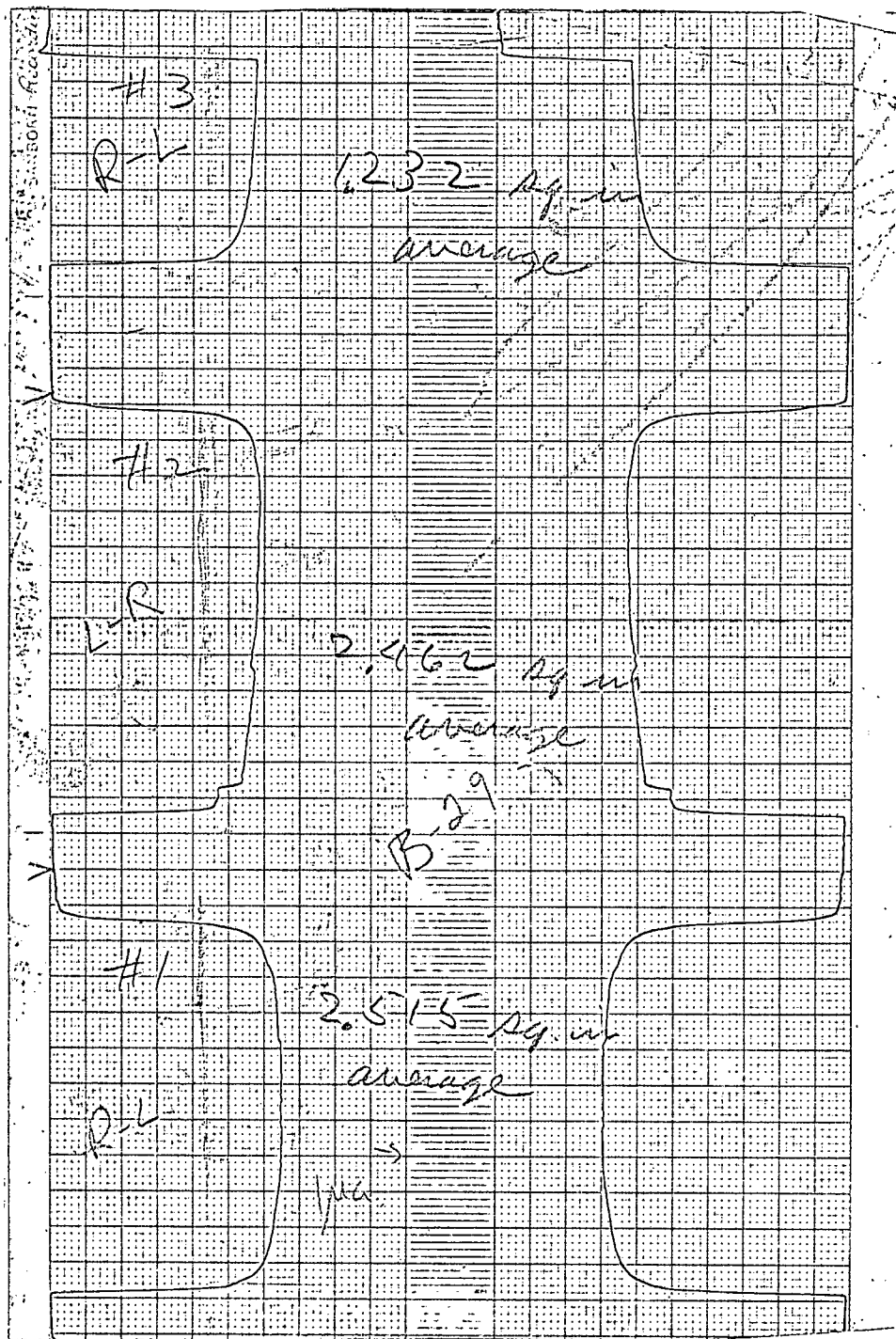


Figure 3.12

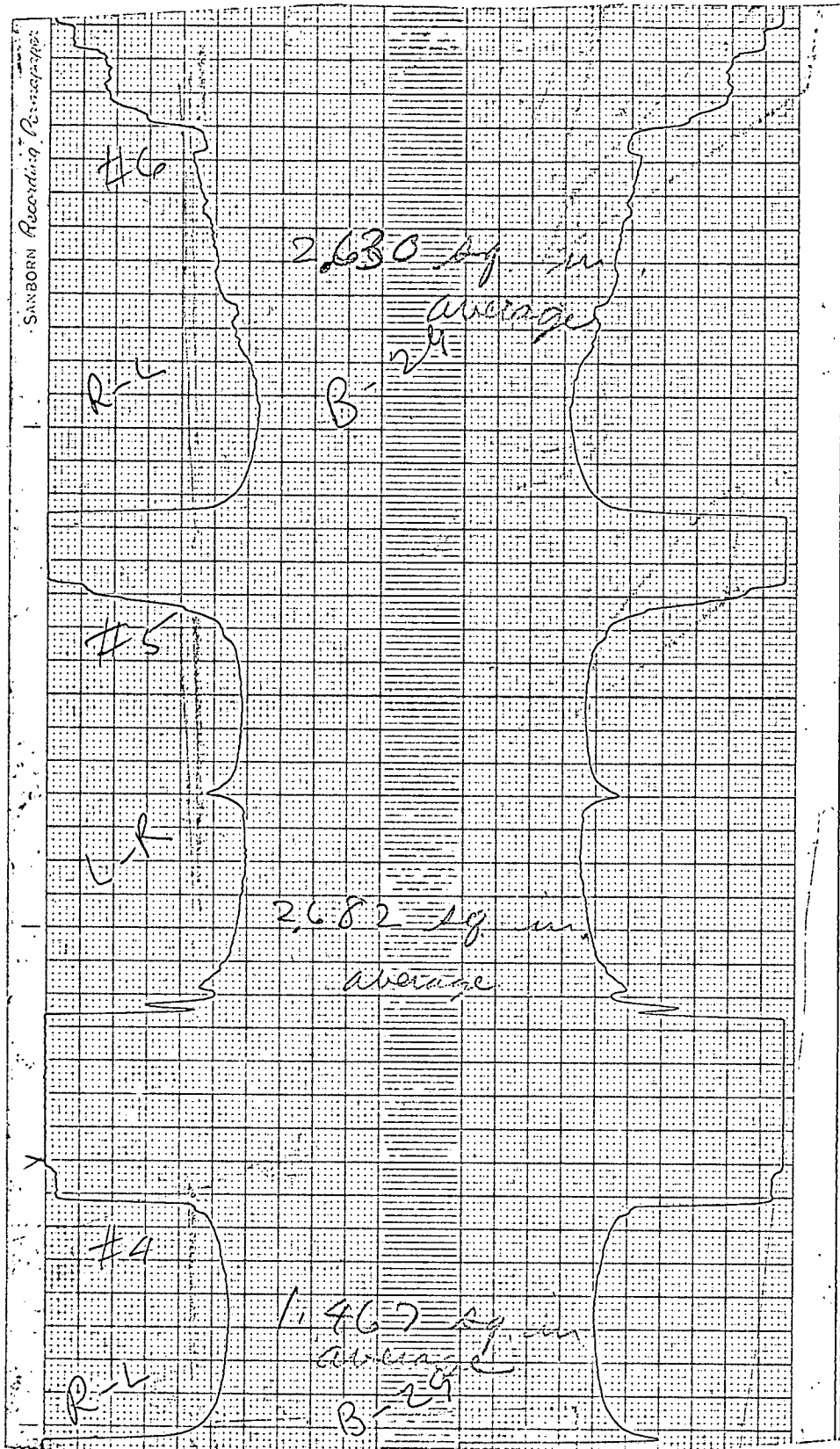


Figure 3.13

that it would be advisable to have a reflector behind the antenna to eliminate the effects of interference behind the antenna. Implementation of these recommendations is described in the following sections.

#### 4. DB-CELL TESTS

##### 4.1 DB-CELL DEVELOPMENT

Concurrent with the microwave experimentation both in the lab and in the field on B-Cells and diodes and their combination, work was performed in the Electro-Chemical Laboratory to develop a cell of somewhat less sensitivity than the B-Cell but with lower resistance and more stable behavior. These experiments resulted in the cell which is designated the DB-Cell. D is for the envelope size and shape, and B is to indicate the high sensitivity of the B-Cells.

The construction and preparation of the B-Cells is described in the final report of Phase I of the Elfin program. These cells used three mil platinum electrodes which were rather fragile. The DB-Cell, on the other hand, uses ten mil platinum electrodes which are clipped short near the glass base bonding the electrodes into the cell. The electrode area is consequently not so small as for the B-Cells and the sensitivity is therefore somewhat less. However, the cell does have a lower resistance and higher internal capacitance. This internal capacitance aids the integration of narrow pulses from a microwave source.

The DB-Cell has three electrodes which extend from the bottom of the cell in contrast to the two electrodes of the B-Cell which extend in opposite directions. The construction of the DB-Cell allows it to be mounted on a standard TO-5 transistor header, sealed and encapsulated to provide better handling capability in the field.

Improvements in electrolytes and cleaning techniques also resulted from the laboratory work. The DB-Cells which were finally used in successful field tests contained an electrolyte of silversulfate dissolved in sulfuric acid. This electrolyte in addition to having low resistance and a high degree of reproducibility also has the advantage of having a very low freezing point which will allow operation in very cold climates. The freezing point varied from one mixture to another but was generally

in the region of  $-40^{\circ}\text{F}$ .

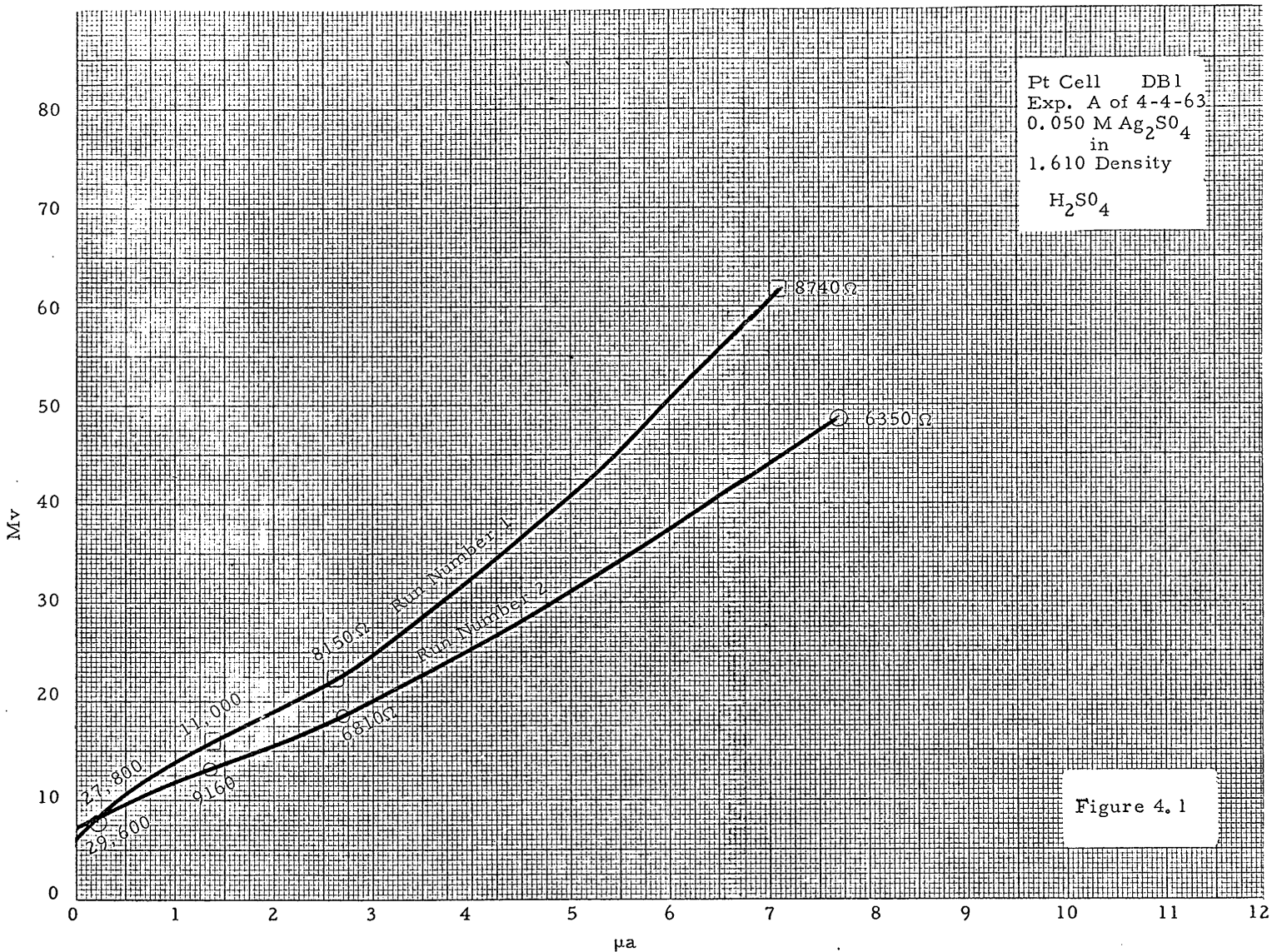
Figure 4.1 illustrates one of the test curves for a DB-Cell using a silversulfate electrolyte. The figure provides a plot of the voltage across the cell as a function of the DC current through the cell. The resulting curves then give an indication of the cell resistance at various operating current levels. These resistances are noted on the graph at various points where they were calculated. It will also be noted that the cell performs reproducibly at voltages less than 10 millivolts across the cell. This factor aids considerably in the integration of small microwave field intensities.

#### 4.2 RF LAB TESTS

Numerous laboratory tests with the DB-Cells were made with a microwave power source radiating in the C-band at approximately 5.6 kilomegacycles. These tests were made on a set-up similar to that described for the diode tests in Section 2. Figure 2.3 is a description of the DB-Cell tests where the load used was either a resistor or a DB-Cell being investigated.

Typical of the results of these tests is the data plotted in Figure 4.2. In this test a Microwave Associates diode 4123A was mounted in front of a copper reflector, a half microfarad capacitor was connected across the leads from the diode to improve the integration of the pulses from the microwave source. One microsecond pulses at a repetition rate of 1000 cycles per second were used in most of the tests. A 10,000 ohm resistor was used in place of the cell for the initial measurements to determine the response of the diode and to provide a reference at the power level being used. The voltage and current through this resistor is shown on the curves marked with the load resistance indicated. The fact that the load resistance varies from 11K to 20K to 110K is result of the fact that the resistance of the microammeter changes on different scales and the load resistance shown is the combined resistance of the load resistor and the internal impedance of the microammeter.





KEUFFEL & ESSER CO. MADE IN U.S.A.  
3 CYCLES X 140 DIVISIONS

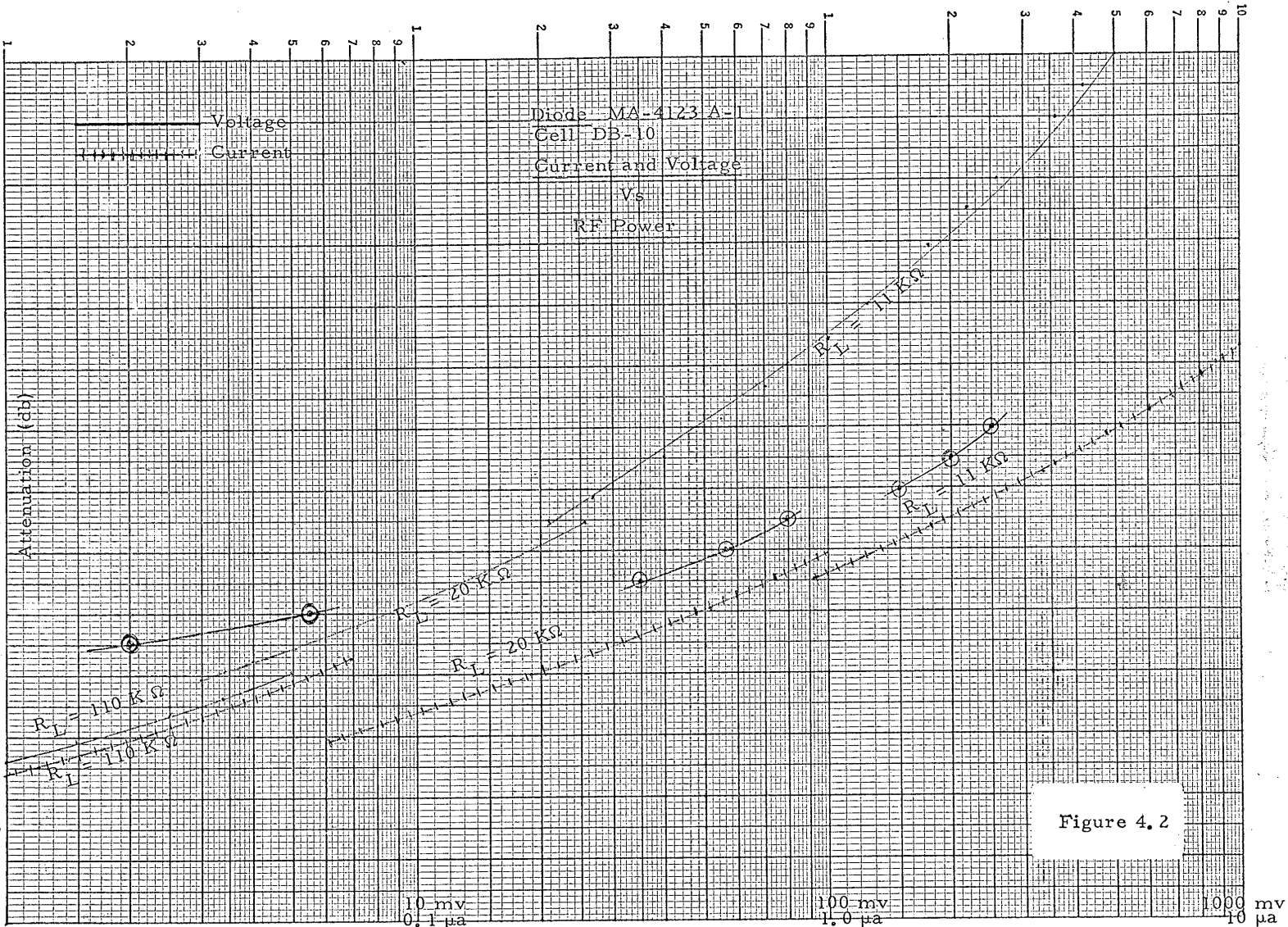


Figure 4.2

The current through the cell is plotted in a set of eight points lying between the current and voltage curves for the load resistance. Results indicate that the cell has an operating resistance in the 1 microampere region of the order of 20,000 ohms. This compares with the diode resistance of approximately 5 to 10,000 ohms in the same current region. Experiments indicated that the cell could integrate nearly as well without the one-half microfarad capacitance being used in parallel as with it. However, since small capacitors of one-half microfarad value were available and did improve somewhat the response of the cell, it was decided to use these in the field tests and in the resulting equipment being delivered.

In addition to the current measuring experiments such as the one described in Figure 4.2, charge integration using the microwave equipment was also investigated and performed satisfactorily and consistent with the laboratory measurements using a DC source rather than microwave generated pulses.

Laboratory tests were also performed to determine whether or not varying the antenna size could be used to give a reliable indication of the radiating frequency. It was not expected that very good results would be obtained in such laboratory tests because of the near field effects and the scattering and interference effects of the various objects in the laboratory. That is to say, a good test range was not available for these laboratory tests. However, the results were nevertheless encouraging and evidence was developed that showed some indication of source field frequency could be obtained by comparing measurements with antennas resonant to different wavelengths.

One such set of data is shown in Figure 4.3 where antennas of length 2.8 cm., 4 cm., 5 cm., and 6 cm., were utilized and a plot of readback time at 1 microampere versus exposure time to the source in minutes was made for the different antennas. The source was the same C-band Klystron used in other tests having a frequency of 5.6 kilomegacycles. The resonant antenna length for this frequency would be approximately 2.8 cm. for a half wavelength dipole. The

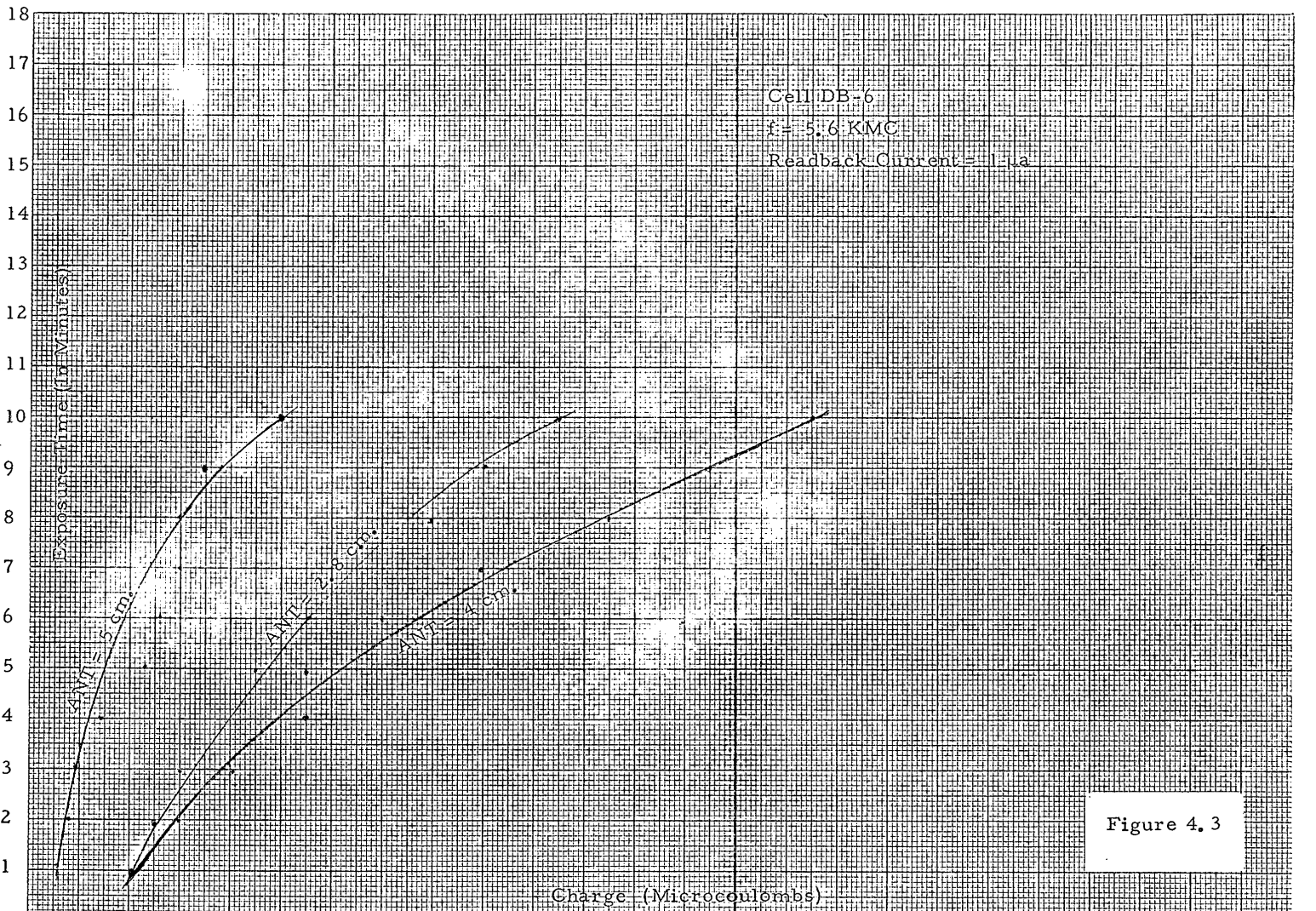


Figure 4.3

results of Figure 4.3 indicate, however, that the 4 cm. antenna length provided somewhat better response than that at 2.8 cm. However, the 5 cm. wavelength is reduced considerably in sensitivity. The measurements with the 6 cm. antenna were very erratic resulting in considerable scatter in the data suggesting sharp interference patterns with the radiating horn. As will be indicated, the field test measurements, where no interference effects are possible, provided much more consistent data and data more readily interpreted.

The results of these various laboratory experiments indicated that the DB-Cells in combination with diodes did provide a sensitivity which was sufficient to yield results in our field tests against the airport radar. These field tests will be described in the following section.

#### 4.3 DB-CELL MICROWAVE FIELD TESTS

Prior to performing the field tests with the DB-Cells it was decided to construct portable equipment which could be taken into the field to allow on-site measurements of the accumulated charge in the E-Cell. This equipment consists of two items described in more detail in Section 5 below. The first of these items is a battery-operated microammeter which provides a full-scale indication of current as low as 100th of a microampere (one-hundredth of a microampere). The scales most commonly used, however, were 1/10 microampere and 1 microampere full scale. The second item is a battery-powered constant source with currents generated at 1/10 microampere, 1 microampere and 10 microamperes. Various switching mechanisms are provided with the source for reversing the direction of current, for adding a capacitor in parallel with the cell, and switches for connecting the cell to an antenna diode combination or to the constant current source for readout. Both instruments were checked repeatedly in the laboratory and used for some of the laboratory measurements described in earlier sections.

The field tests were performed at the site described above in Section 3.3, and were conducted in the following manner. A range

from the radar antenna was chosen and the distance measured off with a one-hundred foot tape to provide an accuracy of sight location of approximately a few feet error. Measurements were taken primarily at distances of 200 feet and 1000 feet from the radar antenna. Measurements taken at intermediate points checked well with the measurements at these two locations. Ranges beyond 1000 feet were not practical because of the terrain and difficulties in estimating the distances properly. The results obtained at a 1000 feet with the radar of 290 watts average power indicate that distances out to 5000 feet would be perfectly practical with radars of somewhat higher average power. Furthermore, estimates of the field strength from the DC current microwave measurements and comparison with laboratory measurements indicate that (as would be expected from antenna beam pattern) our measurements were below the maximum of the main beam by a factor of 10 in power. The use of the equipment on a hill which is swept by the main beam would provide even greater average currents than those obtained.

Once a site had been established and its range to the antenna measured, a non-metallic table was set up and equipment placed on it. A diode antenna placed in front of a reflecting plate was erected on top of the switching box which contained the constant current source. The cell was plugged into a TO-5 socket on the switching box and connections were made to the microammeter.

Prior to integration with the microwave antenna, current would be passed through the cell first in one direction and then in the other, several times, to insure that the cell was in proper working order and to insure that the appropriate electrode was bare of silver.

The switch containing the capacitor circuit would then be closed in order that a 1/2 microfarad capacitance would be connected in parallel across the cell. The cell would be disconnected from the constant current source and connected to the diode antenna with proper polarity. A switch would be thrown closing the circuit at the same time a hand-held stopwatch is started. The diode antenna and reflector



plate had been pointed toward the radar antenna visually in order to give the maximum current through the diode and cell.

At the end of the prescribed integration time which would be of the order of one to five minutes, the switch would be thrown opening the circuit. The cell would then be switched over to the constant current source and the stopwatch rezeroed. When the switch was closed, closing this circuit with the polarity such that the cell would be depleted of the charge accumulated during the integration of the microwave produced currents, the stopwatch would be started and the microammeter would be watched to be sure that a constant current of  $1/10$  microampere or 1 microampere flowed through the cell.

Near the end of the depleting cycle the pointer of the microammeter would begin to drop below the constant current value. When it passed half scale, the stopwatch would be stopped and the time interval noted. The charge accumulated by the cell would then be recorded as the product of the time interval of the stopwatch and the value of constant current through the cell. The cell would then be reconnected to the diode antenna and a new exposure made with the same or somewhat different exposure time.

In general, it is found that the accumulated charge is linearly proportional to the exposure time as would be expected. However, for very short exposures of thirty seconds or less, the rotational rate of the antenna (once every 12 seconds) would introduce scatter in the data if a proportionate number of rotations were not included in the time interval.

Figure 4.4. is a graph of results typical of this kind of field test but in which several different antenna lengths were used. This particular data shows the results for four antennas varying in length from 4 cm. to 7 cm.; the 6 cm. antenna providing the largest average current through the cell.

It will be noticed that the extrapolated lines do not pass through the origin of the graph and apparently yield a finite charge through the

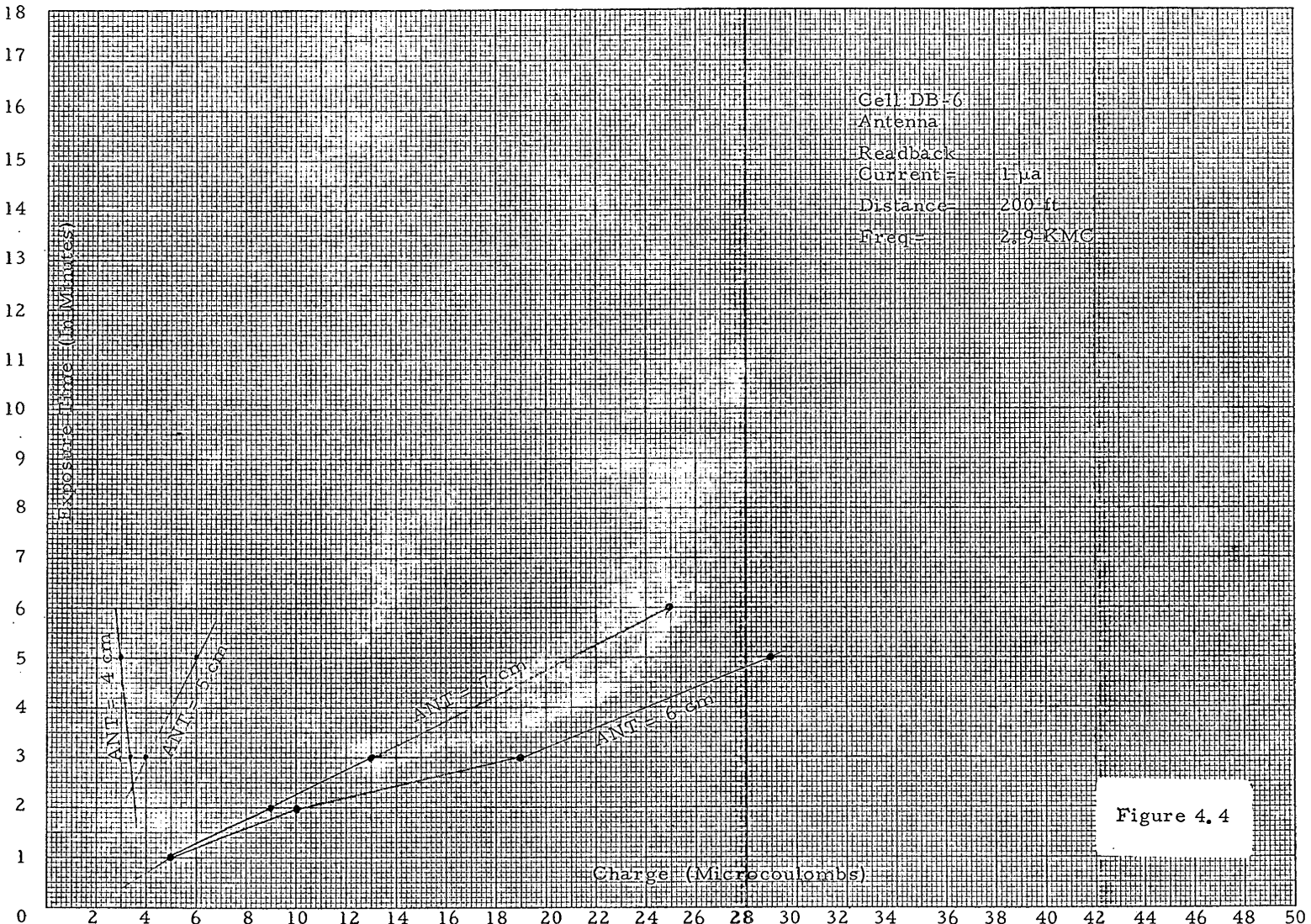


Figure 4.4



cell with zero exposure time. This is due primarily to the capacitance effect of the cell and the parallel capacitor across the cell. With no silver on the anode of the cell, current will still surge through the circuit due to the charging of the parallel capacitances. This effect varies from one cell to another and represents a zero point error in the system technique.

The range at which the data of Figure 4.4 was taken is 200 feet, however, equally reproducible data was obtained out to greater distances as we will see in the next figure. Since the radar frequency is 2900 megacycles, one would expect that the 5 cm. antenna would generate larger currents than the 6 or 7 cm., because of its resonance. However, the use of a reflecting plate and the thin wire of the diode leads which were used as the antenna members will distort somewhat the expected resonant length. This would account for the fact that the antenna of 6 cm. length was apparently more nearly resonant than the 5 cm. antenna. The results of this experiment indicate that a set of antennas of varying length, when properly calibrated against sources of different frequency, will yield a fair indication of the source frequency being measured. The results of Figure 4.4 suggest that frequency could be determined to approximately 10 or 20% with little difficulty.

Figure 4.5 indicates the kind of result which can be obtained at 1000 feet from the 290 watt radar. The data is very consistent within the accuracy of measurement of the time interval over a range of exposure times from 6 minutes down to 10 or 15 seconds. Most of the data was taken by deplating the cell at a constant current of 1 microampere. However, for the very short exposure times when a very small charge was accumulated, greater accuracy was obtained by using a 1/10 microampere deplating current which allowed longer time intervals for the same accumulated charge.

It should be noted that a 15 second exposure encompasses only one sweep of the radar beam and this accumulated charge was readily measured at the range of 1000 feet with an entirely passive system. The results of these experiments indicate that the equipment as

K<sup>o</sup>Σ KLUFFEL & ESSER CO. MADE IN U.S.A.

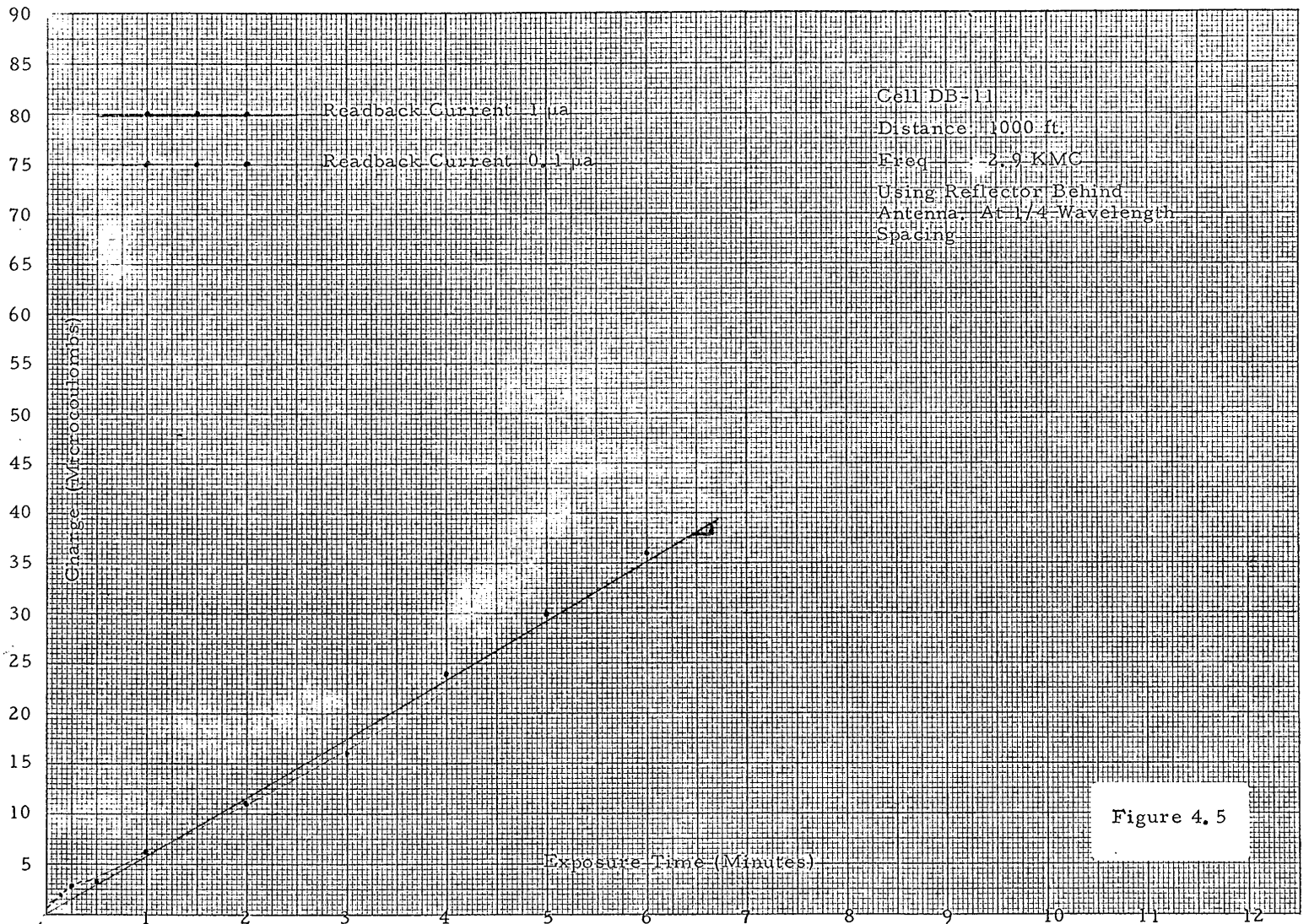


Figure 4.5

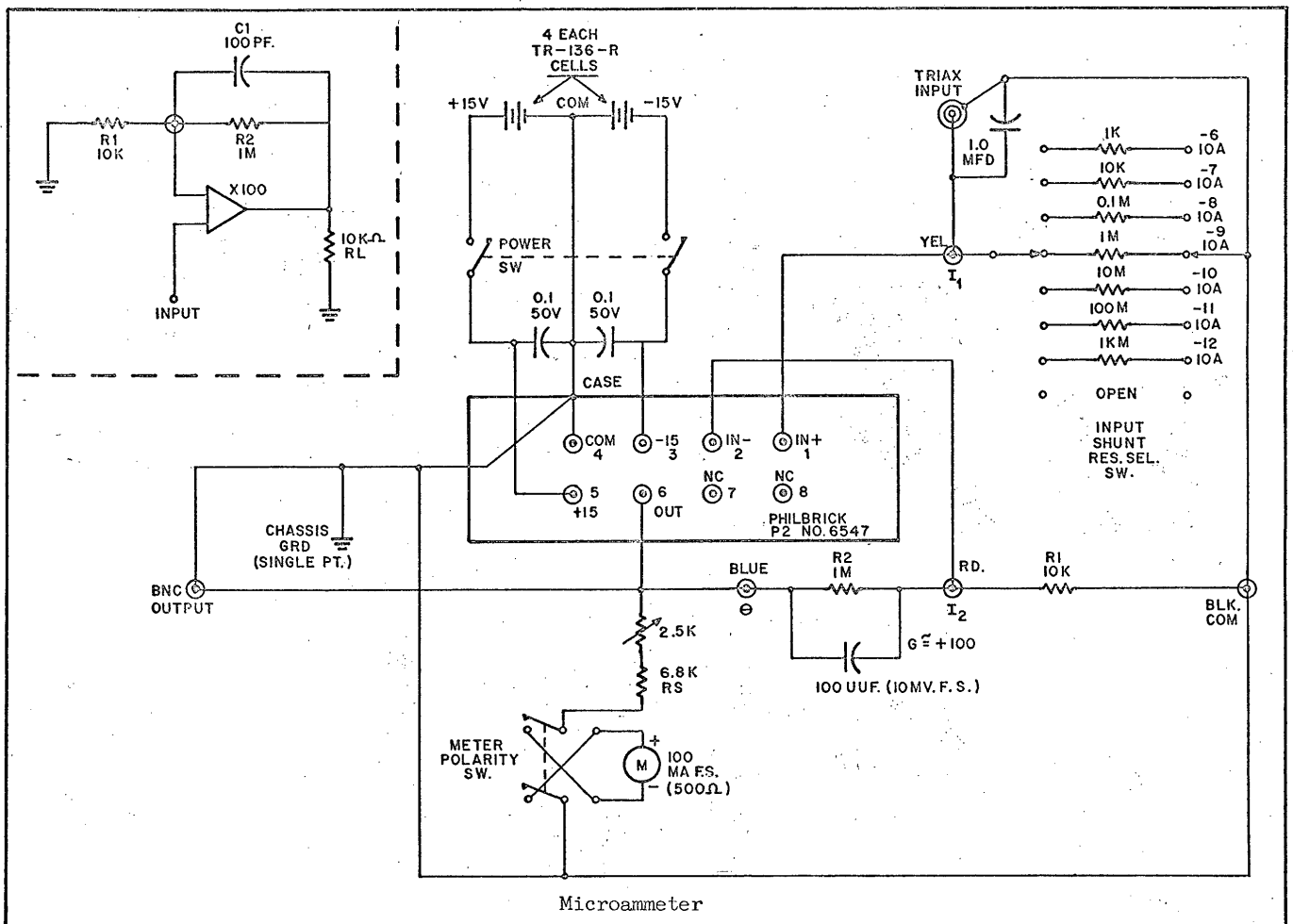
designed can meet the original requirements of making passive measurements of radar power and frequency at ranges from 1000 feet to 5000 feet. In addition to the cell-antenna-diode combination, very little equipment is required. Only a small microammeter, a constant current source, and a stopwatch is necessary to read the accumulated charge in the cell.

## 5. EQUIPMENT OPERATION

The final equipment consists of three different items-- one a microammeter, two a constant current source and switching network, and three the diode-antenna-cell combination package. The use of each of these equipments will be described below.

The microammeter is a battery operated device with capability of measuring currents below  $10^{-8}$  amperes. The front face of the instrument contains three switches, an input and output jack, and a dial for indicating current. There is also an opening in the front face which allows access to a trimming potentiometer for zeroing and calibration. One switch is simply the battery switch which turns the circuit on and off. Another switch reverses the meter polarity. The third switch is a multiple position switch which can change the scales from one current range to another by factors of ten. The instrument presently indicates scales of  $1 \mu\text{a}$ ,  $1/10 \mu\text{a}$ , and  $1/100 \mu\text{a}$ , however, a change has been made through the internal circuit so that each of these scales should be increased by a factor of ten as the circuit is presently constituted. When in doubt about the scale ranges of the microammeter it can be checked against the constant current source, the operation of which is indicated below. The input jack provides the connection for the current to be measured and the output jack is the output of the DC amplifier which constitutes the principle circuit of the microammeter. This allows external monitoring of the current through the microammeter.

The circuit of the device is shown in Figure 5.1 and it will be found that the input impedance of the microammeter is 1000 ohms on the  $1 \mu\text{a}$  scale. The instrument is powered by four Mercury cells type TR-136-R. The device should be checked periodically against the constant current source to be sure that the batteries in both the microammeter and current source are working properly. The principle component of the microammeter is a Philbrick No. 6547 DC amplifier which is a solid state device of high reliability. The output meter is simply a standard 100 microampere full-scale meter



which will read both positive and negative currents, zero being indicated at the center of the scale.

Prior to using the instrument, the input connection should be shorted and the zero on the instrument adjusted after sufficient time for the instrument to achieve equilibrium has been allowed. This zero adjustment is made through the top of the case through the appropriate aperture with a small screwdriver, preferably non-metallic. Once the instrument is zeroed its calibration can be checked against a standard current source. In field operation the output jack is never used and the current is read directly from the meter face.

The second item is the constant current source which contains a TO5 transistor socket into which the cell is mounted. There is an on-off switch for controlling the current from the internal battery, a switch marked left-right and right-left which indicates the direction of current through the cell mounted in the transistor socket. The center electrode of the cell is not activated in this circuit when it is plugged into the socket in a proper fashion. When the switch is in the left-right position it indicates that the left electrode of the cell is positive and the right is negative so that silver, therefore, moves through the cell from the left to the right electrode. The right electrode is that electrode nearest the little metal tab which radiates from the base of the transistor header. There are three toggle switches mounted on the face of the instrument, one which is a shorting switch for the purpose of zeroing the microammeter, another is a switch marked DC and Pulses which when in the pulse position adds a half microfarad capacitor in parallel across the cell terminals. The third toggle switch is marked Readback / RF and determines whether the box is being used as a constant current source in the Readback position for the deplating of the cell or used in the RF position to connect the cell across a diode externally connected to the red and black wires extending from the instrument. The switch labelled Z-function

provides three values of constant current which are set by the voltage of the Mercury cells inside the instrument and large calibrated resistors in series with the cell. A jack is provided for connection to the microammeter so that the current through the cell can be monitored. When the microammeter is not connected it is necessary to have the toggle above this jack in the short position to provide a complete DC path through the cell. The circuit for the field test unit is shown in Figure 5.2.

In using the field test unit and microammeter to check the operation of a cell in the field the following procedure is used. The cell is plugged in to the socket and the switch is thrown to the Readback position; the microammeter is connected and the shorting switch on the test unit is thrown. The power switches are turned on and the microammeter is zeroed. The constant current source is turned on and the Z-function switch is set to the appropriate scale for the microammeter. The left-right and right-left switches are thrown to check the constant current through the microammeter for calibration purposes. The shorting switch is then opened and it is noted whether or not current flows through the cell. The polarity is then reversed and it is again noted whether or not the current is flowing through the cell. Once it has been determined that one electrode, either the left or right, is bare and there is silver on the other electrode in sufficient amount to perform a test, this silver is transferred to that electrode which will be connected in the right polarity to the diode for transfer to the bare electrode.

If pulses are to be integrated the appropriate switch is thrown. The shorting switch is closed and the internal readback power is opened. The cell and diode are now ready to integrate microwave current. This is initiated by throwing the readback switch to RF for an appropriate time interval. At the end of that time interval the switch is replaced to the readback position and the shorting switch is opened connecting the microammeter in series with the cell. The polarity switch is put in the proper position for replating

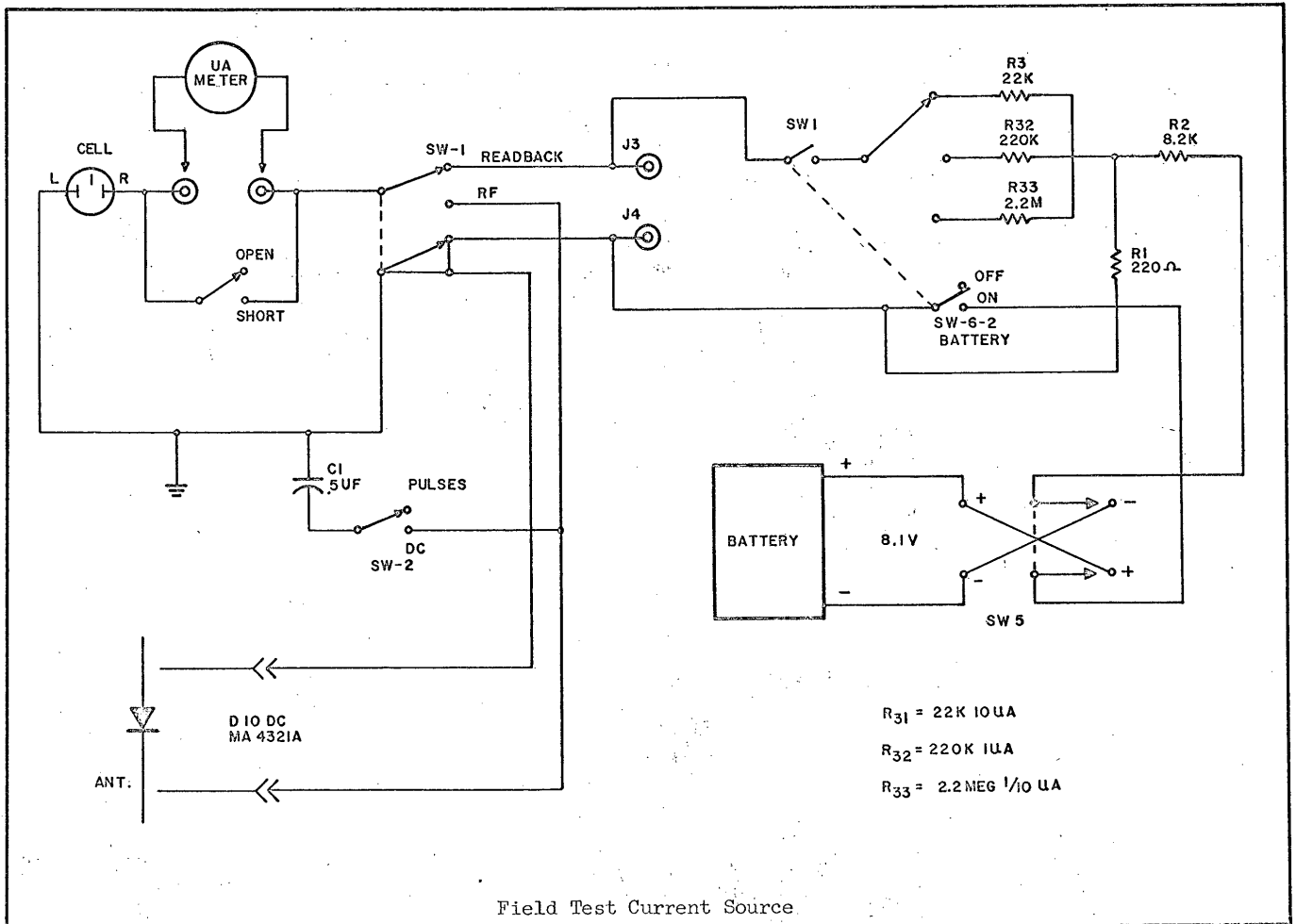


Figure 5.2



of the silver that had been plated during the RF operation and the scales of both instruments are set to their proper value. The power is turned on for the internal readback current source and the time is noted on the microammeter for the cell to be depleted. When this has been accomplished the power on the constant current source is turned off, the shorting switch is thrown, and the cell is ready to perform a new integration when the readback switch is thrown to the RF position.

The third item is the portable field integrating device which allows field measurements without use of the field test unit described above. These packages each consist of two antenna diodes cut to be resonant at different frequencies, two sockets which hold DB integrating cells and a socket which holds a Mercury switch. Tiny capacitors of 0.47 microfarads are also connected in the circuit to aid pulse integration. The diodes are mounted approximately one-quarter wavelength from the base plate provided this distance doesn't exceed the maximum dimensions set for the device.

An examination of the device will indicate that the circuit is connected in such a manner that the cells do not integrate in one position when the Mercury switch is open and they both integrate when the device is inverted 180° so that the Mercury switch is closed. A slight tapping of the device when the orientation is changed may be necessary to release the Mercury from one position to another. The device is used operationally as follows. E-Cells which have been plated with the silver on the proper electrode and the other outer electrode bare are plugged in to the device while it is in the inverted position with the mercury switch open. The device is then carried to the sight location where measurement is to be made. At that point it is re-inverted and tapped to close the Mercury switch. At the end of the proper time interval it is inverted again and tapped so that the Mercury switch opens. The device is then brought back to the field test unit in the proper orientation. The cells are then unplugged and inserted in the field test unit, depleted at the constant

0.68 mJ  
?

current, and the time interval for deplating noted. Reference to calibration charts for that cell-antenna-diode combination provides and indication of the microwave field intensity. Such calibration charts have not at present been prepared because of the lack of a suitable test range over which the microwave field strength is known. Some indication can be obtained, however, by comparing the results with those given in the figures of Section 4.

## 6. CONCLUSIONS

The high sensitivity B-Cell developed under phase one of the program did not prove satisfactory for field integration of pulsed radars because of the high internal resistance associated with the small electrodes of the B-Cells, the poor integration of pulses due to the small inter-electrode capacitance, and the erratic behavior of the cells due primarily to the use of the silver nitrate electrolyte. Variations with the B-Cell were experimented with until a design evolved called the DB-Cell which used somewhat larger electrodes and a silver sulfate, sulfuric acid electrolyte. This cell provided the lower internal resistance, the higher integrating capacitance, and the reliability that was required for a successful field integration unit. In addition the electrolyte provided a low temperature operation which was not available with the B-Cell developed previously.

Laboratory and field tests indicated that the DB-Cells in conjunction with diodes which served as antennas by trimming their leads to the proper length provided reproducible integration of very low microwave field intensities. In particular, field intensity measurements out to 1000 feet from a radar of 290 watts average power were reproducible to a few percent. Extrapolation of these results indicate that measurements out to 5000 feet against radars of one or more kilowatts average power can be readily made.

Experiments using antennas resonant to different frequencies indicate that the frequency of the radiating source can be determined to approximately ten or twenty percent accuracy when the integrated results from the different antennas are compared.

Several Elfin devices were constructed which contain antennas and cells in pairs and are activated by the opening and closing of the Mercury switch. The switch closing can be implemented by inverting the device and opened by re-inversion so that no mechanical switches are necessary. Simple readout equipment has been developed using a small battery operated constant current source

*Mercury  
restoration  
line*

and a battery operated microammeter.

The devices constructed and tested including the readout equipment are primarily of a laboratory and field experimental nature. Once the equipment has been evaluated and it is decided that the concept is worth continuing what remains to be done is to build rugged operational equipment which can be taken directly in to the field and used with a high degree of reliability.

Recent experiments in the company supported cell development program indicate that even greater cell sensitivity can be obtained with the DB-Cells than was reported in the tests under this program. Work is continuing in cell development for this application and related applications. Greater reliability and sensitivity in the use of E-Cells for the application described in this report can be expected in future programs as a result of the development effort. Discussion of more sophisticated forms of Elfin devices to provide better frequency coverage and estimates of other microwave field parameters are being conducted.

THE RELATION OF ELECTRO-CHEMICAL  
PRINCIPLES TO SELECTED EXPERIMENTS

## I.

## DEFINITION OF TERMS AND SYMBOLS

$E$  = emf of cell when acting as a galvanic cell. It is a back emf opposing the applied emf  $E_a$ .  $E$  is often called the emf of polarization. It is a variable depending on the electrolyte, nature of the electrodes, electro-chemical reactions, current density, over-voltage at each electrode, standard emf  $E^{\circ}$  of each electro-chemical reaction, temperature, and other factors. (Reference 1, pp. 647-674).

$i$  = Current through cell.

The above three variables are related by the following equation.

$$E_a - E = i R_c \quad (1)$$

where

$R_c$  = resistance of electrolyte between the two electrodes and is a constant for a given cell at a given temperature and pressure.

$E_o$  = emf across cell at cut-off point of current-time curve when the current  $i$  is zero. It is also the open circuit voltage.

$a_{Ag^+}$  = activity of silver ions

$a_{H^+}$  = activity of hydrogen ions

$a_{SO_4}^-$  = activity of sulfate ions

$(Ag^+)$  = concentration of silver ions in gm-ion weights per liter of solution

$(H^+)$  = concentration of hydrogen ions in gm-ion weights per liter of solution

$(\text{So}_4^{=})$  = concentration of sulfate ions in gm-ion weights per liter of solution

$(\text{HSO}_4^{-})$  = concentration of bisulfate ions in gm-ion weights per liter of solution

$a_{an}$  = activity of silver ions adjacent to anode during flow of current

$a_{ca}$  = activity of silver ions adjacent to cathode during flow of current

$a$  = activity of silver ions in main body of electrolyte

$P$  = partial pressure of oxygen in the air above the electrolyte and in the electrolyte in atmospheres

$c. d.$  = current density

$E_x$  = equilibrium emf of "x" electrode

$E_y$  = equilibrium emf of "y" electrode

$\pi_x$  = equilibrium potential of "x" electrode

$\pi_y$  = equilibrium potential of "y" electrode

$w_x$  = over-voltage at "x" electrode

$w_y$  = over-voltage at "y" electrode

In general, x may indicate the anode, right electrode or reaction occurring at the anode and y the cathode, left electrode or reaction occurring at the cathode.

$R$  = the gas constant = 8.314 joules degree<sup>-1</sup> mole<sup>-1</sup>

$F$  = the Faraday = 96,489 coulombs

$T$  = the absolute temperature in degrees Kelvin

$E^\circ$  = standard electrode emf

$\pi^\circ$  = standard electrode potential

$E$  =  $-\pi$  (Reference 1, p. 600)

$E^\circ$  =  $-\pi^\circ$  (Reference 1, p. 600)

$$E = (E_y + w_y) - (E_x + w_x) \quad (2)$$

$$E = (\pi_x - w_x) - (\pi_y - w_y) \quad (3)$$

The "potential" of an electrode is defined as the potential of the electrode minus the potential of the solution adjacent to the electrode (Reference 1, p. 600).

## II

LOSS IN AREAS IN CURRENT-TIME CURVES DURING  
TRANSFER OF SILVER BETWEEN ELECTRODES

In the following, the conditions in the two cases are considered, viz., (1) when the Pt-to-glass seals are perfect, and (2) when the Pt-to-glass seals are defective, i. e., when crevices exist between the Pt and the glass in the seal. From experimental evidence and theoretical considerations, these two cases will be considered in the following hypothesis.

A. Perfect Pt-to-Glass Seals for Each Electrode

This condition may exist either because the Pt-to-glass seal was originally perfect or because the crevices were completely filled in by gold plating.

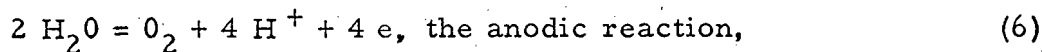
At cut-off the back emf is given by the following equation:

$$E = (\pi_{O_2} - w_{O_2}) - (\pi_{Ag} - w_{Ag}) \quad (4)$$

where

$$\pi_{O_2} = \pi_{O_2}^{\circ} + \frac{RT}{4F} \ln(P \times a_{H^+}^4) \quad (5)$$

for



$$\text{and } \pi_{Ag} = \pi_{Ag}^{\circ} + \frac{RT}{F} \ln a_{Ag^+} \quad (7)$$

$$\text{for } Ag = Ag^+ + e, \text{ the cathodic reaction.} \quad (8)$$

For 0.10 N AgNO<sub>3</sub>, saturated with air, pH = 6.7 and at 25° C.



$$\pi_{an} = \pi_{o_2} \cong 0.82 \text{ volt}$$

and  $\pi_{ca} = \pi_{Ag} \cong 0.73 \text{ volt by calculation. (Reference 2, p. A19)}$

$$w_{o_2} \cong -0.45 \text{ volt over-voltage on smooth Pt, (Reference 1, p. 659)}$$

$$w_{Ag} \cong 0 \text{ (Reference 3, p. 444)}$$

$$E \cong (0.82 + 0.45) - (0.73 + 0)$$

$$E \cong 1.27 - 0.73 = 0.54 \text{ volt}$$

It is to be emphasized that the above equations describe the conditions at cut-off only. *(when H<sup>2</sup> reaction begins)*

The value of  $\pi_{o_2}$  may vary somewhat due to the variable local concentration or pressure of dissolved or absorbed oxygen at the anode. This accounts for the fact that E and E<sub>a</sub> may be greater than 0.54 volt in some instances.

#### B. Defective Pt-to-Glass Seals for One or Both Electrodes

This condition may exist because of the fact that the Pt-to-glass seals were originally imperfect. When the electrodes are gold-plated the crevices may not be fully filled up with gold plating, thus accounting for seals which are still defective.

Before cut-off when silver is being transferred from anode to cathode, the back emf is given by the following equations:

$$E = (\pi_{an} - w_{an}) - (\pi_{ca} - w_{ca}) \quad (9)$$

where

$$\pi_{an} = \pi_{Ag}^{\circ} + \frac{RT}{F} \ln a_{an} \quad (10)$$

$$\pi_{ca} = \pi_{Ag}^o + \frac{RT}{F} \ln a_{ca}. \quad (11)$$

$a_{an}$  = activity of silver ions adjacent to the main anode surface

and

$a_{ca}$  = activity of silver ions adjacent to the cathode.

$w_{an}$  and  $w_{ca}$  are approximately zero (Reference 3, pp. 444 and 447).

At this stage silver is being plated on to the entire Pt cathode inside and outside the crevices from the Pt anode which had previously been plated with silver in the prior run.

During cut-off the value of  $\pi_{ca}$  remains the same as before but the value of  $\pi_{an}$  (and consequently of E) increases because of the following considerations:

Before cut-off the value of  $\pi_{an}$  is determined by  $a_{an}$ , the silver ion activity in the region adjacent to the Pt anode outside the crevices. At cut-off, however, the Pt anode outside the crevices becomes completely depleted and silver ions start to deplete from the crevice anode surface and to migrate away. As the opportunity of these ions to migrate away is considerably less (because of the blocking effect of the walls of the crevices) than that of the ions in the open areas around the Pt anode before cut-off, their concentration (and activity) build up to a considerably higher value than  $a_{an}$ .

Letting  $a_{cr}$  = activity of silver ions in crevices

and  $\pi_{cr}$  = electrode potential determined by these ions,

$$\pi_{cr} = \pi_{Ag}^o + \frac{RT}{F} \ln a_{cr}, \text{ anode potential after cut-off, (12)}$$

and  $\pi_{an} = \pi_{Ag}^o + \frac{RT}{F} \ln a_{an}$ , anode potential before cut-off. (13)

$$\text{As } a_{\text{cr}} \gg a_{\text{an}},$$

$$\pi_{\text{cr}} \gg \pi_{\text{an}}.$$

When the crevices are not large,  $a_{\text{cr}}$  is sufficiently large so that

$$\pi_{\text{cr}} = \pi_{\text{Ag}}^{\circ} + \frac{RT}{F} \ln a_{\text{cr}} = \pi_{\text{O}_2}^{\circ} + \frac{RT}{4F} \ln (P \times a_{\text{H}^+}^4). \quad (14)$$

As the second expression is the potential of the normal anode reaction at cut-off, it is then seen that  $E$  has the same value here as in A when the cell has perfect Pt-to-glass seals and that  $E_a = E$  and the current is zero. Because of the zero current, the initial deplating of the crevice anode surface during the time the current decreases to zero, therefore, ceases. It is thus seen that silver gradually accumulates in the crevices in each successive run. This, then, is an explanation for the gradual progressive decrease in areas of the current-time curves.

Exp. F of June 3, 1963, B31 (gold-plated), Example 13.

Exp. B of April 4, 1963, DB1, Example 16; and Exp. C of June 3, 1963, DB 22 (gold-plated), Example 24, are illustrations of cells with good original seals or with good seals after being gold-plated.

When, however, the crevices are larger,  $a_{\text{cr}}$  is less and

$$\pi_{\text{cr}} < \pi_{\text{O}_2},$$

$$E < E_a$$

$$i > 0 \text{ (at cut-off)}$$

and the normal anode potential  $\pi_{\text{O}_2}$  due to the reaction



is not quite attained.

Exp. E of June 3, 1963, Parts II and III, for cell DB 24, Example 26, Charts 47 and 48 is a good illustration of a defective Pt-to-glass seal of the right electrode which even gold-plating did not fill up. Note the residual currents trailing the R → L runs (no. 8 of Part II and no. 4, and no. 6 of Part III). In contrast it is seen that there is no residual current at the end of any L → R run. There is also a progressive decrease in areas of these curves which is consistent with the theory set forth in this section.

An explanation is in order regarding the cause for the improvement in area tests for DB4 with use, Charts 34-36, (Exps. C of April 10, 1963, D of April 11, 1963, G of April 11, 1963, C of April 15, 1963 and G of May 9, 1963). Sanborn charts are reproduced only for the first and final experiments, Examples 21 and 22, in the above series. In all these experiments the cell contained 0.025 M  $\text{Ag}_2\text{SO}_4$  in 1.520  $\text{H}_2\text{SO}_4$ . In the first experiment there is a small decrease in area when plating silver back and forth between left and right electrodes (Chart 34); while in the final experiment constant areas are obtained as seen from Charts 35 and 36. Considering that  $a_{cr} \gg a_{an}$ , there is a possibility for  $\text{Ag}_2\text{SO}_4$  and/or  $\text{AgHSO}_4$  to precipitate in the anode crevices. While only very small amounts may form during or just prior to cut-off in each run, after a great many runs sufficient silver salts may accumulate to completely fill up the crevices, thereby, preventing silver to plate in this area in all subsequent runs. This, of course, will result in constant areas. It still remains to be explained why the  $\text{Ag}_2\text{SO}_4$  and/or  $\text{AgHSO}_4$  do not gradually dissolve out of the crevices when the cell is not in operation. About all that can be said at present is that either the re-solution of the precipitated silver salts is a very slow process or that, after precipitation in the crevices, the silver salts may slowly change to another allotropic form which is very insoluble in the sulfuric acid electrolyte. Considering that at the

anode and particularly in the crevice region ( $\text{SO}_4^{=}$ ) and ( $\text{H SO}_4^{=}$ ) as well as ( $\text{Ag}^+$ ) are larger than in the main electrolyte, it is seen that the solubility products ( $\text{Ag}^+$ )<sup>2</sup> ( $\text{SO}_4^{=}$ ) and/or ( $\text{Ag}^+$ ) ( $\text{HSO}_4^-$ ) may be exceeded. No data is given on the solubility of  $\text{Ag HSO}_4$  in References 5 and 6; however, in the latter reference, p. 132, two allotropic forms of silver hydrogen sulfate are listed,  $\alpha$   $\text{Ag HSO}_4$  and  $\beta$   $\text{Ag HSO}_4$ .

If  $\text{Ag HSO}_4$  is appreciably soluble, there is, of course, no solubility product for it but this fact would not prevent its being deposited in the crevices if its concentration exceeded its solubility in this area.

## III

## DIFFUSION CURRENTS

If the applied emf,  $E_a$ , across a cell is gradually increased;  $E$  and  $\pi_{an}$  increase and  $\pi_{ca}$  decreases in the equation.

$$E = (\pi_{an} - w_{an}) - (\pi_{ca} - w_{ca}) \quad (9)$$

where  $w_{an}$  and  $w_{ca}$  are essentially zero (Reference 3, pp. 444 and 447).

It is assumed in the above equation that the only reactions occurring are the dissolution of silver at the anode and its deposition at the cathode. From the equations,

$$\pi_{an} = \pi_{Ag}^o + \frac{RT}{F} \ell n a_{an} \quad (10)$$

and

$$\pi_{ca} = \pi_{Ag}^o + \frac{RT}{F} \ell n a_{ca} \quad (11)$$

(Reference 3, p. 447) it can be seen also that  $a_{an}$  increases and  $a_{ca}$  decreases.

However, as  $E$  continues to increase,  $a_{ca}$  continues to decrease until it finally reaches a constant and negligibly small value compared to the silver ion concentration in the main body of electrolyte. The decrease in the silver ion concentration at the cathode is caused by the fact that their discharge rate at this electrode is greater than the rate at which they are supplied to the cathode surface from the solution. When this small and constant value of  $a_{ca}$  is reached, the corresponding current is defined as the limiting current.

From the equation:

$$\pi_{ca} = \pi_{Ag}^o + \frac{RT}{F} \ell n a_{ca} \quad (11)$$

it is seen that  $\pi_{ca}$  also reaches a minimum and constant value.

Consideration of the equation:

$$E = (\pi_{an} - w_{an}) - (\pi_{ca} - w_{ca}) \quad (9)$$

where

$w_{an}$  and  $w_{ca}$  are practically zero, poses the question of whether or not  $\pi_{an}$  increases when  $E$  increases further. As  $\pi_{an}$  is determined by  $a_{an}$  and as the latter has to remain constant when the current is constant, the only way for  $\pi_{an}$  to increase is by the elimination of the original assumptions on which the above discussion is based, i. e., by the setting in of another reaction at the anode or cathode or both. This is, in fact, what occurs with further increases in  $E_a$  and of  $E$ . The current then begins to increase with the initiation of new anodic and/or cathodic reactions. In the operation of the cells, however, it is imperative never to increase  $E_a$  (with the resultant increase in  $E$ ) to the point where other reactions set in, e. g., the discharge of  $H^+$  at the cathode to produce  $H_2$ .

Turning our attention now to the factors which determine the rate at which silver ions are supplied to the cathode surface, it is known that these ions reach the cathode, in general, under the influence of two forces, (1) a diffusive force, and (2) an electrical force. (Reference 4, p. 18). The diffusive force is proportional to the concentration gradient existing at the cathode surface. The electrical force is proportional to the electrical potential difference between the cathode surface and solution. In the most general case the limiting current is the sum of the "diffusion" current and the "migration" current. The former is caused by the diffusive force and the latter by the electrical force. When the cell contains silver nitrate or silver sulfate only, both forces are operative at the limiting current but when the cell contains in addition to one of these an "inert" constituent as potassium nitrate or sulfuric acid, respectively, in sufficient amount the electrical force and the resultant migration current become small in comparison to the diffusive force and the resultant diffusion current (Reference 4, p. 18). In the latter cases, i. e., with  $AgNO_3 + KNO_3$  or  $Ag_2SO_4 + H_2SO_4$  in the cell, the limiting current is approximately equal to the diffusion current.

Considering that the silver ions in this latter case are supplied to the cathode mainly by the diffusive force, it is important to consider the diffusion process. The direction of their diffusion is from regions of higher to lower concentration, i. e., toward the cathode. The rate of diffusion is dependent on the concentration gradient and also on certain properties of the ions and solvent, e. g., the viscosity of the solvent. When the limiting current is reached the silver ions are deposited on the cathode as soon as they reach its surface.

In the case of the  $\text{Ag}_2\text{SO}_4 - \text{H}_2\text{SO}_4 - \text{H}_2\text{O}$  electrolytes used in some of our cells, the viscosities are considerably higher than that of 0.10 N  $\text{AgNO}_3$ . From Tables I and II, it is seen that the electrolytes,  $\text{Ag}_2\text{SO}_4$  in 1.520  $\text{H}_2\text{SO}_4$  and in 1.610  $\text{H}_2\text{SO}_4$ , have viscosities over 3.79 centipoise at 20° C. The viscosity of water at 20° C is 1.0050 centipoise (Reference 5, p. 2030). Normally, the addition of acid to an aqueous solution of a silver salt would decrease its resistivity if the concentration of the salt and the viscosity of the solution could be kept constant. In the case of the  $\text{Ag}_2\text{SO}_4 - \text{H}_2\text{SO}_4 - \text{H}_2\text{O}$  electrolytes, however, the viscosity increases with sulfuric acid concentration (Table II) and, as a result, the mobility  $\mu$  of the hydrogen, silver and sulfate ions decreases below the value which would obtain if the viscosity of the solution could have been kept constant. The mobility  $\mu$  of an ion in a given medium is defined as its velocity in cm per second when the potential gradient, in the direction of the velocity, is one volt per cm (Reference 1, pp. 481 and 518). The higher the mobility of an ion, the higher the conductivity, other factors being constant. Whether or not the resistivity of a  $\text{Ag}_2\text{SO}_4 - \text{H}_2\text{SO}_4 - \text{H}_2\text{O}$  electrolyte at constant  $\text{Ag}_2\text{SO}_4$  concentration increases or decreases with increasing percentages of  $\text{H}_2\text{SO}_4$  (starting from zero percent) depends on which factors are predominant, ( $\text{H}^+$ ) and total mobility of all the ions or viscosity at the given  $\text{H}_2\text{SO}_4$  concentration.

In the  $\text{Ag} \rightarrow \text{C}$  charging run shown in Chart 49, Example 27 for DB 29 containing 0.025 M,  $\text{Ag}_2\text{SO}_4$  in 1.520  $\text{H}_2\text{SO}_4$ , it is seen that



the current decreases to an approximately constant value with time. This indicates a rapid decrease in  $\pi_{ca}$  and therefore in  $a_{ca}$  as seen from the equation.

$$E_a - (\pi_{an} - \pi_{ca}) = i R_c \quad (16)$$

where  $E_a$  and  $R_c$  are constant and  $\pi_{an}$  approximately constant. It is, therefore, concluded that the current in this case is a diffusion or near diffusion current. It is apparently mainly caused in this experiment by the high viscosity of 1.520  $H_2SO_4$  which considerably decreases the rate at which silver ions are able to diffuse to the cathode surface at the concentration gradient existing here.

In Example 32, Exp. A of April 4, 1963, for DB1, containing 0.050 M  $Ag_2SO_4$  in 1.610  $H_2SO_4$ , it is seen from Chart 55, that the average current for the C  $\rightarrow$  R portion of the runs is less than the average current for the R  $\rightarrow$  C portion of the runs. It is known from microscopic examination of Pt electrodes that silver never plates evenly over the surface of an electrode or covers the entire electrode for short plating periods but that it congregates at scattered points on the surface. The more silver there is plated on an electrode, the greater the area of these points and therefore, the greater the effective area of the electrode. In these cases of incomplete covering of a Pt electrode by silver, the effective area is, of course, always less than the geometric area of the electrode. During the C  $\rightarrow$  R  $\rightarrow$  C runs in Exp. A because of the initial charging, C has at all times a larger effective area than R. Because of this fact, the c. d. at the cathode is greater for C  $\rightarrow$  R than for R  $\rightarrow$  C as R is the cathode in the former while C is the cathode in the latter.

Figure 4 is a graphical representation of the relationship between c. d. and silver ion activity at the two electrodes. Curve CD is a plot of c. d. vs. silver ion activity at the cathode while curve AD is the plot of c. d. vs. silver ion activity at the anode. OD represents the silver ion activity in the main body of electrolyte, C the area of C and R the area of R. The single primes refer to C  $\rightarrow$  R and the double primes refer to R  $\rightarrow$  C.

$\Delta a_{ca}$  is the decrease in silver ion activity at the cathode due to the current  $i$  while  $\Delta a_{an}$  is the increase in silver ion activity at the anode due to the current  $i$ . It is seen from Figure 4 that at any given current density the decrease in silver ion activity (and concentration) at the cathode is always greater than its increase at the anode. (Reference 3, pp. 437, 438, 457 and 458; Reference 7, p. 49).

From the following equations and Figure 4, it will be shown that  $E' > E''$  and  $i' < i''$ .

$$E' = \frac{RT}{F} \left[ \ln(a + \Delta a'_{an}) - \ln(a - \Delta a'_{ca}) \right] \quad (17)$$

$$E'' = \frac{RT}{F} \left[ \ln(a + \Delta a''_{an}) - \ln(a - \Delta a''_{ca}) \right] \quad (18)$$

From Figure 4, it will be seen that

$$(\Delta a'_{ca} - \Delta a''_{ca}) > (\Delta a''_{an} - \Delta a'_{an}) \quad (19)$$

From Figure 4, it is evident that while:  $(a + \Delta a''_{an}) > (a + \Delta a'_{an})$  (20)

$$(a - \Delta a''_{ca}) \gg (a - \Delta a'_{ca}) \quad (21)$$

and

$$E' > E'' \quad (22)$$

From Equation (22), because

$$E_a - E' = i' R_c \quad (23)$$

and

$$E_a - E'' = i'' R_c \quad (24)$$

$$\text{it follows that } i' < i'' \quad (25)$$

which is what has been observed experimentally (Chart 55).

In Example 37, Exp. C of March 6, 1963, for Ag Au Bottle Cell No. 1b containing 0.005 M  $\text{Ag}_2\text{SO}_4$  in 1.250  $\text{H}_2\text{SO}_4$ , it is evident that there is a diffusion current for the L  $\rightarrow$  R part of the run but no diffusion current for the reverse part. Considering that

in this case, L is a 20 mil silver wire, 58 mm long and R a 20 mil gold wire 5 mm long, it is seen that the difference in effective areas of L and R are much greater than between C and R in DB 1 (Example 32). Because of this and in line with the considerations applying to DB 1, it is evident that the relative difference between the forward and reverse currents should, theoretically, be greater and this is borne out by the curves in Chart 56.

## IV

Ag<sub>2</sub> SO<sub>4</sub> - H<sub>2</sub> SO<sub>4</sub> - H<sub>2</sub>O ELECTROLYTES AND THE  
EFFECTIVE RESISTANCE OF CELLS

The original purpose in selecting these electrolytes was that sulfuric acid of certain density ranges does not freeze above -40°F (-40°C). See Table IV. Sulfuric acid of 1.250 density freezes at -61°F (-52°C). However, the disadvantage of this density acid is that the solubility of Ag<sub>2</sub> SO<sub>4</sub> in it is less than in water (Table III). In 1.300 density, H<sub>2</sub> SO<sub>4</sub> (freezing point -95°F (-70°C) at the minimum solubility (Table III), the solubility of Ag<sub>2</sub> SO<sub>4</sub> is still less. As this acid contains 40% H<sub>2</sub> SO<sub>4</sub>, it is seen from Table III that the solubility of Ag<sub>2</sub> SO<sub>4</sub> does not begin to increase until a somewhat higher density acid is reached. At this point, however, the freezing point is higher. Enough work has not been done yet in the investigation of Ag<sub>2</sub> SO<sub>4</sub> - H<sub>2</sub> SO<sub>4</sub> - H<sub>2</sub> O electrolytes to determine the optimum composition consistent with the best current level, sharpness of cut-off and effective resistance. The higher the silver ion concentration, the lower the effective resistance, other things being equal. The effective resistance is given by the equation:

$$R_{\text{eff}} = \frac{E}{i} + R_c = \frac{\pi_{\text{an}} - \pi_{\text{ca}}}{i} + R_c = \frac{\frac{RT}{F} \ln \frac{a_{\text{an}}}{a_{\text{ca}}}}{i} + R_c \quad (26)$$

The higher the Ag<sub>2</sub> SO<sub>4</sub> concentration, the lower the value of  $(\pi_{\text{an}} - \pi_{\text{ca}})$  and  $R_c$  (Reference 3, p. 438). See Graphs 9 and 10. The silver sulfate concentration, however, should not be so near the saturation point that Ag<sub>2</sub> SO<sub>4</sub> separates out on the anode at the current used in operating the cell as discussed in Section II. The curves shown in Graphs 1 and 2, Examples 30 and 31, where  $E_a$  is plotted vs  $\bar{v} i$  illustrate the large variation between two DB cells containing the same electrolyte.

Example 19, Chart 29, for DB3 containing 0.050 M Ag<sub>2</sub> SO<sub>4</sub> in 1.610 H<sub>2</sub> SO<sub>4</sub>, illustrates a case where there was too long a time

interval between the filling and sealing of a cell. During this time the electrolyte absorbed moisture from the atmosphere as strong sulfuric acid solutions are noted for their hygroscopic properties. This brought the solubility of the silver sulfate nearer the saturation point (Table III), thus resulting in the precipitation of some silver sulfate on the electrodes of DB3 when they were anodes. The silver sulfate thus formed prevented the complete deplating of the anodes in each successive run, thus accounting for the rapid loss in areas. The discussion in the latter part of Section II covers this effect more fully.

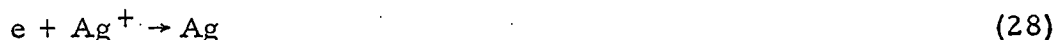
## V

PROGRESSIVE INCREASE IN AREAS IN CURRENT-TIME  
CURVES DURING TRANSFER OF SILVER  
BETWEEN ELECTRODES

In Chart 41, Example 24, for DB 22 (gold-plated electrodes) containing 0.10 N Ag NO<sub>3</sub>, there is a gradual increase in areas with relatively high residual currents. It is thought that during the tail part of each current-time curve, when only the residual current is present, silver is plated onto the cathode from the solution rather than from the anode. During maximum values of the current, the anodic reaction, which is a dissolution of silver from the anode:



and the cathodic reaction, which is the deposition of silver ions on the cathode



occur concurrently with no other reactions taking place but during the flow of the residual current,



is thought to be the anodic reaction which results in the production of oxygen at the anode with a simultaneous decrease in pH of the solution while



still remains the cathodic reaction.

The occurrence of reaction (29) causes  $\pi_{\text{an}}$  to rise with the resultant increase in the back emf and decrease in the current. After many runs it is seen that the total quantity of silver ions in the electrolyte will decrease, causing a progressive increase in current-time areas.

When comparing the curves in Chart 41 with their high residual currents and angular cut-offs to the curves in Charts 42 and 43 for

the same cell, it is observed that in the latter the areas are constant, the residual currents zero and the cut-offs less angular. It is difficult to define in Chart 41 just where reaction (27) stops and reaction (29) begins.

In Chart 40, Example 23 for DB 6 containing 0.050 M  $\text{Ag}_2\text{SO}_4$  in 1.610  $\text{H}_2\text{SO}_4$ , there is a slight progressive increase in areas but with no residual currents. The cut-offs are, however, quite angular which apparently favors the possibility of reaction (29) setting in before the current reaches zero, thus causing a gradual increase in areas and in total silver deposited.

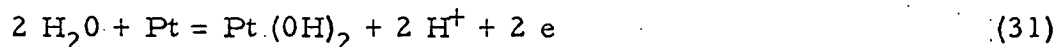
In cycling experiments it is important, therefore, to consider the shape of the cut-off portion of the current-time curve as well as the absence of residual currents in order to obtain constant time intervals for each half-cycle.

## VI

## ANODIC OXIDATION OF PLATINUM AND GOLD

The formation of films of platinous or platinum oxides on Pt electrodes under sufficiently oxidizing potentials and their reduction under appropriate conditions was claimed in the paper of Kolthoff and Tanaka, (Reference 8). In their work, non-oxidizing and non-reducing electrolytes were employed so that the observed effects were entirely due to the potential applied to the Pt electrode. The work of Ross and Shain (Reference 9) showed that if the oxidation potential of a solution of an oxidizing agent is less than that of the Pt (OH)<sub>2</sub> - Pt couple (+0.98 volts) a constant potential is quickly attained for an oxide-free Pt electrode immersed in the solution. The work of Anson and Lingane (Reference 10) proved the existence of oxides of Pt by spectrophotometric analysis of Pt electrodes previously subjected to anodic polarization in sulfuric and perchloric acid. The work of Baumann and Shain (Reference 11) showed that oxidation of gold takes place when a sufficiently high electrode potential is applied. They state that gold is more resistant to oxidation than platinum when complexing anions such as Cl<sup>-</sup> are absent.

The following equations show that the acidity of the electrolyte influences the value of the potential required to oxidize an oxide-free platinum or gold electrode.



$$\pi_{\text{Pt}}^{\circ} = 0.98 \text{ volt (Reference 12, p. 343)}$$

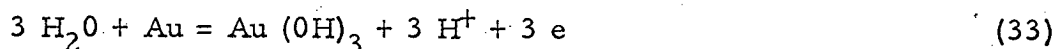
$$\pi_{\text{Pt}} = \pi_{\text{Pt}}^{\circ} + \frac{RT}{2F} \ln a_{\text{H}^+}^2 \quad (32)$$

For a solution of p H = 6.7 as 0.10 N Ag NO<sub>3</sub>,

$$\pi_{\text{Pt}} = 0.98 + 0.059 \log 10^{-6.7}$$

$$\pi_{\text{Pt}} = 0.58 \text{ volt}$$





$$\pi_{\text{Au}}^{\circ} = 1.45 \text{ volt (Reference 12, p. 344)}$$

$$\pi_{\text{Au}} = \pi_{\text{Au}}^{\circ} + \frac{RT}{3F} \ln a_{\text{H}^+}^3 \quad (34)$$

For a solution of p H = 6.7 as 0.10 N Ag NO<sub>3</sub>,

$$\pi_{\text{Au}} = 1.45 + 0.059 \log 10^{-6.7} = 1.05 \text{ volt.}$$

Considering that the mean activity co-efficient of the stronger sulfuric acid solutions, such as used in our cells, is unknown, the value of  $a_{\text{H}^+}$  cannot even be approximated for these electrolytes and as a result  $\pi_{\text{Pt}}$  and  $\pi_{\text{Au}}$  cannot be calculated. However, for two cells, one with Pt and the other with Au electrodes and each containing the same Ag<sub>2</sub> SO<sub>4</sub> - H<sub>2</sub> SO<sub>4</sub> - H<sub>2</sub>O electrolyte ( $\pi_{\text{Au}} - \pi_{\text{Pt}}$ ) is merely the difference of Equations (34) and (32) where the second terms in each equation cancel out. This difference is 1.45 - 0.98 or 0.47 volt.

If decomposition voltage curves are run for these cells the difference of the potentials at the two maxima should give the same value. These maxima can be defined as the maximum currents observed before the decomposition voltages are reached. The decomposition voltage is the voltage at the point where the curve takes its final upward swing. It is, in any case, not an exact value. Maxima can be observed in Graph 4 for DB 16 with platinum electrodes (Example 33) and in Graph 5 for Ag Au Bottle Cell No. 1b with gold electrodes (Example 34). It is unfortunate that these two cells did not contain the same strength electrolytes, however, the difference in their maxima (1.00 volt - 0.72 volt) or 0.28 volt at least furnishes qualitative proof for the formation of oxides of platinum and gold at the potentials existing at these maxima. Ag Au Bottle Cells No. 2 and No. 3 (Examples 35 and 36) also show maxima for the decomposition voltage curves shown in Graphs 6 and 8.

In Table V a comparison between the currents at the maxima and the lengths of the gold electrodes in the three bottle cells discussed is given. It is to be noted that any oxides originally present on the gold electrodes of these cells were reduced by the preliminary cathodizations. In the case of DB 16, the preliminary cathodization removed any Pt oxides on its electrodes. Table V shows a rough proportionality between electrode areas and currents at the maxima which, of course, indicates that higher currents are necessary for the oxidation of larger areas of gold.

As shown by the above theoretical discussion and the four graphs mentioned, the use of gold electrodes permits a higher cut-off voltage than with platinum before oxidation of the anode occurs, assuming the same electrolyte is used in each case. This is equally true for cells containing acid or neutral electrolytes and is shown by the fact that the value of  $(\pi_{\text{Au}} - \pi_{\text{Pt}})$  is independent of p H.

Early work with B cells has demonstrated that a preliminary cathodization of the Pt electrodes (which were not gold plated later) usually resulted in better curves in initial tests. During the continued testing of these cells at various cut-off voltages, it is entirely possible that some or all of the voltages employed have been high enough to cause a gradual oxidation of the electrodes during each successive cut-off. It is not understood why these cells after continued use or most cells with uncathodized electrodes gave poor performances. The fact that cells with gold plated electrodes containing both 0.10 N Ag NO<sub>3</sub> and sulfuric acid electrolytes have given constant areas for current-time curves when transferring silver back and forth between two electrodes may be attributed not only to the elimination of crevices in the electrode-to-glass seals but also to the fact that the gold electrodes remained oxide-free. There is no cell with Pt electrodes containing 0.10 N Ag NO<sub>3</sub> on record which gave constant areas for current-time curves. Of the many cells of this type tested it seems reasonable to assume that at least a few must have had perfect Pt-to-glass seals. On the other hand, practically all the cells with gold plated platinum electrodes containing 0.10 N Ag NO<sub>3</sub> have given constant areas.

TABLE I

## SILVER SULFATE - SULFURIC ACID - WATER ELECTROLYTES

Molarity of $\text{Ag}_2\text{SO}_4$	Weight o/o $\text{Ag}_2\text{SO}_4$	Density of $\text{H}_2\text{SO}_4$	Molarity of $\text{H}_2\text{SO}_4$	Weight o/o $\text{H}_2\text{SO}_4$	Freezing Point (Approx.)
0.005	0.124	1.250	4.34	34.0	-52 C (-61 F)
0.010	0.249	1.250	4.34	34.0	-52 C (-61 F)
0.015	0.373	1.250	4.34	34.0	-52 C (-61 F)
0.020	0.496	1.250	4.34	34.0	-52 C (-61 F)
0.015	0.423	1.102	1.685	15.0	-7.7 C (+18 F)
0.015	0.403	1.155	2.593	22.0	-15 C (+5 F)
0.015	0.388	1.202	3.430	28.0	-27 C (-17 F)
0.015	0.298	1.520	9.60	62.0	-30 C (-20 F)
0.025	0.510	1.520	9.60	62.0	-30 C (-20 F)
0.050	0.958	1.610	11.48	70.0	Indeterminate
0.32	5.47	1.727	14.10	80.0	-10 C (+14 F)

TABLE III

The System Silver Sulfate-Sulfuric Acid-Water at 25°  
(Simons and Ricci, 1946a)

Gms. Ag <sub>2</sub> SO <sub>4</sub> per 100 gms. sat. sol.	Gms. H <sub>2</sub> SO <sub>4</sub> per 100 gms. sat. sol.	Solid Phase	Gms. Ag <sub>2</sub> SO <sub>4</sub> per 100 gms. sat. sol.	Gms. H <sub>2</sub> SO <sub>4</sub> per 100 gms. sat. sol.	Solid Phase
0.833	0.0	Ag <sub>2</sub> SO <sub>4</sub>	6.58	74.95	β-AgHSO <sub>4</sub>
.990	4.75	"	6.54	75.13	"
.946	11.34	"	6.57	75.93	"
.618	21.13	"	7.14	77.9	"
.411	38.12	"	7.97	79.73	"
.400	54.30	"	9.13	80.78	"
.632	62.15	"	9.42	80.92	"
.831	64.97	"	10.85	81.27	"
1.897	70.86	"	11.39	81.21	"
2.273	71.87	"	12.70	80.89	"
2.84	72.60	"	13.58	80.57	"
2.94	72.68	"	5.58	75.43	α-AgHSO <sub>4</sub>
3.89	73.66	"	4.94	76.78	"
4.06	73.78	"	4.34	80.27	"
4.50	74.03	"	4.51	81.59	"
4.74	74.26	"	4.79	82.22	"
5.50	74.26	"	6.13	82.68	"
5.63	74.19	"	7.94	83.01	"
6.57	74.21	Ag <sub>2</sub> SO <sub>4</sub> + β-AgHSO <sub>4</sub>	12.81	81.62	"
6.55	74.47	"	*19.45	77.86	α or β-AgHSO <sub>4</sub> (?)
6.61	74.25	"	*19.82	77.64	"
6.59	74.31	"	*20.81	76.98	"
6.52	74.5	"	*21.01	76.41	"
Av6.57	74.35	"	*21.45	76.32	"
6.18	74.30	Ag <sub>2</sub> SO <sub>4</sub> + β-AgHSO <sub>4</sub>	*21.50	76.55	"
6.23	74.08	"	*21.82	76.17	"
6.32	74.31	"			
6.32	73.95	"			
6.27	74.07	"			
Av6.26	74.14	"			

\*Solubility curves of α and β-AgHSO<sub>4</sub> indistinguishably close.

William F. Linke, Solubilities of Inorganic and Metal Organic Compounds,  
Originated by Atherton Seidell, Ph. D., Vol. I, Fourth Edition, A-IR,  
D. Van Nostrand Company, Inc., 1958, p. 132.

TABLE II  
Viscosity of Sulfuric Acid Solutions

Temperature		Viscosity in Centipoises				
°C	°F	10%	20%	30%	40%	50%
30	86	0.976	1.225	1.596	2.163	3.07
25	77	1.091	1.371	1.784	2.409	3.40
20	68	1.228	1.545	2.006	2.70	3.79
10	50	1.595	2.010	2.600	3.48	4.86
0	32	2.160	2.710	3.520	4.70	6.52
-10	14	.....	3.820	4.950	6.60	9.15
-20	-4	.....	.....	7.490	9.89	13.60
-30	-22	.....	.....	12.200	16.00	21.70
-40	-40	.....	.....	.....	28.80	.....
-50	-58	.....	.....	.....	59.50	.....

G. W. Vinal and D. N. Craig, *The Viscosity of Sulfuric Acid Solutions Used For Battery Electrolytes*, Bureau of Standards, J. Research, 10, 781 (1933), *Storage Batteries*, Fourth Edition, John Wiley and Sons, Inc., 1955, p. 119.

TABLE IV  
Freezing Points of Solutions of Pure Sulfuric Acid

Specific Gravity at 15°C	Freezing Points		Specific Gravity at 15°C	Freezing Points	
	Centigrade	Fahrenheit		Centigrade	Fahrenheit
1.000	0	+ 32	1.450	-29	-20
1.050	- 3.3	+ 26	1.500	-29	-20
1.100	- 7.7	+ 18	1.550	-38	-36
1.150	- 15	+ 5	1.600	*	*
1.200	- 27	- 17	1.650	*	*
1.250	- 52	- 61	1.700	-14	+ 6
1.300	- 70	- 95	1.750	+ 5	+40
1.350	- 49	- 56	1.800	+ 6	+42
1.400	- 36	- 33	1.835	-34	-29

\* Freezing Points Indeterminate

G. W. Vinal, Storage Batteries, Fourth Edition, John Wiley and Sons, Inc., 1955, p. 111.

TABLE V

Comparison of currents observed at maxima in decomposition voltage curves with lengths of gold electrodes.

Example	Bottle Cell	Graph	R (Au)	Current at Maximum
34	Ag Au No. 1b	5	5 mm	0.6 $\mu$ a
35	Ag Au No. 2	6	13 mm	1.2 $\mu$ a
36	Ag Au No. 3	8	58 mm	5.0 $\mu$ a

LIST OF REFERENCES

1. Frank H. MacDougall, Physical Chemistry, Third Edition, The Macmillan Company, 1952.
2. Elfin I, Final Report, C25-7, July 25, 1962.
3. Samuel Glasstone, An Introduction to Electro-Chemistry, D. Van Nostrand Company, 1942.
4. I. M. Kolthoff and James J. Lingane, Polarography, Second Edition, Vol. I, Interscience Publishers, Inc., 1952.
5. Handbook of Chemistry and Physics, 38th Edition.
6. William F. Linke, Solubilities, Vol. I, Fourth Edition, D. Van Nostrand Company, Inc., 1958.
7. William Blum and George B. Hogaboom, Principles of Electroplating and Electroforming, Third Edition, McGraw-Hill Book Company, 1949.
8. I. M. Kolthoff and N. Tanaka, Analytical Chemistry, 26, 632, 1954.
9. J. W. Ross and I. Shain, Analytical Chemistry, 28, 548, 1956.
10. F. C. Anson and J. J. Lingane, Journal of American Chemistry Society, 79, 4901, 1957.
11. Frederic Baumann and Irving Shain, Analytical Chemistry, 29, 303, 1957.
12. Wendell M. Latimer, Oxidation States of the Elements and Their Potentials in Aqueous Solutions, Second Edition, Prentice-Hall, Inc., 1952.



## APPENDIX B

## ELECTRO-CHEMICAL TIMER

## INTRODUCTION

If silver is removed from a platinum electrode and deposited onto a second electrode by means of an electroplating process at constant current, it will be found that the voltage across the electrolytic cell remains constant for the time interval during which most of the silver is removed from the electrode and increases abruptly at the end of the process. If the current is constant, there is an exact relationship between the amount of silver on the anode and the time required to remove it, provided that the voltage across the cell does not exceed a given value. The rise in voltage across the cell at the end of the process is of the order of one volt or less. This is a convenient change for use with solid state devices such as transistor and silicon controlled rectifiers. Using this technique it is possible to build a very precise timer with a minimum of components, occupying a very small volume and providing timing intervals of accuracy of the order of a tenth of a percent. Such a timer is shown in Figure 1 and 2 and its circuit in Figure 3. This timer when combined with a battery of a few volts will fire a squib or flash bulb after a time interval which can range from a few seconds to several months.

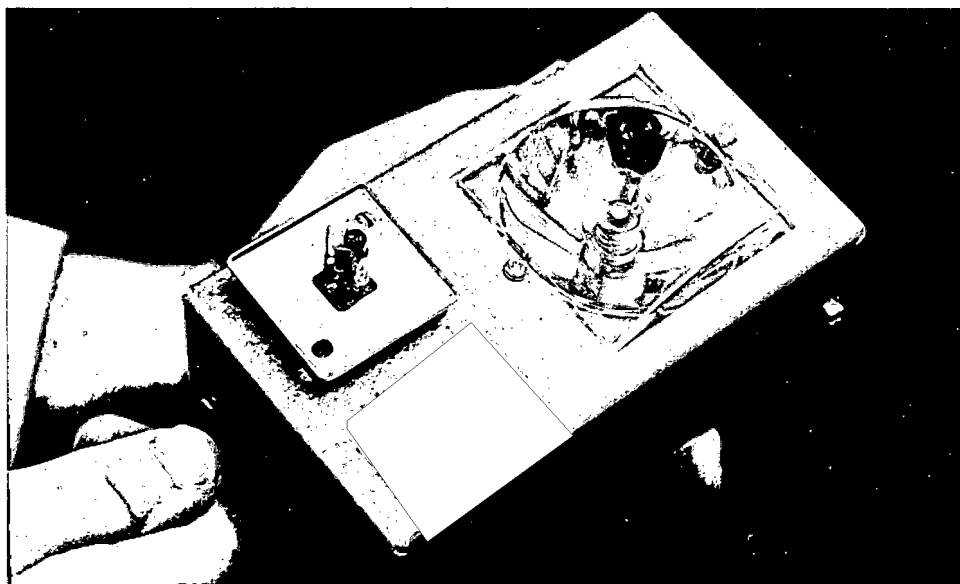
[redacted] has been engaged for the past two years in the development of electroplating cells (E-cells, hereafter) for application to timers, integrators, and computer logic functions. The company has available many items of equipment used for assembly, preparation and test of the E-cells. Precision equipment for charging the cells and setting precise time intervals also exist. In brief, it will be noted that the electro-chemical laboratory of [redacted]

50X1

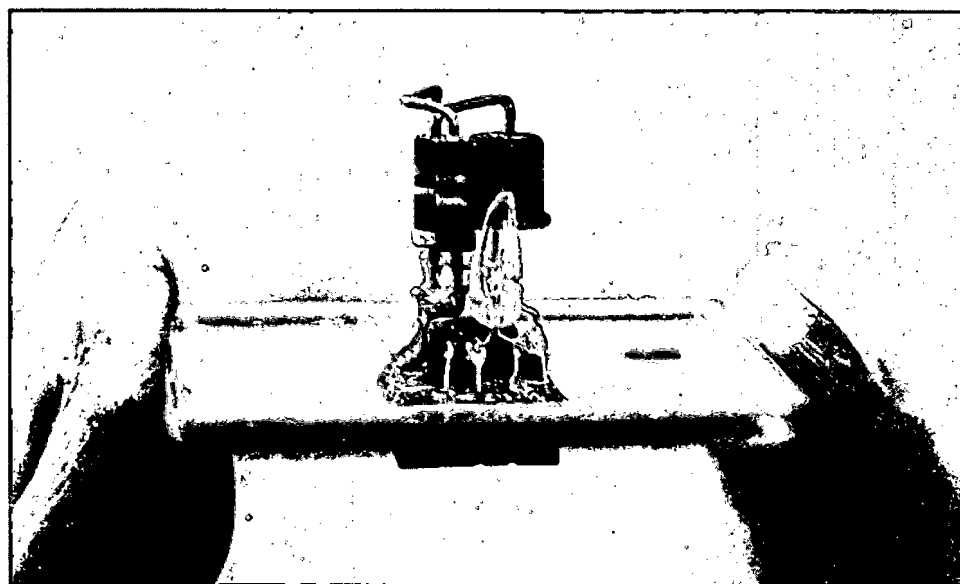
50X1

[redacted] has developed E-cells with sharp cutoff when the silver is removed at a rate of only one millimicroampere ( $10^{-9}$  amperes) current through the cell. The residual current through the cell after the end point is as small as 10 pico amperes ( $10^{-11}$  amperes).

50X1



50X1



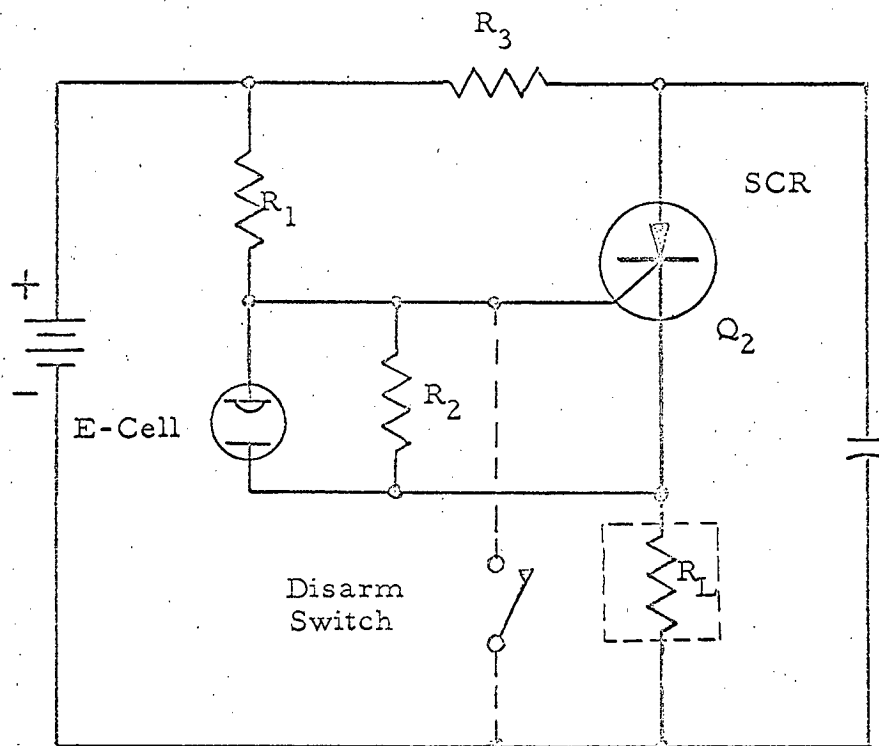


Figure 3  
Basic SCR Circuit

Timing cells have been built and operated in timers several hundred times with a typical accuracy of .2 of one per cent in the timing interval at ambient temperatures. Equipment has been developed around the cell to integrate microwave energy to an accuracy of better than one db whether or not the source is pulsed or constant. The sensitive cells can be connected directly to a variety of transducers without intervening amplification, such as photovoltaic devices, microphones, and antenna diode combinations. The integrated field intensities can be read immediately by plugging the cell which is mounted on a standard TO-5 transistor header into a hand-held instrument which deplates the accumulated silver.

The discussion below considers both the basic operation of E-cells and the application of appropriate solid state circuitry to the E-cells to perform the timing function. Most of the information presented below has never appeared in open literature and is primarily the result of intensive activity in electro-chemistry at  over the past two years.

50X1

## E-CELL PRINCIPLES AND OPERATING CHARACTERISTICS

### Electro-Chemical Principles

This section will not discuss the well-known principles of electro-chemistry which can be found in many of the excellent texts such as those by Glasstone and Kortum-Bockris. Such texts discuss the basic properties of electrolytes and their conductivity as well as the concepts of electrode potential, over potential, polarization, and reference electrodes.

Instead we will concentrate specifically on those features which are most directly related to the use of an E-cell in a timer. The features of interest involve properties of the electrolyte, of the interface between the electrolyte and the electrodes, the electrode itself, and the crystallization of the silver or other plated material on the electrode. Our discussion will consider primarily the plating of silver onto platinum electrodes, although nearly all the considerations apply equally as well to other combinations. The operation of gold electrodes has been found to be very slightly different from that of

platinum electrodes and materials such as copper and nickel have been plated with much the same success as silver. However, experience has shown that there is good reason for using silver on platinum and consequently, this will occupy our attention primarily.

The choice of an electrolyte involves many considerations. Its resistance should be small in order that it will not interfere severely with the regulation of the current source. It should be reasonably stable so that voltages applied to the electrolyte after the silver has been removed from the anode will not trigger other reactions which will introduce errors in the time interval; and finally its temperature characteristics should be such that the electrolyte does not freeze at the low end of its operating and storage range nor change chemically at the high end by means of hydrolysis or other chemical reactions.

It is well known that the resistance of an electrolyte generally decreases as the concentration of the salt in the electrolyte increases. The salt concentration cannot be made too high however, because at very low temperatures the solution can become supersaturated and salt crystals would precipitate interrupting the flow of current to the electrode. Also, very high concentration of the electrolyte can effect the crystal structure of the silver being deposited on the electrode and provide crystals which do not adhere properly to the electrode surface.

The resistance can be lowered best by keeping the cells small and the electrodes reasonably close together, but not too close that silver crystals can provide an electronic short between the electrodes. The electrode area can also be increased to lower the resistance, but this increase degrades the low current characteristics of the cell as will be discussed below. Experience indicates that electrolyte concentration in the region of .1 normal to 1 normal is sufficient to provide cells with resistance of a few hundred ohms or less.

Silver nitrate though commonly used, is unsatisfactory for most E-cell applications where accuracy, stability and many cycles of operation are required. The reason is that the nitrate ion itself is not a very stable ion and readily breaks down into nitrous oxide and water. If the voltage across a cell with a bare platinum anode is

allowed to rise over .7 of a volt this process takes place spontaneously and not only provides a current when the cell should be nonconducting, but also causes chemical reactions which seriously degrade the surface of the electrode so that later operation is found to be very erratic.

In order to use semiconductor switches in conjunction with the E-cell, such as the use of a silicon controlled rectifier, it is desirable to have voltage changes across the cell of .8 of a volt or larger for reliable operation. Several such electrolytes are available. One, which is a mixture of silver cyanide and potassium cyanide, allows one volt to be put across the cell without detrimental effects. This is due to the stability of the cyanide ion and the fact that the silver ion is more tightly bound in solution by the cyanide complex formation,  $\text{Ag}(\text{CN})_2^-$ .

If a potential less than one volt is placed across two platinum electrodes inserted in an electrolyte most of the voltage drop will occur across electrode-electrolyte interface which is only a few atomic diameters thick. This interface behaves like the parallel plates of a capacitor with negative charges on the cathode being opposed by positive silver ions in the electrolyte. At the other electrode, positive charges hold the negative ions in an array very close to the electrode surface. The result is exactly analogous to the polarization of a dielectric in a parallel plate capacitor; and indeed, electrolytic capacitances are used for this purpose. It is found that with platinum electrodes and silver concentrations of approximately one normal, the capacitance of the interface is approximately 20 microfarads per square centimeter of electrode area. For very rough, uneven electrodes the true surface area must be used rather than the geometric envelope. This capacitance effect is very important in many applications where sharp cutoff times are required or where the integration of very small quantities of charge is under consideration.

A further contribution of the interface is its effect on the overall resistance of the cell during conduction of silver from one electrode to another. It will be found that as the current is decreased through a given cell that the resistance begins increasing rather abruptly at a certain low current level depending upon the electrode area. If one

looks at a plot of the potential across the cell as a function of the current passing through it, instead of obtaining a straight line through the origin, the potential varies as  $\log(1 + i/i_0)$  plus the resistive drop of the electrolyte. At very low current levels, this potential drop across the interface becomes more important than the resistive drop of the electrolyte.

Perhaps the most important phenomenon controlling the application of E-cells to timers and sensitive integrators are the crystallization effects of the silver on the platinum electrodes. Both platinum and silver have the same cubical crystal structure with approximately the same lattice constant. Consequently, when silver plates onto a platinum electrode, the silver crystal structure tends to be an extension of the platinum crystals and the bonding at the interface is very good. However, the points where the silver crystals form and the nature of the crystals themselves varies considerably with different operating conditions and chemical composition of the electrolyte.

For example, if the current density is too large for a given electrolyte concentration, treeing of the crystals will occur. This results from the fact that the silver ions in the solution very near the electrode are quickly depleted. The extremities of the silver crystals formed which reach out into the more concentrated portions of the electrolyte are favored in crystal formation. The result is that long spindly crystals are created which adhere at only one point to the platinum electrodes and are easily broken loose by shock and vibration.

A comparable but not so serious effect occurs when very pure silver nitrate solutions and solutions of other simple silver salts are used as electrolytes. It is then observed that the crystal deposit tends to be in the form of a few large cubical crystals rather than a lot of small crystals closely bound to the electrode. This has two effects. When large crystals are formed, the ratio of the surface area of contact to the electrode to the total mass of the crystal is small so that the crystals are more subject to shock and vibration.

A purely electrical effect is important also. As the silver is depleted from the electrode, then the resistance of the electrode-electrolyte interface is proportional to the area of the silver crystals

exposed to the electrolyte. As the crystals get smaller and smaller, this area decreases and the resistance at the end point of the deplating process rises rather sharply. However, when only a few large crystals are being removed from the anode, then the change in resistance at the end point is much more gradual, since the surface area exposed to the electrolyte is relatively small to begin with. For timer applications, this results in what is known as a long cutoff time.

Perhaps of most interest from a theoretical point of view are the recrystallization effects of the silver on a platinum electrode. Regardless of how it is formed, a microscopic examination of the platinum electrode will reveal a surface of very rugged structure. Platinum wire is typically polycrystalline and the surface contains many edges and corners and similar discontinuities at edges and vertexes of crystals. As the silver is deposited the crystals form preferentially on those points of the platinum crystal which reach into the silver solution for two reasons. As mentioned above the concentration of the silver ions is greater at the points and more importantly, the electric field intensity is greater at these points. Consequently, the crystal structure first formed appears as small cubical crystals which are situated at corners and edges of the platinum crystals.

Thermal agitation and transfer of silver ions back and forth across the boundary cause these crystals to diffuse and migrate away from the edges into the crevices of the platinum crystals where the silver is more tightly bound. If this electrode is made an anode instead of a cathode, then it will be found that the energy to remove this silver is somewhat greater as time progresses than if it were deplated immediately. If a large amount of silver is deposited then the silver rearranges itself into more compact forms of lower potential energy. If the silver is allowed to stand for awhile before it is deplated, the voltage required to initiate deplating is somewhat higher than if the deplating were to take place immediately after deposition. Once the deplating has started and the crystal structure is broken into, the voltage required to continue the process returns to the normal value. These effects in one way or another influence the accuracy and reproducibility of electroplating cells used for timer application.



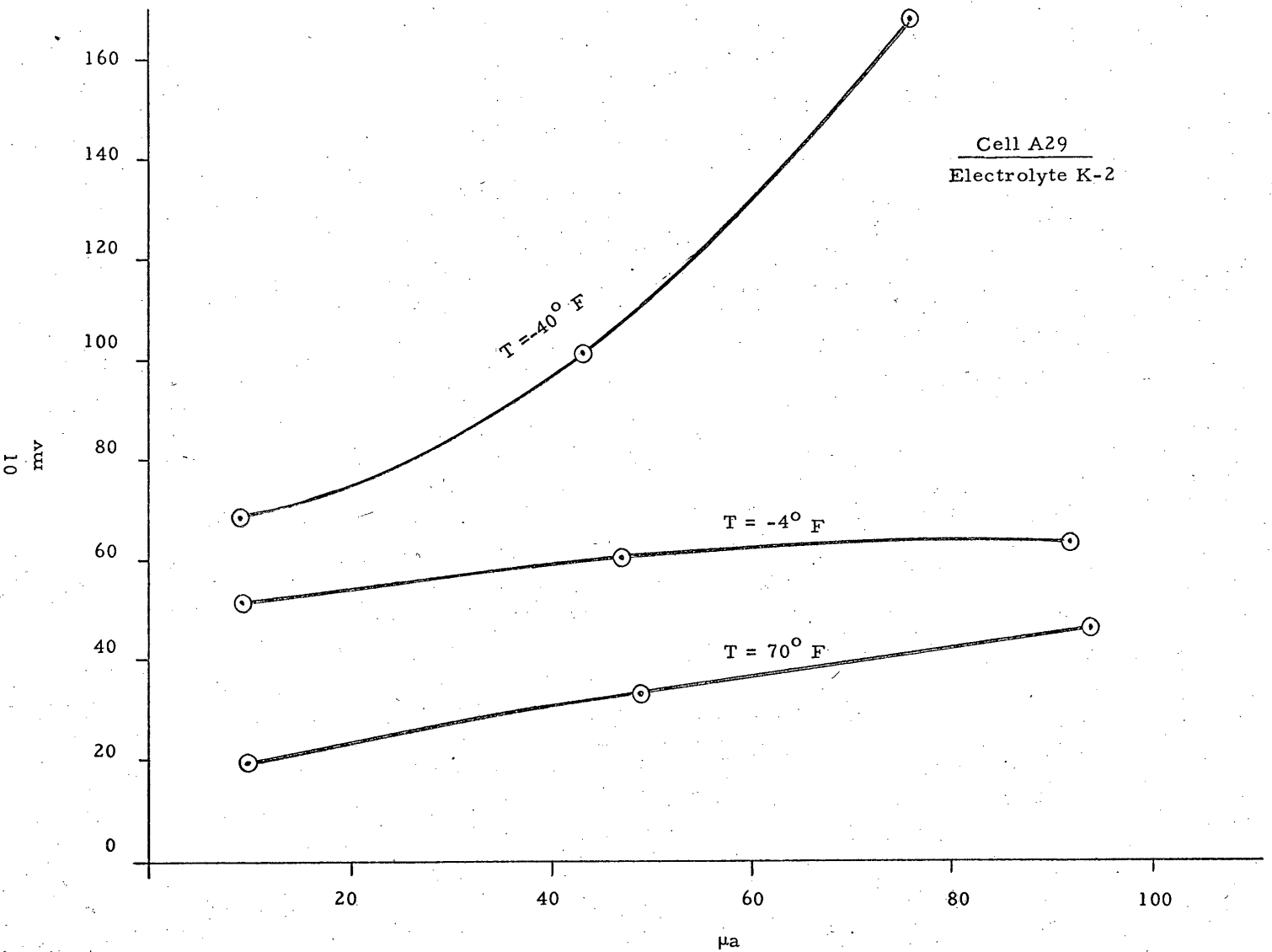
### Operating Characteristics

Only the more important operating characteristics will be considered here. The most important of these are the cell resistance characteristics, the recovery and reproducibility and finally, the accuracy and sharpness of the cutoff time. The resistance of a cell at various current levels and three different temperatures can be inferred from Figure 4 in which the voltage across the cell is plotted versus the current through the cell during its conduction mode. The extrapolated curves do not pass through the origin because of the interface voltage drop which was described above. If data for very small current values is taken, it will be found as illustrated in Figure 5 that the curves actually do go through the origin. Figure 6 shows a similar curve for a cell of higher sensitivity.

In our early work on the investigation of electroplating cells for timer and integrator applications, it was found that if a given quantity of silver were plated on one electrode and then transferred back and forth between electrodes and the current time relationship recorded, that there was an apparent decrease in the total quantity of silver being transferred. The smaller the amount of silver involved, the more rapid the percentage decrease during each cycle. This lack of reproducibility was found to be due to a number of factors, the first of which was inadequate chemical purity. This would seem like an obvious consideration, however, it should be pointed out that the degree of impurity is extremely important. Current passing through a cell at a 100 microampere rate is transferring silver from one electrode to another at only 1/10th of a microgram per second. Consequently, a few micrograms of the wrong impurity can alter the total amount of silver being transferred by many seconds.

Once adequate purity was obtained, it was found that there was still a variation reliability depending upon the condition of the electrode surface. Through many months of trial and error, it was found that the electrode surface could be properly prepared by going through several stages of treatment which had the effect of smoothing the surface and removing monomolecular layers of platinum oxide.

Cell Resistance Characteristic



### Cell Resistance Characteristic

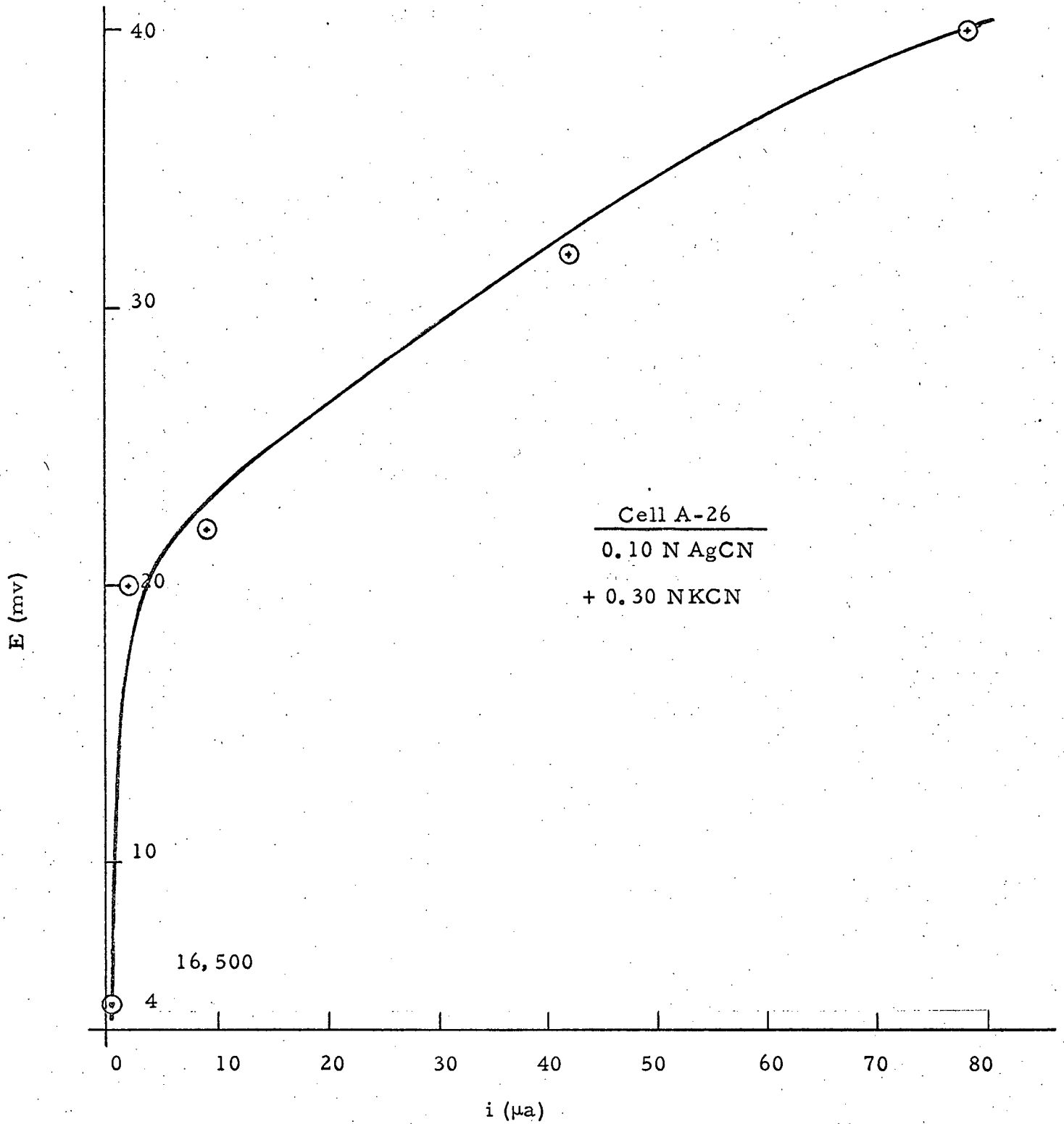


Figure 5

Cell Resistance Characteristic

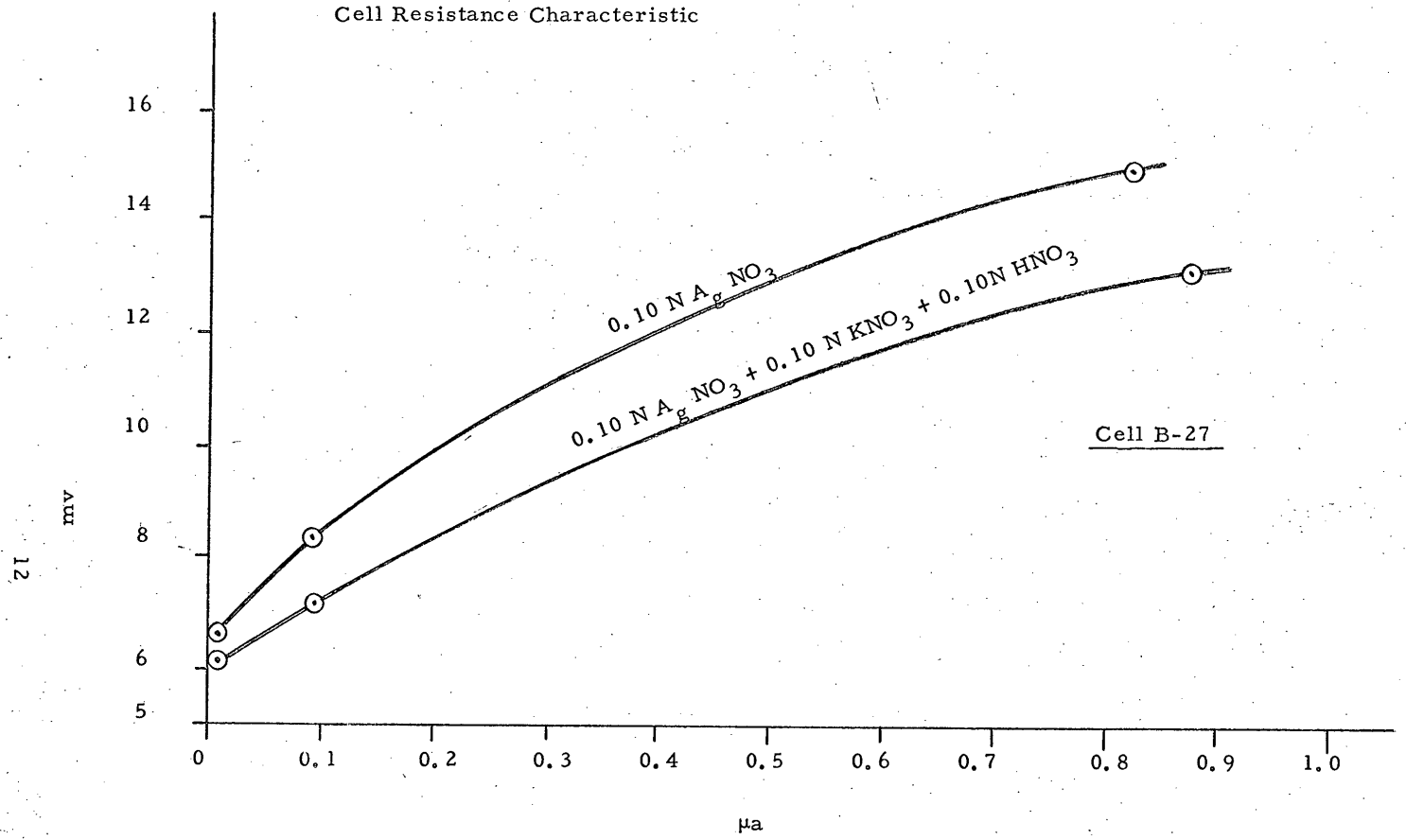


Figure 6

When both chemical purity and surface preparation were accomplished, it was then found that the degree of recovery of silver between cycles was a function of the maximum voltage that was used to remove silver from the anode. In line with our discussion above on crystallization effects, it was found that if too small a voltage were used, then the silver deposited in the platinum crevices was removed only very slowly because of the time required for the silver to diffuse to the edges of the platinum crystals. If the cycle was reversed before this slow diffusion effect took place then a certain amount of silver remained behind in the crevices. As many cycles were performed this silver in the crevices built up to a level which was very difficult to recover. On the other hand, if the voltage across the cell were made too large then side chemical reactions due to impurities which were not removable from the electrolyte would take place causing current to flow giving the appearance of a larger amount of silver on the electrodes. With any particular electrolyte and cell configuration, it is necessary to find the proper operating voltages in order that accurate recovery can be obtained.

This is illustrated in Figure 7. In this figure a cell was cycled back and forth every minute for several days. During the first two days, the voltage was set at a level which caused a slight increase in the current time product during each cycle and a gradual lengthening of the time to deplete the silver at a fixed current level was observed. The voltage was then reduced across the cell to a level which had been found favorable under previous operating conditions and the current time product remained constant within the accuracy of the measurement for a time interval of six days or several thousand cycles. An examination of the cell's characteristics after many thousand cycles of operation at the proper voltage showed that they did not change or perhaps improved slightly; the resistance being somewhat lower and the cutoff time being somewhat shorter than when the test was started.

The accuracy of a timer insofar as the E-cell characteristics are concerned involves the reproducibility described in the paragraph above, the variation of the cell resistance insofar as it effects the current source

Life Cycle Test

Cell Ay  
Electrolyte K7

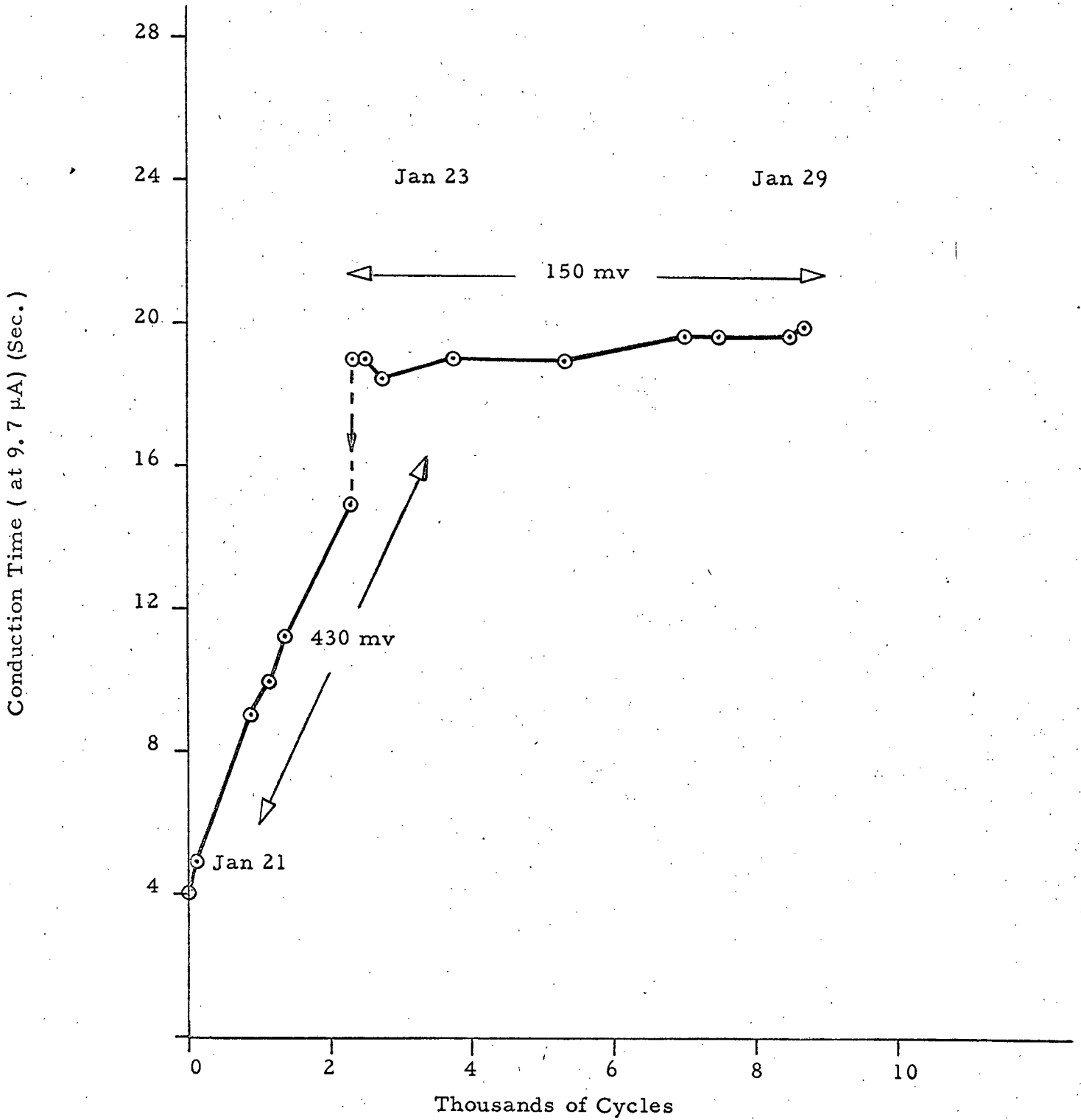


Figure 7

which is deplating the cell, and the sharpness of reproducibility of the cutoff time or more accurately, the rate of change of resistance at the end of the plating cycle. The cutoff time was described as being a function of the rate at which the crystal surface area changed near the end of the plating process. It is also related to the total number of crystal centers formed on the electrode and the extent to which the platinum electrode has been covered with silver. \* Since a larger amount of silver initially plated onto the electrode results in a larger percentage of the crevices between the platinum crystals being filled, it is observed as expected that the cutoff time in seconds tends to be longer, the longer the total time required to deplate the silver from the electrode.

Experience indicates that the time required for the voltage across the cell at the end of the deplating process to rise from about 20% of its maximum value to 80% of its maximum value is approximately equal to 1% of the total deplating time, and its reproducibility under normal conditions allows one to set a threshold which is crossed with an accuracy of approximately one-tenth of a percent of the total time. More accurate cutoff times than this are not required for most programs. However, in other work being undertaken by   techniques to improve this cutoff time are being investigated. It will be important here only to investigate and control the variation in the cutoff time as it is affected by various environmental changes.

50X1  
50X1

#### E- CELL CONSTRUCTION, PREPARATION, AND TESTING

Cells of various sizes and configuration have been constructed of glass, plastics and other materials; electrodes of platinum, gold and gold plating on other metals have also been investigated. After several months of experimentation to develop a cell which is easily constructed, durable and highly reliable, a design has been achieved

\* For short time applications, the capacitance of the electrode-electrolyte interface is also important.

which fits very well the requirement of the present proposal. This design is illustrated in Figure 8. It consists of a small glass envelope with three electrodes of 10 mil platinum wire which extend from the cell at the bottom and are soldered or welded to a standard TO-5 transistor header.

Once the cell has been filled and the center electrode charged with silver, it is sealed at the top by a variety of techniques depending on the environmental requirements of the cell. Most frequently the cell is capped with an epoxy sealer or an inert silicone rubber seal. Special techniques have been developed to protect the electrolyte from any contamination of the sealing material. The cell envelope is fixed firmly to the header by an epoxy cement and the entire unit is potted in silicone rubber inside a cylindrical container providing shock resistance and durability under extreme environmental conditions.

Other techniques for cell construction oriented toward mass production are presently under development and these techniques will be applicable to the present problem if such large production is required. The material cost for the cell described above are less than \$1.00, and the cost of the cell as described in production quantities should not be excessive although such a costing has not been accomplished at present.

Cells are presently prepared in batches of 20 and go through numerous steps before the device is finished. (The cell envelopes are presently prepared by hand but in very large quantities are easily manufactured by machine). The envelopes are cleaned and the electrodes are treated with a series of chemicals to prepare the surface. The electrodes are cathodized to remove any traces of oxides and filled with an electrolyte designed specifically for the application under consideration. The cells are charged with silver in groups and the current is controlled carefully by a constant current source and is cut off automatically at the proper time.

Once the cells are sealed, they are put through a variety of tests which determine their operational characteristics and compare them to previously determined specifications. Temperature cycling



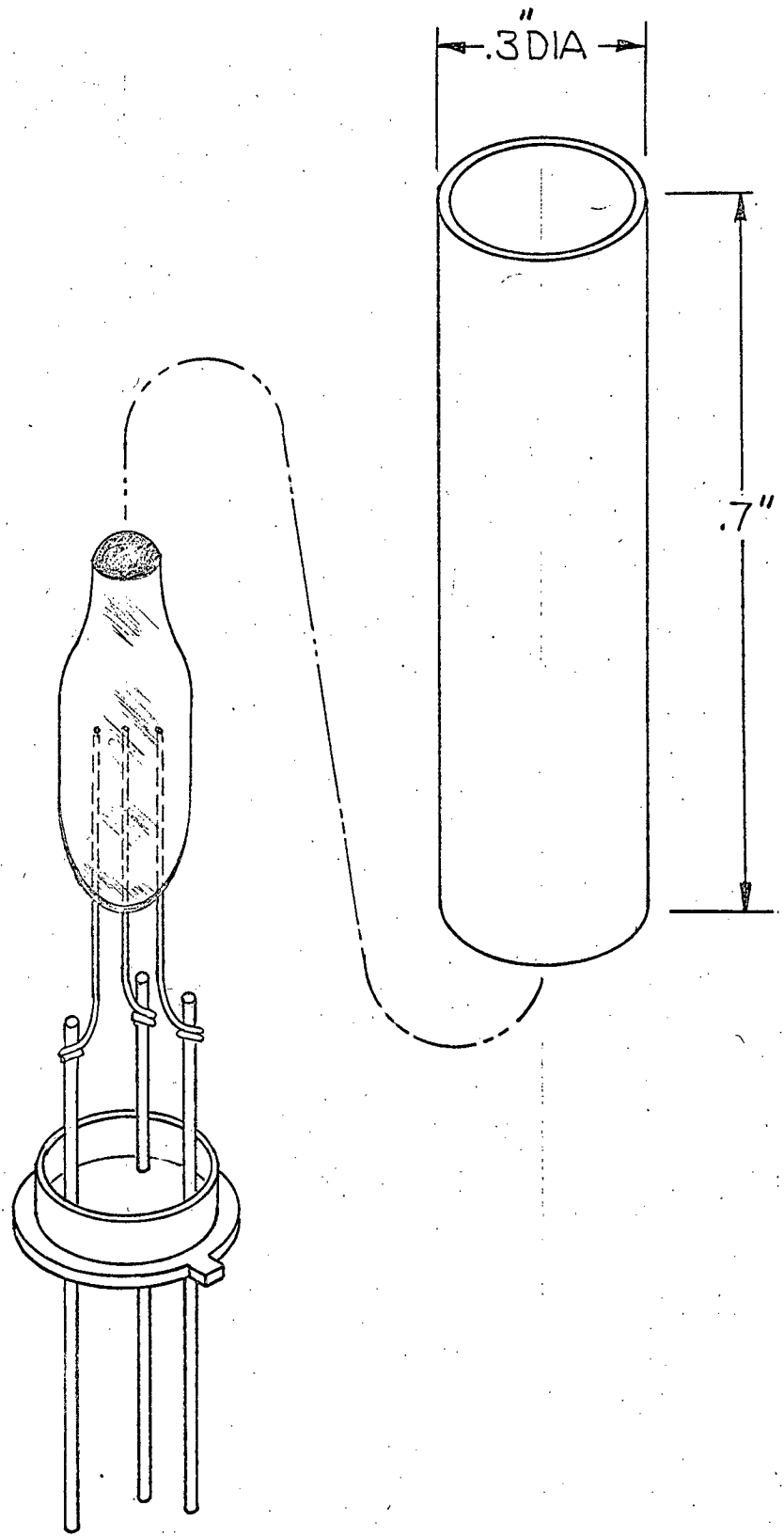


Figure 8

E-Cell Configuration

and renewed testing is performed as required by the application. The tests are designed to determine reproducibility of charge and discharge, current time product, resistance at two different current levels, and to measure the speed and constancy of the cutoff time. In some cases, additional tests are added which are oriented toward the specific application.

#### ASSOCIATED ELECTRONICS, E-CELL TIMER

The electronic circuitry to complete the timing and actuation function established by the electrolytic cell must be inherently a simple, rugged and reliable as the E-cell itself. In addition, it must provide an operational system to utilize the E-cell in its most optimum form.

has developed in various programs many techniques and circuits which permit optimum operation of the cell, yet maximize the reliability of the electronics itself.

50X1

#### Basic Circuit Considerations

Since E-cells can be made which operate reliably over a current range from as small as a millimicroampere to well over several amps, some flexibility is available to the circuit designer. Considerations of size and battery life dictate that as low a current as convenient be utilized in the cell. In order that simple and reliable solid state circuit components can be used, the cell currents are usually chosen in the range of one to one hundred microamperes. For reliable operation a voltage change across the cell at the end of the plating process, greater than .8 of a volt is desirable. This eliminates the use of silver nitrate as an electrolyte in the cell, but allows several other electrolytes to be used successfully.

The circuit should be designed so the resistance variation of the cell with temperature does not seriously influence the current source. In practice it is found that the largest contribution to the error of a timer is in the lack of constancy of the current source. When great accuracy is required, special attention to the design of a constant current source will yield excellent results.

In addition to the obvious requirements of simplicity, reliability, long-shelf life and low-power consumption, it is valuable to design a circuit which can be used with the cell repeatedly for non-destructive testing. Lack of experience with E-cell characteristics often results in the design of circuits which lead to voltages greater than one volt being applied across the cell at the end of its plating period. Excessively high voltages will usually destroy the operating characteristics of the cell as the result of oxidation of the electrodes and excessive precipitation of silver compounds.

### Circuit Designs

The solid state circuits which have been used most frequently with E-cells for timer applications fall into three classifications:

1. Transistor circuits.
2. Silicon-controlled rectifier circuits.
3. Uni-junction (or four layer diode) and SCR combination circuits.

The advantage of the transistor circuitry is that transistors are relatively inexpensive and provide simple operating circuits. On the other hand, these circuits are less stable under temperature variation and require a fixed relationship between the cell deplating current and the load current so that when large load currents are required, fairly large deplating currents may be necessary, raising the energy requirements for the circuit during long-time operation.

On the other hand, an SCR circuit requires a given minimum current change at the cell to trigger its operation and very large currents are passed through the load once the SCR has been fired. The SCR circuits have proven to be highly reliable and require relatively low power consumption, but there is at present a slightly larger cost for the SCR component.

The uni-junction SCR combination circuits have the advantage that they can be triggered with very small currents as low as 1/10 microampere and still provide large current surges through the load as is characteristic of SCR operation. This low current through the E-cell which results in lower power consumption and longer operational

lifetime in most cases will be offset by the factor of decreased reliability due to the doubling of the number of components. Furthermore, the 20 to 50 microampere operation of the SCR circuits is already sufficiently small that at this current drain most batteries last out their shelf life.

Some basic circuits will be presented which indicate operational principles with the E-cell. These circuits are generic in nature and would be adapted to specific applications. Figure 9 shows the fundamental diagram for the operation of the electrolytic cell as a current-time integrator. In this circuit it is assumed that the electrolytic cell has at its anode, an amount of plating material proportional to a current-time integral corresponding to a several hour timing period. A series resistor  $R_1$ , which is many times larger in impedance than the electrolytic cell during the conducting state is placed in series with the cell and the combination placed across the battery supply. Resistor  $R_2$  shown in dotted lines may be placed in parallel with the electrolytic cell in order to limit the voltage rise across the electrolytic cell to a safe limit. This safe limit is determined by the voltage at which disassociation of the electrolyte takes place. It is to be noted that resistor  $R_2$  is not necessary for the operation of the cell. If the device were to be used in an application wherein it is self destroying upon actuation, the need for resistor  $R_2$  would be non-existent.

The graphs of Figure 10 describe the operation of the circuit in Figure 9. Assuming the electrolytic cell has silver on the anode, the voltage across the cell when the circuit is activated will be as indicated in Figure 10a, relatively low. The electrolytic cell conducts at a current which is determined by Resistor  $R_1$ . Thus when a current-time integral exhausts the silver on the anode, the electrolytic cell no longer conducts effectively. The voltage abruptly rises to a value limited by resistor  $R_2$  and the current through the cell abruptly drops to almost zero. It is this voltage transition which is used to obtain a contact closure.

The basic operation described in Figure 9 can now be implemented with the addition of one transistor and a load resistor to obtain conduction

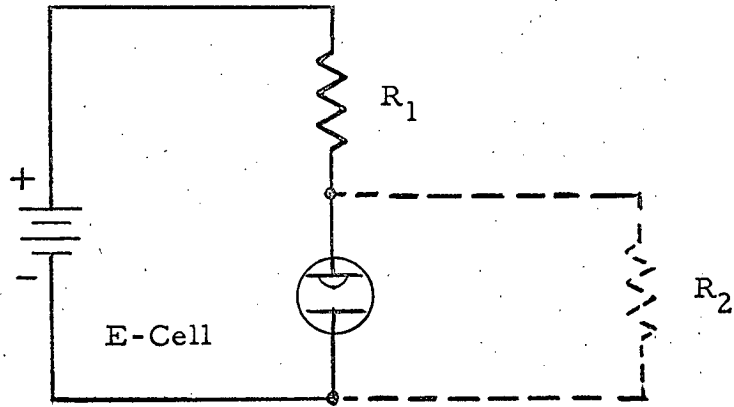


Figure 9  
E-Cell Deplating Circuit

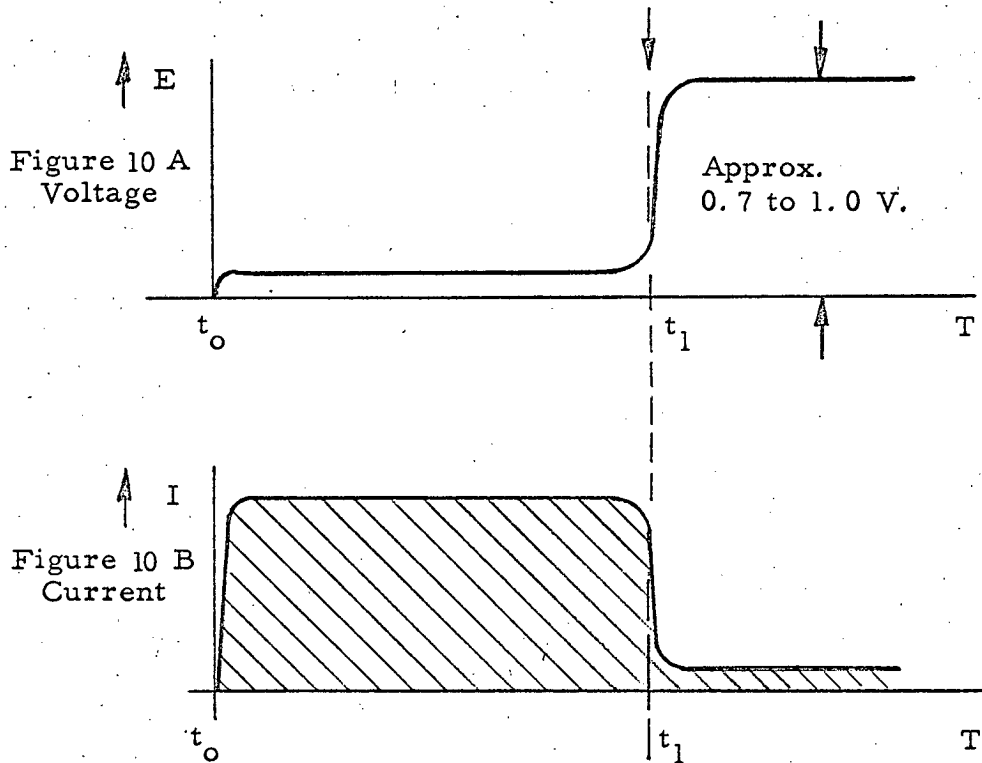


Figure 10  
E-Cell Voltage/Current-Time Relationships

through a load upon the transition of the E-cell from its conducting to its non-conducting state. Figure 11 shows such an example of a simple circuit. During the time delay period the electrolytic cell is a low impedance and has a very low voltage drop across it. Consequently, transistor  $Q_1$  is in a non-conductive state. When the current-time integral has been completed through the electrolytic cell by the passage of current  $i_1$ , the cell abruptly becomes an open circuit with the resultant rise in base voltage to the emitter voltage of  $Q_1$ . This rise results in  $Q_1$  conducting heavily and hence providing the equivalent of a contact closure.

Figure 12 shows a more reliable circuit capable of taking advantage of the fact that the electrolytic cell is a switching device. This circuit replaces the analog control device  $Q_1$  with a much more appropriate device, a silicon controlled rectifier  $Q_2$ . The advantage here is that the SCR has a relatively predictable and stable firing potential. The operation of the circuit is such that when the electrolytic cell is conducting, the gate electrode of the SCR is operating at very close to zero potential. This prevents the SCR from firing. However, with the addition of 0.8 volt when the electrolytic cell ceases deplating, the SCR gate electrode is raised above the threshold, guaranteeing firing of the SCR under wide temperature conditions. A further advantage of this circuit is that the current carrying capability of the SCR is not a function of the gate current. As a result, the deplating current at which the electrolytic cell is operated is independent of the ultimate load current. This feature will be particularly advantageous for power consumption. As shown in Figure 12 the circuit is so arranged for use with a squib, such that capacitor  $C_1$  becomes charged very slowly through  $R_4$  during the deplating phase. When the cell has deplated and the SCR has fired, the energy to operate the squib is derived from the storage capacitor. Although a squib type operation is shown in the diagram, the same type circuit can be used without resistor  $R_4$  or the large capacitor  $C_1$  if the cathode of the SCR is tied directly to B+. In this way, direct contact closure is obtained with B+ and up to several amperes can be carried through the contacts. This circuit

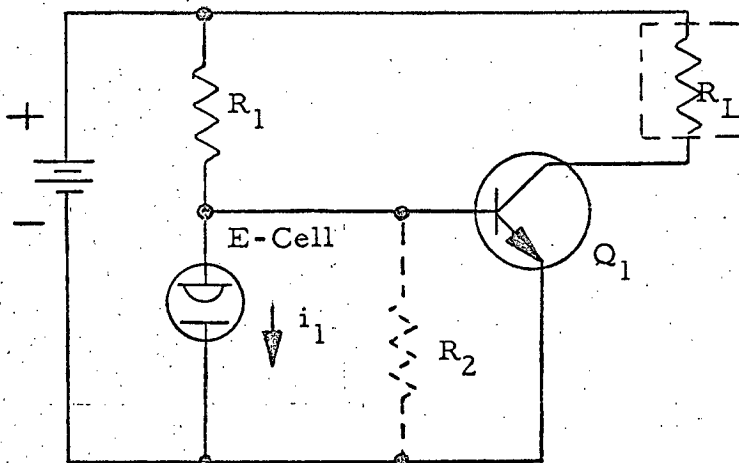


Figure 11  
Basic Transistor Circuit

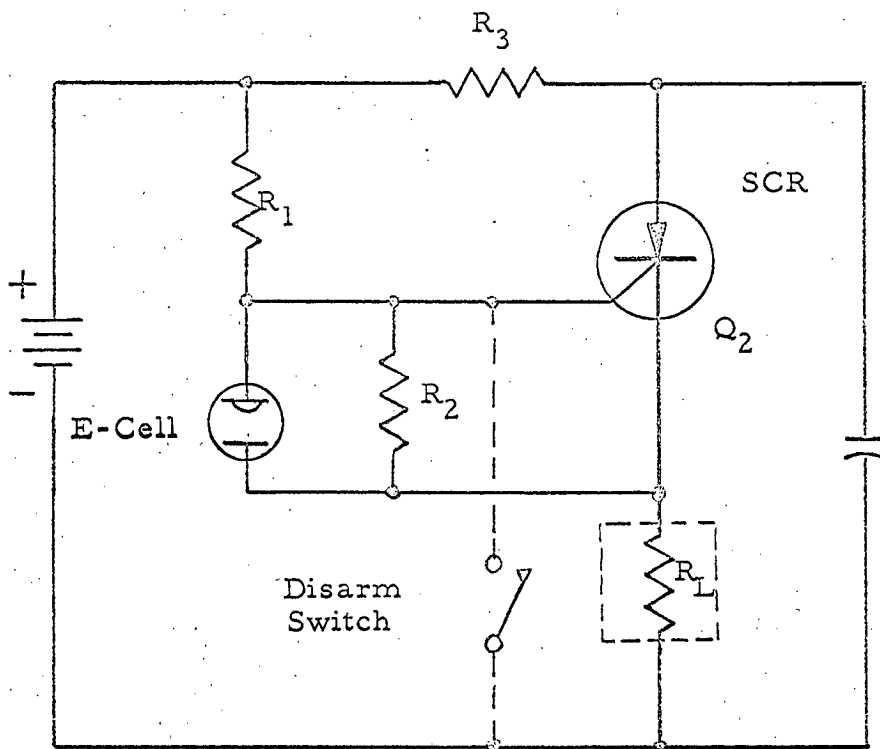


Figure 12  
Basic SCR Circuit



has a further advantage over the previous one in that the load device or squib is now tied to the ground side of the circuit and in much better position for fail-safe features.

An additional feature that can be supplied in such a circuit, is that of providing absolute disarming. This is provided by the insertion of a switch from the SCR gate to ground.

An equipment utilizing an electrolytic cell timer of the type shown in Figure 12 has been developed and is shown in photograph Figure 1. Figure 2 shows a close-up view of the electrolytic cell timer. The actual circuitry of this device occupies approximately 1 cubic centimeter. This timer was developed several months ago by [redacted] and has operated many hundreds of times since then with an accuracy of approximately 1%. 50X1

Another circuit shown in Figure 13, though more complex, has several advantages that may be unique. These advantages are particularly useful in timers that are used for extremely long time delays and conservation of power is one of the prime requirements. Since the electrolytic cell can operate at extremely low values of current, much less than 1 microampere, it would be desirable in some cases to take advantage of this unique property. The circuit of Figure 13 does just this. This device is very similar to that shown in Figure 12 except that a uni-junction or four layer diode device is used as a trigger circuit prior to the silicon controlled rectifier. If the electrolytic cell divider circuit is operating at 1/10th microampere, it could not establish a sufficient signal to drive the SCR; hence, the four layer diode or uni-junction stage is used ahead of it.

This type of circuit has been developed at [redacted] where operation down to very low values has been obtained with reliable operation. 50X1  
50X1

#### General Operational Performance

Requirements of this program outline three specific areas of operational performance in addition to the more general requirements of

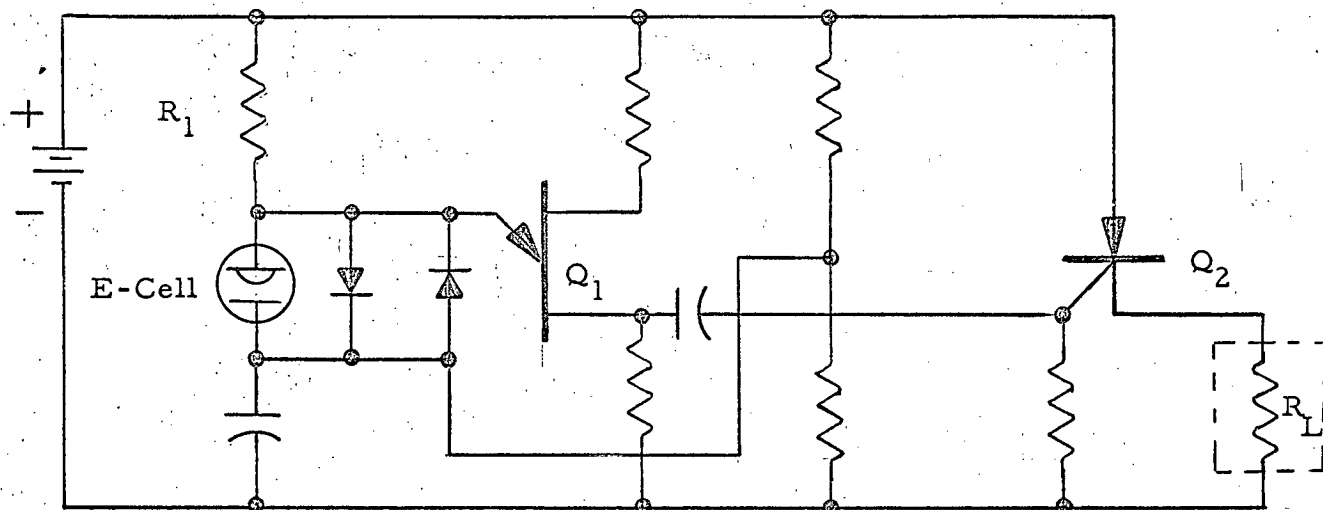


Figure 13

Basic Uni-Junction --SCR Circuit

environment. These specific areas are (1) time-delay accuracy (2) operating and storage temperature range and (3) long shelf life.

The fundamental accuracy of the time delay is a function of several independent parameters. First and dominant is the requirement that the electrolytic cell be depleted at a fixed current. The quantity stored by the electrolytic cell is charged. The time interval is known only to the accuracy that the deplating current is known. It can be assumed that any battery will vary in potential with temperature and discharge. Therefore, it is obvious that a voltage regulating function may have to be included in the timer circuit if such a regulated source is not available to the timer from other accessory equipment.

The required regulating function has been solved in other E-cell timer developments by the use of a zener diode to provide regulation. Recent zener diodes requiring only a few hundred microamperes to achieve operation in their stable region, are very satisfactory for the task without adding serious power drain.

It would be desirable to operate the zener diode at a zener potential of 5.1 volts. In this range the maximum temperature stability inherent in the diode without compensating circuitry is obtained; however, the voltage is greater than required by the rest of the circuitry. With simple compensating forward drop diodes a stable zener reference can be made for any practical operating potential. In any event, a simple, reliable and proven technique exists to reduce the variation of deplating current to less than one per cent and hence an inaccuracy error of less than 1%. With more exotic, though readily available, zener diodes the error due to deplating current inaccuracy could be reduced to as low as 0.1% or less assuming, of course, the proper selection of the series resistor.

Variation in E-cell impedance versus temperature and possibly storage time can also affect the deplating current. However, as indicated earlier, the  electrolytic cell is a much lower impedance than the resistor placed in series with it. For example, if the deplating current is operated from a 2-1/2 volt reference source the series

50X1

resistor might well be 50 to 100 K. Since the cell impedance is approximately 1 K at these current levels the cell impedance could vary over a range of 2 to 1 and still not affect the deplating current by more than one or two percent.\*

As pointed out earlier the very nature of the  E-cell virtually eliminates the contributions of inaccuracy from the associated electronic circuitry because the cell in itself is almost a bi-stable element requiring the electronics only to detect an abrupt large signal change. Hence, small drifts in the firing potential of an SCR for example is inconsequential. This advantage is not present in some other electrolytic devices where the elapsed time is measured by a slow, small variation in potential drop across the cell. The basic characteristics of the timer for variations with temperature are basically those of the E-cell and are discussed earlier in this discussion. The associated circuitry contemplated is based upon silicon semiconductor devices such that the ability to obtain reliable operation of these elements over a range of  $-25^{\circ}\text{F}$  to  $+160^{\circ}\text{F}$  is common engineering practice. Similarly the one year shelf life required and 10 year life desired are achievable with the same simple associated electronic components.

50X1

## MANUFACTURING DESIGN, FABRICATION, AND ENVIRONMENTAL TEST

### Manufacturing Design

The mechanical design of the electrolytic timer will most likely take the form of a printed circuit or welded module device which can be epoxy cast or foamed as required. All the solid state components to be used in the device will be of conventional high reliability type such that they can be packaged in a convenient and compact form. The electrolytic cell has been described previously and will operate in any position. The general performance of small glass components have proven their high quality and reliability from a mechanical standpoint in such applications as diodes and capacitors. During the course of the PHASE A effort,

\* The temperature coefficient of resistance for the E-cell is negative and compensates partially the positive coefficient of most resistors.

environmental tests will be performed on both the electrolytic cell and other critical individual components to ensure a conservative high reliability design.

As a general practice in developments of this nature, [redacted] performs both a reliability study of all parts and develops a plot of operational loci versus loci of specified limits for each component. In the case of the reliability study, data accumulated by the individual component manufacturers can be used in addition to standard referenced data, such as the Diamond Ordnance Fuze Laboratories Reliability Engineering Notes.

#### Functional Testing

The development of an electrolytic timer which requires many hours to perform functional tests, places some interesting demands on the testing techniques employed to reduce test time. In addition, some provisions must be made for resetting the electrolytic cell after each use. Fortunately, these problems have already been encountered by [redacted] and such test equipment is being constructed.

The problem of simulated testing of the timer over short periods of time to determine the general operability of the unit can be readily handled by the use of a 3 electrode cell.\*

The source electrode has plated on it, at the factory, a quantity of plating metal proportional to the current-time integral necessary for the operational timing period. The working electrode is a noble metal electrode containing no plated material. The test electrode is the third electrode which contains only a small sample of plated material, for example, a sufficient amount for 5 or 10 minutes timing at the current rate being used in the timer. All 3 terminals of the electrolytic cell are brought out of the timer device and appropriate connection is made through external circuitry. Hence, in the actual application device the

---

\* The third electrode also provides a means of resetting the timing intervals.

50X1

50X1

50X1

test electrode is not hooked up at all and the source electrode is tied to ground through an external connection and the working electrode is tied to the series resistor which determines plating current in the timer.

During a test operation, the timer is mounted on a test fixture which has a switch to determine whether the source electrode or the test electrode will be tied in series with the series resistor determining deplating current. Hence, after a particular environmental test, if it is desired to ascertain the functional operability of the unit, the test electrode and the working electrode can be tied into the circuit. In this way the electrolytic timer goes through a time function determined by the plating material originally established on the test electrode. This might be only several minutes; hence, the total operation of the circuit can be ascertained without erasing or destroying the current-time integral memorized on the source electrode.

After the operational test has been completed, the working electrode and test electrode are disconnected by a switch on the test equipment from the other timer circuitry and instead connected to a plating circuit of opposite polarity to that used in the timer, such that the plated material which is now on the working electrode, is returned to the test electrode, so that the device will be ready for retest at a later time. In addition, if it is necessary to ascertain whether the source electrode is still in operating condition a further test can be made by tying the source electrode and working electrode to the electrolytic timer and operating this for 2 to 3 minutes. If under this condition no actuation of the electronics occurs and current of the specified quantity does flow through the cell, it can be assumed by such a test that the electrolytic cell is still in operating condition and the electronics have demonstrated their ability to perform the contact closure. These various short tests described here contribute to the complexity of the timer only by the addition of one contact on the connector of the unit. No internal components are added to provide for this type of testing capability. All such extra components are included only in the test apparatus.

When actual operational tests are performed utilizing the source electrode and the full timing period of the device, the timer can be reset by use of the test apparatus to replat the source electrode from the working electrode in a similar manner as discussed above in resetting the test electrode. Here again, the resetting time can be reduced from the several hours required for the deplating function. This is accomplished by the use of a higher current determined by a resistor placed in the test apparatus to deplate the cell. In some designs it is found that resetting of the electrolytic cell can be accomplished as fast as 1/100th of the deplating time. In most timers, effort is made to include as fast a resetting time as practical.

#### CONCLUSIONS

The experience of  in electro-lytic timers closely matches many timer requirements. Timers have been built with high reliability, accuracy, reproducibility, and wide environmental stability. It remains for any specific application to build a timer which incorporates all the appropriate requirements in one device and test it thoroughly.

50X1

The extensive experience with E-cells and related circuits summarized in the Technical Discussion evidences a variety and subtlety of phenomena unsuspected by those with little experience in the field. This accumulated knowledge of a basic and fundamental nature provides an excellent foundation for undertaking further development.